HETEROGENEOUS PHOTOCATALYTIC DEGRADATION OF ORGANIC POLLUTANTS IN WATER OVER NANOSCALE POWDERED TITANIUM DIOXIDE

K. M. MEZUGHI

PhD

UNIVERSTY OF BRADFORD

2010

HETEROGENEOUS PHOTOCATALYTIC DEGRADATION OF ORGANIC POLLUTANTS IN WATER OVER NANOSCALE POWDERED TITANIUM DIOXIDE

The photocatalytic degradation of organic compounds in water (Reactive Orange 16, Triclocarban, Clopyralid and Estrogens (estrone, 17β-estradiol, and 17α-ethinylestradiol)) was studied; the reaction kinetics and the effect of the operating parameters on the performance of the system were determined; a comparison with other advanced oxidation processes (O_3, H_2O_2, UV) was also made.

Khaled M. Mezughi

Submitted for the Degree of
Doctor of Philosophy

School of Engineering, Design and Technology

University of Bradford

United Kingdom

2010

ABSTRACT

Organic contaminants from industrial and/or domestic effluents may be harmful to humans directly or indirectly by degrading the quality of the aquatic environment. Consequently these contaminants must be reduced to levels that are not harmful to humans and the environment before disposal. Chemical, physical and biological methods exist for the removal of these pollutants from effluents. Among the available chemical methods, heterogeneous photocatalytic oxidation has been found particularly effective in removing a large number of persistent organics in water. In this study, photocatalytic degradation was explored for the removal of reactive azo-dye (textile dye), triclocarban (disinfectant), clopyralid (herbicide) and three endocrine disrupting compounds (EDCs) (estrone, 17β-estradiol and 17α-ethinylestradiol) from synthetic effluents. The major factors affecting the photocatalytic processes including the initial concentration of the target compounds, the amount of catalyst, the light intensity, the type of catalyst, the electron acceptor, the irradiation time and the pH were studied. Other oxidation techniques including (O_3, H_2O_2, UV) were also studied.

Generally UV light is used in combination with titanium dioxide, as photocatalyst, to generate photoinduced charge separation leading to the creation of electron-hole pairs. The holes act as electron acceptors hence the oxidation of organics occur at these sites. These holes can also lead to the formation of hydroxyl radicals which are also effective oxidants capable of degrading the organics.

The results obtained in this study indicated that photolysis (i.e. UV only) was found to have no effect on the degradation of reactive azo-dye (RO16). However, complete photocatalytic degradation of 20 mg/L (3.24×10^{-2} mM) RO16 was achieved in 20 minutes in the presence of 1g/L TiO_2 Degussa P25 at pH 5.5. Comparison between various types of catalysts (i.e. Degussa P25, VP Aeroperl, Hombifine N) gave varied results but Degussa P25 was the most effective photocatalyst hence it was selected for this study. For RO16 the optimum catalyst concentration was 0.5 g/L TiO_2 with initial concentration of 20 mg/L RO16. It was found that the disappearance of RO16 satisfactorily followed the pseudo first-order kinetics according to Langmuir-Hinshelwood (L-H) model. The rate constant was k= 0.0928 mol/min. Photodegradation of TCC was studied in 70%v acetonitrile: 30%v water solutions. UV light degraded TCC effectively and the reaction rates increased with decreasing initial concentration of TCC. UV/TiO_2 gave unsatisfactory degradation of triclocarban (TCC) since only 36% were removed in 60 minutes with initial concentration of TCC 20 mg/L. The degradation of clopyralid and the EDCs was studied using three oxidation systems UV/TiO_2, UV/H_2O_2 and O_3. Complete degradation of clopyralid (3,6-DCP) was achieved with UV/TiO_2 in about 90 minutes at an optimum catalyst concentration of 1g/L. Zero-order kinetics was found to describe the first stage of the photocatalytic reaction in the concentration range 0.078-0.521 mM. At pH 5 the rate constant was $2.09\times10^{-6} \pm 4.32\times10^{-7}$ $M.s^{-1}$.Complete degradation of all the three EDCs was achieved with UV/H_2O_2 in 60 minutes at catalyst concentration of (2.94×10^{-2} M). On the other hand complete degradation of the EDCs was achieved in just 2 minutes with ozonation. For high concentration EDCs, TiO_2/UV gave low efficiency of degradation as compared with ozone and H_2O_2/UV. First-order kinetics was found to describe the photocatalytic reaction of the EDCs.

Acknowledgements

All praise to the gracious, the greatest **Almighty Allah** who blessed me with the courage and made my efforts fruitful for the completion of this research to a happy ending. Without Allah's assistance, a project like this would never have come to fruition.

I would like to express my sincere gratitude to Dr. Chedly Tizaoui, my supervisor, for his invaluable guidance and advice, continuous co-operation, valuable comments, suggestions, unlimited help and support throughout this work.

I would also want to extend my sincere gratitude to my co- supervisor Professor Hadj Benkreira for his wonderful guidance, encouragement and support from the beginning of my study.

I would like to thank the Education Service Department of the Libyan Government for sponsoring me for this PhD research study at the University of Bradford.

Thanks also go to all staff members of School of Engineering, Design and Technology. In particular, I would like to thank Mr John Purvis, Mr. Michael Cribb, Mr. Ian Mackay, Mr. Andrew Healey, Mr. Stuart Fox, Mr. Dave Steel and Mrs. Belinda Hill for their help and support. I would also like to thank my colleagues Mr Aminu Tukur, Dr. Mawaheb Dardar and Mrs Helen Essandoh.

I want to express my gratitude to my parents for their enormous love, and my brothers and sisters for their unconditional support and encouragement. My warmest thanks go to my great wife Layla and my lovely daughters (Fatima and Hiba) for their love, understanding and patience during my study.

DISCLAIMER

The work submitted in this thesis is genuinely carried out by me and has not been submitted to any other organization for any other degree.

The following publications have been based on this work:

Mezughi, K., Tizaoui, C., 2009. Heterogeneous Photocatalytic Degradation of the Antiseptic Triclocarban, 5th International Conference on Oxidation Technologies for Water and Wastewater Treatment, (March 30-April 1), Berlin, Germany, (PC 253).

Tizaoui, C., Mezughi, K., 2009. The degradation of the herbicide clopyralid by heterogeneous photocatalysis, 3rd Developments in Water Treatment and Supply Conference (June 01-02), Buxton, UK.

Tizaoui, C. Mezughi, K., Bickley, R. J., Heterogeneous photocatalytic degradation of the herbicide clopyralid and comparison with UV/H_2O_2 and ozone oxidation techniques, submitted to Water Research (Impact Factor 4.355).

Table of Contents

List of Figures

List of Tables

List of Abbreviations and Symbols

Abbreviations

AOPs	Advanced Oxidation Process
COD	Chemical Oxygen Demand
EDCs	Endocrine-Disrupting Compound
RO16	Reactive orange 16
3, 6-DCP	Clopyralid
TCC	Triclocarban
E1	Estrone
E2	17β-Estradiol
E3	Estriol
EE2	17α-Ethinylestradiol
EPA	Environmental Protection Agency
Eq.	Equation
PTFE	Poly tetrafluroro ethene
SE	Steroid Estrogen
TOC	Total Organic Carbon
UV	Ultraviolet
NTP	Normal Temperature and Pressure
BET	Surface area

Symbols

A, B	reactant or reagent
Ac	acceptor
Cat	catalyst
D	donor
c	concentration of reactant [μg L^{-1}]
c_0	initial concentration of reactant [μg L^{-1}]
e^-	electron
h^+	positively charged hole
$h\nu$	photonic energy
I	irradiation intensity [mW cm^{-2}]
k	apparent reaction rate constant [min-1]
K	Langmuir adsorption coefficient of reactant [L mg^{-1}]
m	concentration of TiO_2 [g L^{-1}]
q	equilibrium surface concentration [mg g^{-1} TiO_2]
R^2	correlation coefficient
T	time [h]
V	volume[L]

Chapter One

Introduction

1.1 General

This chapter introduces the context under which this study has been carried out. Particular focus will be given to water as being one of the essential elements on earth necessary for all life. Humans can survive without food for periods much longer than they can do without water. Indeed, a constant supply of water is needed to replenish the fluid lost through normal physiological activities such as respiration, sweating and urination. The water to be consumed by humans has to be wholesome, so proper care is needed to ensure that the water used is clean and fit for drinking purposes. Any contamination in water may lead to diseases, bacterial and fungal attacks, and sometimes even fatal consequences. For example there are many sources of ground water pollution that can cause nasty tastes and odours, and that may be a risk to human health. Contamination of surface and ground waters may occur naturally or as a result of human activities such as agricultural runoff and industrial discharges. Examples of water contaminants include:

Microorganisms: There are many types of microorganisms that can cause human illnesses or result in discolouration of water or produce nasty tastes and odours. Microorganisms include bacteria, viruses, algae and parasites. Shallow wells are highly at risk of contamination by microorganisms, as are those located near farms, wildlife hotspots and high risk flood zones. Water run-offs from these areas can usually cause contamination.

Nitrates and nitrites: Nitrates are linked to the blue baby syndrome. High levels of nitrates arise usually as a direct result of human activities. They are contained in fertilisers used on farms, which are of potential contamination to ground water. If large amounts of contaminated waters are consumed, human health can be jeopardised.

Micropollutants: Many industrial processes generate wastewater streams contaminated with organic compounds harmful to human health and the environment. Water pollution by micro-pollutants such as pesticides, textile, dioxins, organic compounds and so on is a worldwide problem at present (Mumma, 1995).

In order to solve the problem of water contamination, many researchers are on the track to develop new technologies capable of removing a range of water contaminants. One of the promising technologies is photocatalysis, which is the subject of this work. Photocatalysis was found to be effective in removing a wide range of organic and inorganic compounds and has been applied successfully in treating both drinking and waste waters (Hughes et al., 1996).

1.2 Water Pollution

All life forms require access to water. However nowadays water pollution is an issue to be faced. Water pollution is wide spread and almost affects all sources of water supplies such as lakes, rivers, underground water and oceans. Water pollution can be the result of natural phenomena such as volcanoes, storms and earthquakes, but the main contribution comes from human activities.

Wastewaters discharged by factories and sewage treatment plants are the most polluters of concern. Wastewaters contain toxic and hazardous substances such as heavy metals, organic toxins, and solids. Sometimes the pollutants in water include a wide spectrum of

chemicals or pathogens. Many of the chemical substances are toxic or even carcinogenic. Waters contaminated at unacceptable levels are harmful once they are discharged into fresh water. They can affect animals and humans alike. Pollutants in water can be absorbed by plants as well and may enter the food chain.

Other problems that may arise from the existence of pollution in the environment is the fall of acid rain, which can cause fish death for example. Research studies have shown that fishes cannot cope with waters at pHs in the region of pH 4.5 -5, (Wellburn, 1988). Acid water affects human health, animals' health and can be absorbed by plantations (Mellanby, 1992).

Some non-toxic discharges such as oils, nutrients or organic matter give negative effect to the environment due to deoxygenation of the water. Oil floating on water causes death of fishes or plants due to high oxygen demand in the water. Nutrients encourage bacterial and fungal growth causing deoxygenation of the water as well. These negative effects of pollution raise huge concerns about today's environment. A summary of the major forms of environmental pollution is shown in Table 1.1.

Table 1. 1: Major forms of environmental pollution.

Air Pollution	The release of wastes into air, such as the release of carbon monoxide, carbon dioxide, chlorofluorocarbons (CFCs) or nitrogen dioxide from industries or vehicles.
Water Pollution	The unhealthy water discharged by factories. Water pollution problems will be discussed later.
Soil Contamination	Chemicals such as heavy metals, acids, hydrocarbons etc. that are released to soil or underground.
Radioactive Contamination	This includes the atomic release from technology.
Noise Pollution	The noise released by factories, aircrafts or roadways.
Thermal Pollution	The temperature of water bodies changes due to human activities.

1.2.1 The sources of water pollution

There are many causes of water pollution but two general categories exist: direct and indirect contaminant sources. Direct sources include effluent outfalls from factories, refineries, and waste treatment plants etc. that emit fluids of varying quality directly into urban water supplies. In the United States and other countries, these practices are regulated, although this does not mean that pollutants can not be found in these waters. Indirect sources include contaminants that enter the water supply from soils/groundwater systems and from the atmosphere via rain water. Soils and groundwaters contain the residue of human agricultural practices (fertilizers, pesticides, etc.) and improperly disposed of industrial wastes. Atmospheric contaminants are also derived from human practices (such as gaseous emissions from automobiles, factories and even bakeries). Contaminants can be broadly classified into organic, inorganic, radioactive and acid/base. Examples from each class and their potential sources are too numerous to discuss here.

1.2.2 The effects of water pollution

The effects of water pollution are varied. They include poisonous drinking water, poisonous food animals (due to these organisms having bioaccumulated toxins from the environment over their life spans), unbalanced river and lake ecosystems that can no longer support full biological diversity, deforestation from acid rain, and many other effects. These effects are, of course, specific to the various contaminants.

1.3 Water Treatment Processes

In this section, a brief summary of the conventional treatment processes is made.

1.3.1 Physical Methods

Screens: These are used to filter the water and are usually used at the beginning of the purification process to remove solids from the water.

Sand Filtration: The filter in this case is made of a multiple layers of sand that varies in size. When the water flows through the sand, solid particles are filtered out.

1.3.2 Cross Flow Filtration

Microfiltration: This type of filtration is designed to remove very small particles from the water that range in size from 0.1 to 1.5 μm.

Ultrafiltration: This type of filtration removes even smaller particles from the water that range in size from 0.005 to 0.1 μm.

Nanofiltration: This type of filtration removes particles from the water that range in size from 0.0001 to 0.005 μm.

Reverse Osmosis: This type of filtration is effective at removing the smallest of particles with a size of up to 0.001 μm.

1.3.3 Chemical Methods

Chemical Addition: Oxidising agents are effective at killing certain microorganisms and reducing agents can be added to neutralise the oxidising agents to prevent harm to humans and the environment.

Clarification: This process removes suspended solids through a number of different processes. This method is effective at removing large particles but may not filter out all of them, further treatment may be needed.

Deionisation and Softening: Ion exchange systems absorb certain anions and cations in order to deionise the water. The water softeners are often used as ion exchangers; they work by removing calcium and magnesium ions from the water, and then replace them with positively charged ions. This reduces the hardness of the water.

1.3.4 Disinfection

Disinfectants are used to kill any remaining microorganisms in the water; it is an important process of water treatment as it can prevent pathogenic microorganisms from causing human diseases.

Chlorine Disinfection: Chlorine is capable of killing many microorganisms, but when it reacts with substances that may be present in the water, dangerous carcinogenic chemicals may be formed such as trihalomethanes (THM_S) and haloacetic acids (HAA_S).

Ozone Disinfection: This type of disinfection works by using oxygen atoms to destroy pollutants through oxidation.

UV-Radiation: This type of disinfection is growing in popularity. It is more natural in its way of killing microorganisms as it uses UV rays to kill germs.

1.3.5 Biological Methods

Water purification can also be done biologically using microorganisms such as bacteria. These microorganisms decompose organic matter within the water and therefore reduce the amount of organic suspended matter. There are two types of treatment that use either anaerobic or aerobic bacteria. Table 1.2 shows water problems and some common treatments.

Table 1. 2: Typical water problems and some common treatments.

Common Water Problems	Treatment
Bacteria	Disinfection
Fuel products	Carbon filter
Hard water	Water Softener
Hydrogen sulfide gas	Oxidizing filter, followed by a carbon filter, or chlorination followed by a sediment filter
Iron particles	Water softener or iron filter
Metals	Reverse osmosis unit or distillation
Nitrates	Reverse osmosis unit or distillation
Pesticides	Carbon filter
pH	Neutralizing filter
Sediment	Fiber filter
Taste and odours	Carbon filter

1.4 Organic Pollutants

A wide variety of organic pollutants especially pesticides are introduced into the water system from various sources such as industrial effluents, agricultural run off and chemical spills (Cohen et al., 1986 and Muszkat et al., 1994). Their toxicity, stability to natural decomposition and persistence in the environment has been the cause of much concern to the societies and regulation authorities around the world (Dowd et al., 1988). The control of organic pollutants in water is an important measure in environmental protection. Among many processes proposed and/or being developed for the destruction of organic contaminants, biodegradation has received the greatest attention. However,

many organic chemicals, especially those that are toxic or refractory, are not amendable to microbial degradation.

There are many powerful anti-cancer drugs (Cytotoxic drugs) that are used by an increasing amount of patient but these drugs can be excreted unchanged from the human body directly into the sewage. These drugs used by cancer patients are normally water soluble and are very hard to destroy using conventional water treatment procedures, which adds more strain on sewage treatment plants. There are many substances, both natural and synthetic which have the potential to mimic or interfere with the functioning of the human endocrine system. These are collectively known as Endocrine Disrupters (EDCs) a general, non scientific, term used to describe all kinds of substances thought to be able to act in this way. The phenomenon was first identified in the 1980's as a consequence of observations of gender changes in fish in some rivers, (Jobling et al., 1998).

Azo dyes are ubiquitous commercial chemicals that present unique environmental problems. More than 300 million pounds of dyes are produced annually in the United States. Colored dye effluents pose a major problem for the manufacturing plants as well as water-treatment plants downstream. Quite apart from the aesthetic undesirability of coloured streams resulting from dye waste, the azo dyes in particular can undergo natural anaerobic degradation to potentially carcinogenic amines.

1.5 Photocatalysis

The efficient treatment of wastewater and contaminated drinking water is important due to increasing population and decreasing energy resources that many parts of the world currently face. An ideal process for waste water treatment would be an inexpensive process that achieves complete mineralisation of all contaminants in the waste stream without the formation of hazardous by-products. Currently however, no treatment

technology approaches this ideal situation. Heterogeneous photocatalysis is an advanced oxidation processes (AOP) that has proved promising for the removal of toxic and bio-resistant organic and inorganic compounds from waste water by their total conversion into species that are non-toxic. It gives a good chance of offering a technology well suited to the above requirements.

Photochemical methods for water treatment must be applied in the context of existing water treatment technologies. They may not be well suited for applications involving highly contaminated domestic or food industry waste waters; but are highly attractive as an additional stage of treatment for many waste waters containing non-biodegradable compounds such as dyes, pesticides, herbicides, pharmaceutical and personal care products, and hormones.

Currently no literature exists on the use of photocatalysis for the degradation of the personal care product triclocarban. Also knowledge is limited on the degradation kinetics of endocrine disrupting compounds [estrone (E1), 17β-estradiol (E2) and 17α-ethinylestradiol (EE2)] present simultaneously as contaminants in wastewater. On the other hand, the photocatalytic degradation of RO16 and clopyralid has not been studied extensively hence this research was carried out to investigate the kinetic degradation of the above mentioned compounds and the effect of the operating parameters to help improve the understanding of their behaviour during photocatalysis.

1.6 Aim and Objectives

The overall aim of this work was to investigate the oxidation of a selection of organic pollutants including a reactive azo-dye (RO16), a disinfectant triclocarban (TCC), a herbicide clopyralid (3, 6-DCP) and endocrine disruptors [estrone (E1), 17β-estradiol (E2) and 17α-ethinylestradiol (EE2)] in water using photoassisted heterogeneous

photocatalysis over titanium dioxide and compare performances with other oxidation techniques including O_3 and UV/H_2O_2.

The particular objectives of the study are:

1. To study the effects of operating parameters on photocatalytic processes such as pH, initial concentration of substance, concentration of catalyst, power of UV light, and electron acceptor.
2. To investigate the adsorption capacities of TiO_2 and determine the optimal TiO_2 concentrations.
3. To investigate the performance of different catalysts and study the potential for their re-use.
4. To study the degradation kinetics of the pollutants of concerns.
5. To gain fundamental understanding of the photocatalytic system used in this study.
6. To compare the performances with other oxidation processes including UV/H_2O_2 and ozone.

1.7 Thesis Plan

An extensive experimental study has been carried out to address the aims and objectives of this thesis. Results and discussions alongside conclusions and future work are presented in this thesis. The thesis is structured as follows:

Chapter 1 presents a brief introduction on water and photocatalysis importance and sets the scene for the work. The aim and objectives of this work have also been stated in Chapter 1.

Chapter 2 provides the general background and shows an in depth literature review related to the topics of this work.

Chapter 3 is concerned with the materials, methods and experimental procedures that were used in this study.

Chapter 4 analytical results.

Chapter 5 includes the experimental results and their discussions.

Chapter 6 summarizes the conclusions reached during the course of this work and proposes future work.

Chapter 7 comprises of appendices and references.

Chapter Two

Literature review

2.1 General

There are many natural cycles in the ecosystem, for example the carbon cycle, the nitrogen cycle and the phosphorous cycle. These natural processes, in principle, recycle essential mineral nutrients that sustain life. Mankind however operates on that nutrient flow rather than on nutrient cycling (Serpone et al., 1988). That is, nutrients are extracted from the Earth's crust and the wastes are returned to rivers, lakes, and eventually the ocean. These wastes come from various sources, including chemical fertilizers, pesticides and herbicides from domestic and agricultural applications, human and animal wastes, and oil and grease from motor vehicles. Industries while processing raw materials and manufacturing goods to fulfil its ‘‘mission’’ to provide a better material life to mankind, produce large amounts of wastes, which lead to the release of pollutant directly into the environment. Other routes of aquatic environment contamination arise from effluents from wastewater treatment plants, accidental spills, and uncontrolled or poorly chosen landfill hazardous waste sites (EPA 1979). Several types of organic chemicals cause disagreeable tastes and odors in drinking water, and other types are known to be toxic.

Treatment technologies which have been developed and are currently in operation include physical, biological, and chemical processes. Physical processes include methods such as air stripping, steam stripping and carbon adsorption. Biological processes use microbial treatment to remove the pollutants while chemical methods employ ozone or chlorine for oxidation processes. As a result, environmental, social and

economic pressures for the elimination of pollution hazards have led to the development of destructive processes that should ideally produce a totally harmless effluent. Recently photocatalysis is an attractive technology to degrade harmful chemicals in the presence of light.

2.2 Advanced Oxidation Processes (AOP)

In the past 15 years, a large number of research projects have been addressed to a special class of oxidation techniques defined as Advanced Oxidation Processes (AOPs), pointing out its potential prominent role in wastewater purification (Ollis and Ekabi, 1993). It was shown that AOPs could successfully solve the problem of water pollutants working at or near ambient temperature and pressure (Bahnemann et al., 1994; Bolton and Cater, 1994). All AOPs are characterized by the same chemical feature: the production of hydroxyl radicals $^{\bullet}OH$. These radicals are extremely reactive species and attack most organic molecules with rate constants usually in the order of 10^6-10^9 mol l^{-1} s^{-1} (Hoigne, 1997). $^{\bullet}OH$ radicals are also characterized by a low selectivity of attack which is a useful attribute for an oxidant used in wastewater treatment and for solving pollution problems. The versatility of AOPs is also enhanced by the fact that they offer different possible ways for $^{\bullet}OH$ radicals production, thus allowing a better compliance with the specific treatment requirements. Table 2.1 shows that $^{\bullet}OH$ has the highest thermodynamic oxidation potential, which is perhaps why $^{\bullet}OH$ -based oxidation processes have gained the attention of many advanced oxidation technology developers. In addition, most environmental contaminants react 1 million to 1 billion times faster with $^{\bullet}OH$ than with O_3, a conventional oxidant (US EPA, 1998).

Table 2.1: Oxidation potential of several oxidants in water (Carey, 1992).

Oxidant	Oxidation potential (eV)
Positively charged hole h^+ on TiO_2	2.42
Hydroxyl radical •OH	2.18
Ozone	2.07
Hydrogen peroxide	1.77
Permanganate ion	1.67
Chlorine	1.36
O_2	1.23

AOPs can be classified according to the reaction phase (homogeneous or heterogeneous) or to the methods used to generate the $^{\bullet}OH$ radicals (chemical, electrochemical, sonochemical or photochemical). The main use of AOPs is illustrated in Figure 2.1.

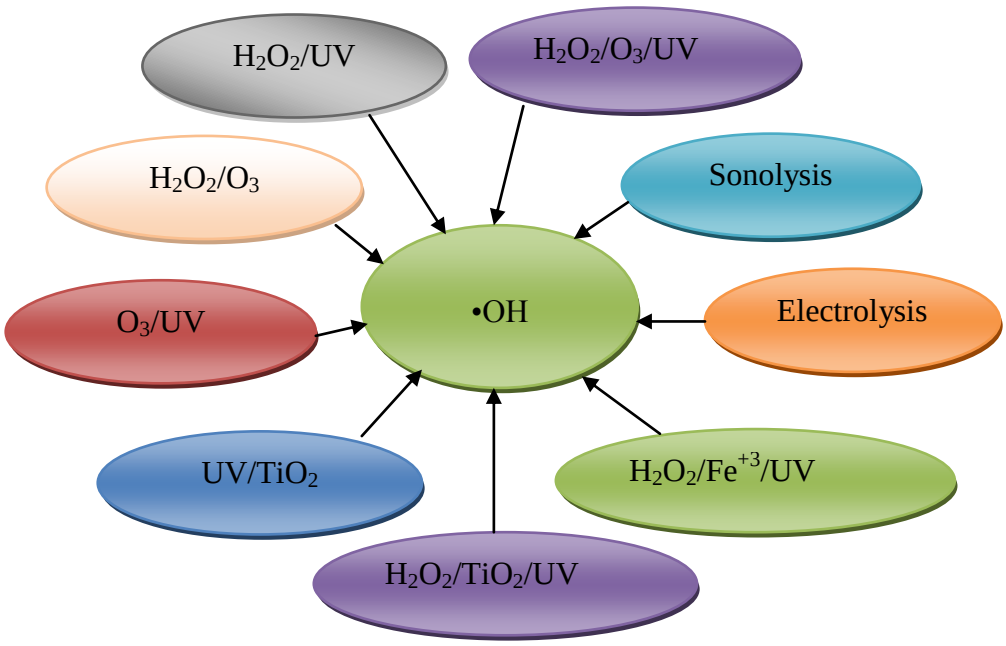

Figure 2.1: Main advanced oxidation processes (AOP).

The focus of this study was on UV/TiO_2, UV/H_2O_2 and O_3. A brief introduction to these processes will be presented in the following paragraphs and a detailed discussion on the UV/TiO_2 system, the main subject of this study, is presented in Section 2.5.

2.2.1 The Photocatalytic Process (*UV/TiO₂*)

During, the photocatalytic process, the illumination of the semiconductor photocatalyst with ultraviolet radiation activates the catalyst, establishing a redox environment in the aqueous solution (Zhang et al., 1994). The energy difference between the valence and conduction band is called the band gap energy (Hoffmann et al., 1995).

The semiconductor photocatalyst absorbs impinging photons with energies equal to or higher than its band-gap or threshold energy. Each photon of the required energy that hits an electron in the occupied outer orbital of the valence band of the semiconductor atom can elevate that electron to the unoccupied conduction band leading to excited

state conduction band electrons and positive valence band holes as shown in Fig. 2.2 (Schiavello and Sclafani, 1989).

The fate of these charge carriers may take different paths (refer to Figure 2.1). First, they can get trapped, either in shallow traps (ST) or in deep traps (DT). Second, they can recombine, nonradiatively or radiatively, dissipating the input energy as heat. Finally, they can react with electron donors or acceptors adsorbed on the surface of the photocatalyst (Hoffmann et al., 1995). In fact, it was shown that any photoredox chemistry occurring at the particle surface emanates from trapped electrons and trapped holes rather than from free valence band holes and conduction band electrons (Serpone et al., 1996). The competition between charge carrier recombination and charge carrier trapping, followed by the competition between recombination of trapped carriers and interfacial charge transfer are what determine the overall quantum efficiency for interfacial charge transfer. Also of great importance are the band positions or flat band potentials of the semiconductor material. The flat band potential (V_{fb}) locates the energy of both the charge carriers at the semiconductor-electrolyte interface and depends on the nature of the material and the system equilibria (Litter, 1999). This value therefore is indicative of the thermodynamic limitations for the photoreactions that can take place.

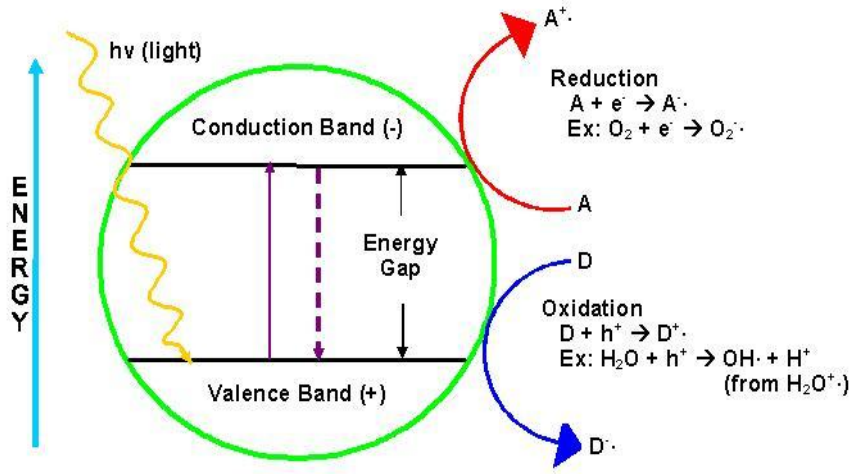

Figure 2.2: Schematic of an irradiated TiO_2 particle.

When considering the interactions between the generated charge carriers and a desorbed species on the semiconductor surface, the heterogeneous photocatalytic process can also be expressed as a series of complex reactions (Reactions 2.1-2.12) (Litter, 1999). Reaction 2.1 represents the formation of the charge carriers upon the illumination of TiO_2. If these generated charge carriers are not involved in any further reactions, they can quickly recombine. The holes react with physisorbed water or chemisorbed OH^- to produce hydroxyl radicals (Reactions 2.2 and 2.3). The hydroxyl radicals are thought to be the main oxidants responsible for the degradation of the organics (D: electron donors) (Reaction 2.4). The electrons react with the dissolved oxygen to lead superoxide ions (Reaction 2.5). These can also form hydroxyl ions after further reactions (Reactions 2.6-2.10). The direct reaction between the organic molecules and the holes can also lead to the destruction of the organics (Reaction 2.11) and between the electrons and the electron acceptors (A) (Reaction 2.12).

$$TiO_2 \xrightarrow{h\nu} TiO_2\left(e^-_{cb}, h^+_{vb}\right) \rightarrow recombination \tag{2.1}$$

$$TiO_2(h^+_{vb}) + H_2O_{ads} \rightarrow TiO_2 + HO^{\bullet}_{ads} + H^+ \tag{2.2}$$

$$TiO_2(h^+_{vb}) + HO^-_{ads} \rightarrow TiO_2 + HO^{\bullet}_{ads} \quad (2.3)$$

$$HO^{\bullet}_{ads} + D_{ads} \rightarrow D_{oxid} \quad (2.4)$$

$$TiO_2(e^-_{cb}) + O_{2ads} + H^+ \rightarrow TiO_2 + HO^{\bullet}_2 \rightarrow O^{\bullet -}_2 + H^+ \quad (2.5)$$

$$HO^{\bullet}_2 + TiO_2\left(e^-_{cb}\right) + H^+ \rightarrow H_2O_2 \quad (2.6)$$

$$2HO^{\bullet}_2 \rightarrow H_2O_2 + O_2 \quad (2.7)$$

$$H_2O_2 + O^{\bullet -}_2 \rightarrow HO^{\bullet} + O_2 + HO^- \quad (2.8)$$

$$H_2O_2 + h\nu \rightarrow 2HO^{\bullet} \quad (2.9)$$

$$H_2O_2 + TiO_2(e^-_{cb}) \rightarrow HO^{\bullet} + HO^- \quad (2.10)$$

$$TiO_2(h^+_{vb}) + D_{ads} \rightarrow TiO_2 + D^+_{ads} \quad (2.11)$$

$$TiO_2(e^-_{cb}) + A_{ads} \rightarrow TiO_2 + A^-_{ads} \quad (2.12)$$

The UV/TiO_2 process is known to have many important advantages, in particular:

i. A large number of organic compounds in water can be completely mineralised (Blake, 2001).

ii. The inputs to the photocatalytic technology are only air and electric power, and no added chemicals are involved, except the addition of TiO_2 which can be separated from water after use.

iii. The rate of reaction can be high if high power lamps or large surface areas of the photocatalyst are used.

iv. Titanium dioxide is available at relatively modest price, is non-toxic and would be recycled on a technical scale.

v. UV lamps are inexpensive, long lasting and can be produced in various sizes.

vi. This technology has a potential to use solar radiation because it is operated in UV-A region (UVA: 320 - 400 nm, UVB: 280 - 320nm and UVC: below 280nm).

vii. The photocatalyst is not consumed in the overall reaction.

2.2.2 UV light/Hydrogen peroxide

Hydrogen peroxide is widely used; it is a safe, effective, powerful and versatile oxidant. The main applications of H_2O_2 are oxidation to aid odour control and corrosion control, organic oxidation, metal oxidation and toxicity oxidation. The most difficult pollutants to oxidize may require H_2O_2 to be activated with catalysts such as iron, copper, manganese or other transition metal compounds.

The dissociation of hydrogen peroxide in water is shown in Equation (2.13)

$$H_2O_2 + H_2O \rightarrow HO_2^- + H_3O^+ \quad (2.13)$$

The application of UV light to a solution of H_2O_2 leads to the formation of hydroxyl radicals (Equation 2.14). Other reaction steps may also take place and lead to the consumption of the formed radicals and the production of hydrogen peroxide (Equations 2.15-2.19).

$$H_2O_2 + h\nu \rightarrow 2HO^\bullet \quad (2.14)$$

$$H_2O_2 + HO^\bullet \rightarrow HO_2^\bullet + H_2O \quad (2.15)$$

$$H_2O_2 + HO_2^\bullet \rightarrow HO^\bullet + H_2O + O_2 \quad (2.16)$$

$$2HO^{\bullet} \rightarrow H_2O_2 \quad (2.17)$$

$$2HO_2^{\bullet} \rightarrow H_2O_2 + O_2 \quad (2.18)$$

$$HO^{\bullet} + HO_2^{\bullet} \rightarrow H_2O + O_2 \quad (2.19)$$

2.2.3 Ozonation (O_3)

Ozone is unstable gas comprising of three oxygen atoms, the gas will readily degrade back to oxygen and during this transition a free oxygen atom or a free radical is formed. The free radical is highly reactive and short lived; under normal condition it will only survive for milliseconds. Ozone is a colourless gas that has an odour similar to smell of the air after a major thunderstorm. Ozone has greater disinfection effectiveness against bacteria and viruses as compared to chlorination. In addition, its oxidizing properties can also reduce the concentration of iron, manganese, sulphur and reduce or eliminate taste and odour problems in drinking water. Ozone oxides the iron, manganese, and sulphur in the water to form insoluble metal oxides or elemental sulphur. These insoluble particles are then removed by postfiltration. Organic particles and chemicals will be eliminated through either coagulation or chemical oxidation. Ozone is unstable, and it degrades over a time frame ranging from few seconds to minutes. The rate of degradation is a function of water chemistry, pH and water temperature (Langlais 1991). Ozone can react with contaminants (substances) by either direct reaction as the O_3 molecule, or by indirect reaction with hydroxyl free radical. These different reaction mechanisms lead to different oxidation products and are controlled by different type of kinetics (Gottschalk et al., 2000).

The direct oxidation (M + O_3) of organic compounds by ozone is a selective reaction with slow reaction rate constants, typically being in the range of k_d = 1.0-1000 (s^{-1}). The

reaction of the ozone molecule with the unsaturated bond of the organic compound occurs in three ways. These reactions are *cycloaddition* due to the 1,3 dipole structure of ozone, and *electrophilic* and *nucleophilic* reactions, and usually occur in solutions containing organic pollutants (Gottschalk et al., 2000).The indirect reaction of ozone involves radicals. Indirect reaction in an ozone oxidation process can be very complex (Gottschalk et al., 2000). The first reaction that takes place is ozone decomposition which is accelerated by initiators. The mechanism can be divided in three different steps. First step is initiation which is formation of superoxide anion radical $(O_2^{\bullet -})$, second step is propagation which is formation of hydroxyl radicals and re-initiation of the chain reaction, and third step is termination which is re-formation of the superoxide anion radical.

*Initiation step***:** The first reaction is the formation of a superoxide anion radical $(O_2^{\bullet -})$ and one hydroperoxyl radical $(HO_2^{\bullet})$.

$$O_3 + OH^- \rightarrow O_2^{\circ -} + HO_2^{\circ} \quad (2.20)$$

$$HO_2^{\circ} \leftrightarrow O_2^{\circ -} + H^+ \quad (2.21)$$

*Propagation step***:** Second reactions form the ozonide anion radical $(O_3^{\bullet -})$

$$O_3 + O_2^{\circ -} \rightarrow O_3^{\circ -} + O_2 \quad (2.22)$$

$$HO_3^{\circ} \leftrightarrow O_3^{\circ -} + H^+ \quad (2.23)$$

$$HO_3^{\circ} \rightarrow OH^{\circ} + O_2 \quad (2.24)$$

$$OH^{\circ} + O_3 \rightarrow HO_4^{\circ} \quad (2.25)$$

$$HO_4^{\circ} \rightarrow O_2 + HO_2^{\circ} \quad (2.26)$$

Following the formation of hydroperoxide radical ($HO_2^{\bullet}$), the chain reaction can start again (see the initiation step).

Termination step: Third reactions between some organic or inorganic compounds with OH° to produce radicals that do not lead to the formation of $HO_2^{\circ}, O_2^{\circ -}$ and thus the initiation step is blocked.

$$OH^{\circ} + CO_3^{2-} \rightarrow OH^{-} + CO_3^{\circ -} \quad (2.27)$$

$$OH^{\circ} + HCO_3^{-} \rightarrow OH^{-} + HCO_3^{\circ} \quad (2.28)$$

$$OH^{\circ} + HO_2^{\circ} \rightarrow O_2 + H_2O \quad (2.29)$$

2.3 Comparison of different Advanced Oxidation Processes

It is worth comparing different AOP processes in order to evaluate relative merits of each, although different processes will respond differently depending on the nature of the compounds that are present in a given water.

Ultraviolet light with ozone enhances not only the rate of complete destruction, but also the range of compounds attacked. Basically the systems are aqueous and saturated with ozone, and are irradiated with UV light of 254nm wavelength (photolysis).

Corresponding oxidative degradation rates are much higher than those observed in experiments where either UV light or ozone has been used separately (Legrini et al., 1993). However, the most serious and specific problem is the low ozone solubility in water.

The mechanism by which UV/H_2O_2 breaks down organic molecules is similar to that for UV/O_3. The absence of ozone is attractive, because both capital and operating costs

associated with ozone generation on site are reduced. This process has several advantages including:

i. The oxidant is commercially available.

ii. Hydrogen peroxide can be stored on site and it is thermally stable.

iii. Hydrogen peroxide is infinitely soluble in water.

2.4 Photocatalysis

As outlined earlier, a photocatalytic process is among the group of processes called Advanced Oxidation Processes (AOPs). In AOPs, highly reactive radicals, principally hydroxyl radicals ($HO^{\bullet}$), are produced and these radicals can mineralise organic compounds to carbon dioxide, water and mineral acids. In general AOPs can be categorized into two groups: homogeneous and heterogeneous processes. In homogeneous reactions, hydrogen peroxide, ozone and/or UV lights are utilised while in heterogeneous processes photoreactive semiconductors such as titanium dioxide TiO_2 are employed. In comparison with homogenous reactions, the use of heterogeneous reactions has several advantages, including the capability of mineralisation of a wide range of organic compounds, the possibility of reuse of photocatalysts, and the utilisation of solar light to excite the catalysts. Moreover, as oxidation and reduction reactions simultaneously occur in the photocatalytic process, organic and inorganic pollutants can be treated at the same time.

2.4.1 Heterogeneous Photocatalysis

Heterogeneous Photocatalysis has been examined and explored extensively as a potentially viable alternative technology to classical "best" technologies for both environmental detoxification and for energy production (Shaw et al., 1992). Both fundamental and applied investigations have been pursued over the last two decades.

This technology employs illuminated semiconductor particulate materials, e.g. TiO_2, as photocatalysts to produce both reducing and highly oxidizing species on the particle surface poised to unleash redox processes in aqueous media, many of which would not otherwise be possible by normal chemical means. Indeed heterogeneous photocatalysis has seen its initial development with the several studies in the late 1970s to early 1980s (Diffey and Robson 1989) which explored ways to photogenerate clean alternative fuels (e.g. dihydrogen from water) with the realization that processes carried out with organized assemblies afforded some advantages over homogeneous processes.

Semiconductor materials provided several interesting features toward this end, not least of which was chemical stability and the possibility to modify the semiconductor particle surface, itself possessing good catalytic characteristics, by addition of functional or bifunctional catalysts (e.g. Pt and RuO_2) to improve the overall catalytic functions and to accentuate process kinetics.

In the last two decades Serpone's laboratory has made significant contributions to heterogeneous photocatalysis both in (a) demonstrating the general usefulness of photocatalysis (Knowland et al., 1993) and in its development (Gulston and Knowland, 1999) toward a viable technology with potential attributes in energy conversion and in resolving environmental issues, together with (b) efforts to unravel and understand the events occurring at the particle surface and at the particle/solution interface by application of various time-resolved methods (e.g. picosecond laser spectroscopy (Damiani et al., 1999) and pulse radiolysis (Turro, 1978).

Several issues hampered the progress in the fundamental understanding and the underlying issues of heterogeneous photocatalysis with semiconductor particulates (Chignell et al., 1980): namely, the description of such terms as (i) photocatalysis (i.e., what is photocatalysis?), (ii) turnover quantities (viz, turnover numbers, turnover rates

and turnover frequencies; liberally used but too often incorrectly), (iii) quantum yields (here also too often misused), and (iv) the utilization of the Langmuir-Hinshelwood kinetic model to describe the mineralization process kinetics and to associate it automatically as a proof of concept or notion that reactions take place at the surface of the photocatalyst particle without any corroborating independent evidence to that effect. In fact, for item (iv) it is to note briefly that process kinetics, as too often reported in heterogeneous photocatalysis, are model independent and are simple manifestations of saturation-type kinetics commonly observed even in homogeneous phase processes.

Much of the discussions in the 1990s on the heterogeneous photocatalytic mineralization of organic contaminants, mediated by titania particulates (mostly in the anatase form), centered on the mechanistic details to improve the photocatalytic activity of the photocatalyst, and to understand the role and importance of free versus surface-bound oxidizing radicals (e.g., $^{\bullet}OH$ radicals) on the one hand and direct hole oxidation on the other. It was clear by the mid-1990s that if the potential of TiO_2, as the photocatalyst material in photocatalytic processes was to be maximized, a better understanding of the chemical nature of the photogenerated electrons and holes, and of the roles these species played in heterogeneous reactions at the TiO_2/solution interface was required. Despite the many efforts since the early 1990s (Sawyer, 1991), the mechanistic details of the photocatalyzed oxidative degradation of organic substances remains nonetheless a matter of current debate.

2.4.1.1 Photocatalytic Reactions

The majority of work concerning the environmental applications of heterogeneous photocatalysis has focused on the remediation of polluted water streams. Reactions in the aqueous phase can be more complex than those found in the gas phase due to the

additional variables (e.g. pH, concentration of photocatalyst, and partial pressure of dissolved oxygen) that must be accounted for and carefully controlled. Despite these additional factors in aqueous reactions, the initial process of band gap excitation generating electrons in the conduction band (possessing reducing power) and holes in the valence band (possessing oxidizing power) are essentially the same as those for reactions in the gas phase. In both aqueous and gas phase, the charge transfer reactions that follow band gap excitation are still unclear and a matter of controversy.

Aqueous remediation schemes have demonstrated the complete or partial mineralization (i.e. conversion of organic contaminants to inorganic compounds such as CO_2 and H_2O) of literally hundreds of different organic compounds. Chlorinated and unchlorinated alkanes and alkenes, aliphatic and aromatic alcohols and carboxylic acids, dyes, PCBs, surfactants and pesticides have been shown to oxidatively degrade in illuminated aqueous suspensions of TiO_2, and much of the published work has been reviewed **(**Linsebigler et al., 1995 and Hoffmann et al., 1995).

Many inorganic compounds (ammonia, cyanide, and phosphates) are also subject to oxidative degradation at semiconductor surfaces in the aqueous phase (O'Shea et al., 1997). Wastewater containing heavy metal ions (e.g. Pt) is also effectively remediated through heterogeneous photocatalysis via reductive deposition mechanisms (Ollis et al., 1991).

Based on the above literature survey this work will focus on using TiO_2/UV to degrade a range of chemicals including an azo dye (RO16), triclocarban, clopyralid and endocrine disruptors.

2.5 Semiconductors used as photocatalysts

Titanium dioxide TiO_2 is the semiconductor most commonly used in photocatalytic processes. However, due to its wide band gap, TiO_2 absorbs only UV light, limiting its

practical applications if sunlight (less than 5% of UV light in the solar spectrum) is to be utilised. Besides TiO_2, there are several chalcogenides (oxides and sulfides) that have been investigated for photocatalytical processes. Theses are semiconductors such as ZnO, WO_3, CdS, ZnS and iron oxide. However, they all suffer shortcomings compared to TiO_2. ZnO (Eg = 3.2 eV) is unstable in aqueous solutions, while CdS (Eg = 2.4 eV) and ZnS (Eg = 3.6 eV), when illuminated with light, suffer from photoanodic corrosion.

2.6 Light and energy

Light is transmitted in discrete packets of energy (photons) and has a frequency and wavelength. The relationship between these two properties is given by the Plank Law of Radiation:

$$u = h\nu = hc/\lambda \tag{2.30}$$

$$U = N_A h\nu = hcN_A/\lambda \tag{2.31}$$

where u is the energy (J) of one photon, ν is the frequency (s^{-1}), λ is the wavelength(m), c is the speed of light (2.9979×10^8 m s^{-1}) in vacuum, h is Planck's constant (6.6261×10^{-34} J. s), N_A is the Avogadro number (6.02214×10^{23} mol^{-1}), and U is the energy per einstein (one mole of photons). Using these two equations, the photochemical effects of light could be better understood.

2.6.1 Photochemical wavelength range

Generally, photochemical reactions are carried out in the wavelength range of 100~1000nm. The energy of light with wavelengths longer than 1000nm is too low to induce the chemical change, while the ionization and molecular

disruptions prevail if the species absorb the high energy from photons with wavelengths shorter than 100nm. Based on the forms of energy, the total photochemical wavelength range is divided into bands with specific names as shown in Table 2.2 (Bolton, 1999).

Table 2. 2: Spectral ranges of interest in photochemistry.

Range name	**Wavelength range (nm)**
Near infrared	700 ~1000
Visible	400 ~ 700
Ultraviolet	
UVA	315 ~ 400
UVB	280 ~ 315
UVC	200 ~ 280
Vacuum ultraviolet (VUV)	100 ~ 200

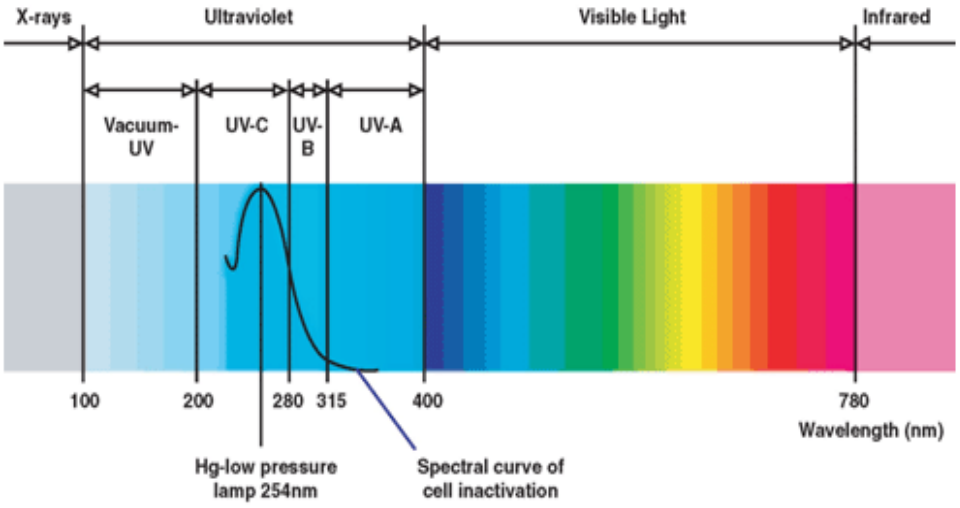

Figure 2. 3: The Electromagnetic Spectrum.

In near infrared range, only some photosynthetic bacteria can initiate the reaction. Most of the photosynthesis in green plants and algae is occurred in the visible light range. Photoreactions of interest are mainly involved in the UV range. According to the human skin's sensitivity to UV light, three sub-ranges are classified Figure 2.3. The UVA range causes the sun tanning, while UVB range can cause sun burning that then eventually induces skin cancer. The UVC range is also called the germicidal range, since it is very effective to kill bacteria and viruses. The vacuum UV range is absorbed by almost all substances, including water and air; it therefore only can be transmitted in the vacuum.

2.6.2 Light sources

In this section, several lamps mostly employed in photochemistries are introduced Jagger (1967), especially those in the field concerned with the present study.

2.6.2.1 Mercury Arc Lamps

The low-pressure mercury lamps contain mercury vapor that is at very low pressure (10^{-3} mmHg) and are operated at room temperature. Under appropriate voltage, the filament generates electrons that can be accelerated by the voltage across the tube. Some of these electrons collide with mercury atoms and produce positive mercury ions. Then the electrons and positive ions excite other mercury atoms by collision to cause them emitting photons. The main emission lines from the low-pressure mercury lamps are centered at 253.7nm and 184.9nm, due to the transitions from the excited states to the ground state in mercury atoms:

$$Hg\left(^3P_1\right) \rightarrow Hg\left(^1S_0\right) + h\nu \quad (2.32)$$

$$Hg\left(^3P_1\right) \rightarrow Hg\left(^1S_0\right) + h\nu' \quad (2.33)$$

When the low-pressure mercury lamp has the envelope from regular quartz, the output is exclusively centered at 253.7nm. Such lamp is also called germicidal lamp since it is effective in inactivating bacteria and viruses, and it also has been widely employed in the UV/H_2O_2 process.

When the mercury pressure in the lamp increases to 1 atm, the lamp is referred to as the medium-pressure lamp. The principal emission of mercury atoms is then reversed as a result of absorption by relatively cool mercury vapor far away from the electrodes, and a broaden emission is produced. The medium-pressure lamp still emits a discrete line spectrum but with a broaden range including the lines in the far- and near- UV regions, and with the maximum emission at 365nm.

The high-pressure arc mercury lamp is the most intense sources of UV radiation. With the increasing of mercury pressure in lamp (several hundred atmospheres), the pressure and operating temperature are raised, which produces a continuous background radiation between the discrete emission lines. The output of the high-pressure lamp is about 10 times of that from the medium-pressure lamps and about 1000 times of that from low-pressure lamps, per unit length of arc. The continuous spectrum makes the high-pressure lamps more versatile since any wavelength may be obtained. However, the emission at 253.7nm in the high-pressure lamps is rather low.

2.6.2.2 Fluorescent Lamps

Fluorescent lamps are good sources for near UV application. This lamp is manufactured by coating a phosphor layer on the inside surface of the low-

pressure mercury lamp envelope, which is excited by the irradiation and fluoresces in the near UV and visible range. The special glass envelope permits only the near UV light to escape from the tube. The range of the lamp output is 300~400nm, and the maximum output is around 360nm. Fluorescent lamps are suitable in the UV/TiO_2 application.

2.6.2.3 Xenon Arc Lamps

Another powerful source of near UV light is the high-pressure xenon arc lamp. This lamp provides a spectrum that is continuous and smooth, which is a good complementary source to the high-pressure mercury arc lamps. Furthermore, unlike the mercury arc, the xenon arc is more stable and easy to operate.

2.6.3 Measurement of Light

Two classes of the light measurement techniques are introduced here: physical and chemical methods. In the physical techniques, the physical effects of the irradiation are measured and converted into a form that causes a change in a measuring device. Radiometer is such a device that senses the total incident irradiance on a detector element. There are two types of light detectors: thermal and photonic (Bolton, 1999).

The thermal radiometer is the device containing a thermopile, an assembly of thermocouples connected in series (Wayne, 1988), to convert all the energy of incident light into heat and to produce a current proportional to the incident irradiance. Light is a form of energy and it may be degraded to heat. If light falls on a black surface, the temperature of the surface will rise, and the temperature increasing can be measured by the thermopile. The thermopile

can achieve the complete absorption of irradiation, regardless of wavelength; hence the thermal detector performs the most reliable measuring of light in the absolute sense and can be used as a standard to calibrate other types of detector.

Thermopiles are very sensitive to the IR emission. Therefore, care must be taken in the measuring since all near room temperature objects, including people, emit significant IR. In the photochemical experiments, it is more convenient to use a photocell to measure the light intensity. The photonic radiometer detector is such a device consisting of a photocell (Bolton, 1999), where the light is absorbed by the semiconductor material, which comprises of P-type and N-type semiconductors with different electrical properties between metal electrodes. Once the negative electrons and positive holes are produced in the semiconductors, the electrodes subsequently convert the incident photon flow into the electrical current. These detectors are highly sensitive but wavelength-dependent. If the incident light is monochromatic, the conversion is easily achieved. However, for a broadband light source, the spectral distribution of the source and the spectral sensitivity of the detector are required in order to convert the radiometer reading into the true values.

Another alternative approach to determine the light intensity is to measure the rate of a photochemical reaction for which the quantum yield is accurately known. This kind of chemical systems is referred to as chemical actinometer. Chemical actinometers are chosen for their insensitivity to wavelength and the experimental parameters. There are three common actinometers that are important to UV application: ferrioxalate actinometer, persulfate actinometer, and iodide/iodate actinometer. The reactions related to these actinometers are shown as follows (Bolton, 1999):

$$Fe(C_2O_4)_3^{3-} + hv \rightarrow Fe^{2+} + 2.5C_2O_4^{2-} + CO_2 \quad (2.34)$$

$$S_2O_8^{2-} + hv \rightarrow 2SO_4 \bullet^- \quad (2.35)$$

$$SO_4 \bullet^- + (CH_3)_3COH \xrightarrow{O_2} H^+ + SO_4^{2-} + organic\ product \quad (2.36)$$

$$8I^- + IO_3^- + 3H_2O + hv \rightarrow 3I_3^- + 6OH^- \quad (2.37)$$

2.7 Titanium dioxide as a photocatalyst

Titanium is the ninth most abundant element in the earth's crust; this study focuses on titanium dioxide (TiO_2) used as a photocatalyst. There are many commercial uses of TiO_2, these include application as an opaque white pigment, for which use, over half of the world's production of TiO_2 is employed, and as a tiller in plastics and rubber (Diebold, 2003).

Titanium dioxide has the formula TiO_2 and has three solid phases, all occurring naturally:

I. Anatase (Figure 2.4-a) has a tetragonal crystal structure that is slightly less ordered than rutile. It transforms to rutile at approximately 750^oC, although very pure anatase is more difficult to convert, retaining the anatase form until 800^oC (Hanley et al; 2002). This transformation is believed to occur at the surface of the particles. Anatase is the most widely used form of TiO_2 for catalytic purposes. Each Ti^{4+} ion is surrounded by a distorted octahedron of six O^{2-} ions. Commercially, anatase is the preferred form for use in the paper, ceramics, rubber, food and cosmetics markets.

II. Rutile (Figure 2.4-b) can be found naturally in relatively pure form containing about 95% TiO_2. It has a tetragonal lattice crystal structure. It is thermodynamically more stable than anatase by approximately 10 kJ mol^{-1} and can be formed as the initial

crystalline product of hydrolysis of chloride solutions (Jayanty, 1972) Each Ti^{4+} ion is surrounded by an irregular octahedron of six O^{2-} ions with a slight orthorhombic distortion. Commercially, rutile is the preferred form of TiO_2 used in the coatings and plastics industries.

III. Brookite (Figure 2.4-c) although naturally occurring it is quite rare in comparison and is generally overlooked due to its low stability and difficulty in preparation. Brookite has an orthorhombic crystal structure and it can be prepared by hydrothermal method.

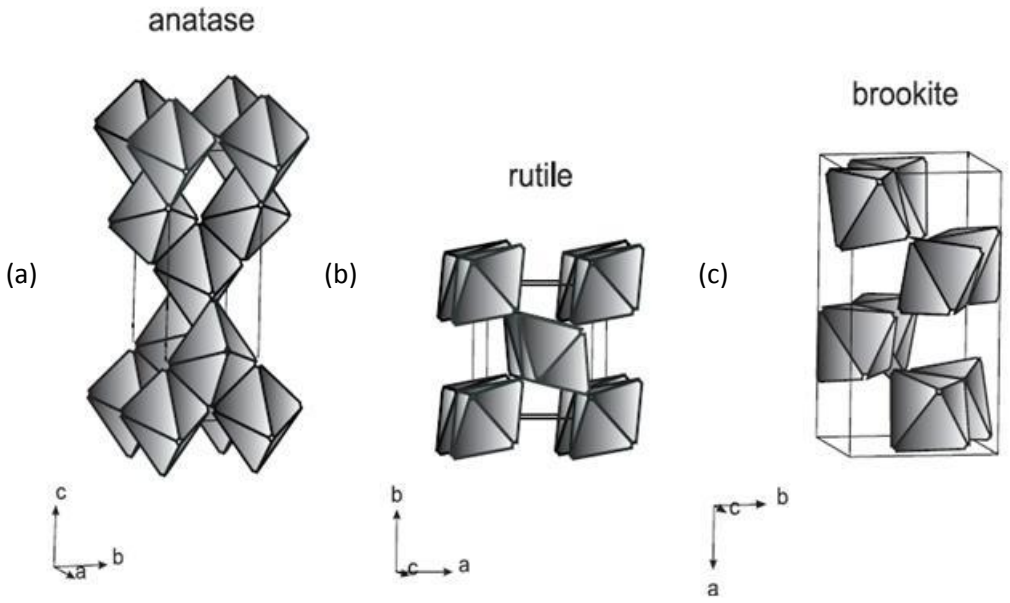

Figure 2. 4: Illustrations of TiO_2 crystalline structures: anatase, rutile and brookite.

2.7.1 Photocatalytic Properties of Titanium Dioxide

Titanium dioxide is one of the most widely used metal oxides in industry. It is applied as a catalyst support and as a catalyst. It is also used as a pigment material, as its high refractive index in the visible range allows preparation of thin films.

Titanium dioxide generally exhibits the highest photocatalytic activity of the photocatalysts. Other semiconductors that can be used as photocatalysts are ZnO, CeO_2, CdS, ZnS, WO_3, etc. However, these semiconductors are not as attractive for photocatalytic oxidation as TiO_2: it is biologically and chemically inert, inexpensive and resistant to photocorrosion and chemical corrosion (Carp et al., 2004). Only ZnO has shown comparable activity (Bahnemann et al., 1991). For this reason the use of other semiconductors in environmental studies is rather limited (Hoffmann et al., 1995).

The photocatalytic efficiency of TiO_2 is dependent on crystal structure, particle size and surface area. In most cases, anatase is the most active crystal form, it is thermodynamically less stable than rutile, but its formation is kinetically favoured at lower temperatures (<600°C). The lower temperature of crystallization of TiO_2 may explain its higher surface area and a higher surface density of active sites for adsorption and catalysis (Herrmann, 1999). Photocatalytic oxidation process effectiveness is governed by the catalyst lifetime and recombination probability of the electron-hole pair. Therefore, anatase is often mixed with rutile, a less catalytically active form, to reduce the rate of recombination of the electron-hole pair (Bhatkhande et al., 2002; Dalrymple et al., 2007). The band gap of anatase is 3.2 eV and it absorbs photons within the near UV range (~380 nm) of the electromagnetic spectrum. However, solar radiation starts at a wavelength of about 300 nm at ground level. Thus, 4-5% of the solar energy reaching the surface can be utilized in photocatalytic oxidation with TiO_2 as the photocatalyst (Zhang et al., 1994).

2.8 Commercially available photocatalysts

The production of titanium dioxide as a photocatalyst is quite limited. Some commercially available photocatalysts include Hombikat UV 100, supplied by Sachtleben Chemie (Lindner et al., 1995), while Degussa P25 is one of the most

commonly recognisable photocatalyst (Levy, 1997). Table 2.3 shows physical characteristics of Degussa P25 and Hombifine N.

Table 2. 3: Relevant physical characteristics of Degussa P25 and Hombifine N.

Catalyst	Hombifine N	Degussa P25
Phases	Anatase%100	Anatase 75%, Rutile 25%
BET (m^2g^{-1})	317	51
Porosity (nm)	Mesopores, ϕ =5.6	Non-porous
Primary crystal size (nm)	≈ 5	≈ 25
Pore volume (cm^3g^{-1})	0.38	0.36

Note: a: adopted from Mills and Le Hunt (1997).

2.8.1 Other applications of TiO_2 photocatalysis

TiO_2 has been applied to various photocatalytic processes in a broad range of application areas. The primary application of TiO_2 photocatalysis lies in water treatment (the mineralisation of organic pollutants in water) (Heintz et al., 2000; Taborda et al., 2001). Other applications include destruction of air pollutants (Fujishima et al., 2000), photocatalytic splitting of water using solar energy conversion based on dye sensitization (Kavan et al., 2001), self cleaning window materials (Yu et al., 2002) and, removal of inorganic pollutants, destruction of bacteria and viruses (Lee et al., 2000). In addition, application of TiO_2 photocatalysis in the analysis of total organic carbon (TOC), the use in the HPLC for analysis of organic compounds and indirect use in the analysis of chemical oxygen demand (COD) (Kim et al., 2000).

2.9 Catalyst recovery

After the photocatalytic degradation reaction, the catalyst has to be reclaimed but in many processes the recovery is not usually addressed because of the particle size of the catalyst which is normally within the nano-size range. There is a range of separation techniques used for catalyst recovery. These techniques are discussed in the following paragraphs.

2.9.1 Gravity sedimentation

Gravity sedimentation is a process to separate or concentrate suspended solid particles partially from liquid by gravity settling (Dahlstrom et al., 1997). Sagawe et al. (2001) have used a batch operation for photocatalytic treatment during the day, with the catalyst settling in a tank overnight. However, this method needs a relatively large reactor and tank, and this process is not continuous. Sedimentation of small particles can be very slow, and convection currents can disturb sedimentation.

2.9.2 Coagulation

Coagulation is a process that brings particles into contact to form agglomerates (Svarovsky, 2000a). Bekbolet (2001) has reported using Fe (II) to coagulate TiO_2 particles in order to increase titanium dioxide removal efficiency. However, this method has the problem that iron affects the water product, as would any other additive.

2.9.3 Magnetic particles of TiO_2

Any particle introduced into a magnetic field becomes magnetized to some extent and acts as a magnetic dipole (Sastry et al., 1997). Jefferson et al. (2001) have discussed using magnetic iron particles to increase the density of TiO_2, and then these particles

can be separated by a magnetic drum separator. However, for fine and weakly paramagnetic particles, sush as titanium dioxide, the capital cost is very high. So only large installations are economically attractive (Svarovsky, 2000a). In addition, it is difficult to recycle TiO_2 particles after they are magnetized because of redispersion problems.

2.9.4 Filtration

Filtration is a separation process of a solids-liquid mixture through a permeable medium that retains the solids and allows the liquid to pass. Filtration equipment retains most of the particles that must be separated. Filtration is convenient and reasonable for continuous operation but many moving parts are subject to wear. The rotary drum filter is the most widely used of the continuous filters.

2.10 Influence of physical parameters affecting photocatalytic reaction kinetics

2.10.1 Catalyst Concentration

The reaction rates have been found to be proportional to the concentration of catalyst in the system, either in static or in slurry photoreactors (Herrmann, 1999). However, the reaction rate levels off or become independent when the catalyst concentration reaches a certain limit (Pareek et al., 2001; Park et al., 2003). This limit depends on the catalyst characteristics, light intensity, and the geometry and working conditions of the photoreactor. It has been reported that the relationship between initial rate and catalyst concentration had similarities with Langmuir type behaviour (Terzian et al., 1995).

2.10.2 Temperature

Photocatalytic systems are operated at room temperature and do not normally require heating. Cooling is necessary when the higher power lamp is used. It has been reported that reaction rate did not change significantly with temperature and a suitable operating temperature is generally between 15ºC and 80ºC (Herrmann, 1999).

2.10.3 UV Light intensity

The rate of reaction has been found proportional to UV light intensity (I); however above a certain value (the value is very variable), the rate shows lesser dependency (Martin et al., 1996; Herrmann, 1999; Park et al., 2003). Many authors suggest that the dependence of rate on light intensity follows an I^f relationship and exponent f changes from 1 at low intensity, 0.5 at intermediate intensity and 0 at high intensity. The transition region varies. The data of Terzian et al., (1995) showed a Langmuir type behaviour suggesting that light absorption creating electron/hole pairs is a similar process to pollutant adsorption on the catalyst surface.

2.10.4 pH value

It has been reported that photocatalytic reaction is faster in alkaline media than in acid media (Terzian et al., 1995). On the other hand, some researchers have claimed that reaction rate achieves a maximum near the point of zero charge of titanium dioxide (pzc≈6.35), (Preocanin and Kallay 2006 ; Poulios et al., 1999). Few studies have shown that there is no significant change in the rate of reaction over quite a wide range of pH (Rao et al., 2003). Point of zero charge is the pH at which the charge on a semiconductor surface is zero, and it means that at this pH the surface is electrically neutral (Serpone et al., 2002). It is possible that more hydroxyl radicals are produced over the surface of TiO_2 when pH is increased (Doong et al., 2000). Although alkaline

media may seem more favourable for the photocatalytic reaction, it is not necessary to make effluent more alkaline because it is an added expense. A neutral effluent is favoured to protect equipment mainly from corrosion in an industrial application.

The surface charge, particle size and band edge position of TiO_2 are strongly influenced by pH. pH controls the protonation state of the surface hydroxyl groups on TiO_2, which is governed by the following acid-base equilibria (Equations 2.38 and 2.39).

$$> TiOH_2^+ \leftrightarrow > TiOH + H^+ \quad (2.38)$$

$$> TiOH \leftrightarrow > TiO^- + H^+ \quad (2.39)$$

In addition, the band edge energy or flat band potential of TiO_2 will change with pH and thermodynamically this change would lead to a change in the oxidation power (Lindner et al., 1995). pH can also influence the energy of the conduction and valence bands of the semiconductor. Furthermore, pH also affects the size of the semiconductor aggregates (Mills and Le Hunt, 1997).

2.11 The Studied Pollutants

Six pollutants of concerns have been studied in this project. These pollutants are a reactive azo-dye (RO16), a disinfectant triclocarban (TCC), a herbicide clopyralid (3, 6-DCP) and endocrine disruptors [estrone (E1), 17β-estradiol (E2) and 17α-ethinylestradiol (EE2)]. Background information related to each of them and the reasons behind their choice are presented in the following paragraphs.

2.11.1 Reactive Orange 16

The removal of colour from the wastewater coming from different industries is a current issue of discussion and regulation all over the world (Da Silva and Faria, 2003). Dyes are used in many industries like textile, paper, plastic, leather, ceramic, cosmetics, ink, food processing etc. (Sharma et al., 2002). There are many classes of dyes such as

acidic, basic, neutral, azo, disperse, direct, reactive etc. Out of these dyes azo dyes are most frequently used. These contain one or more azo bonds $(-N=N-)$ in their structure (Stylidi et al., 2004). Some of these dyes are toxic and potentially carcinogenic. About 15% of dyes of the total world production are lost during synthesis and carried away in the wastewater. Several studies on the physical, chemical and biological degradation of dye containing wastewaters have been reported in the literature (Chang and Lin, 2000; Mccallum et al., 2000). Physical methods do not degrade the pollutants but they only transfer them from the liquid phase to the solid phase, thus causing secondary pollution. Chemical methods have been proved to be expensive as they require high dosage of chemicals and produce large quantity of sludge. Biodegradation of dyes has been shown to be ineffective (Wong et al., 2003).

Heterogeneous photocatalysis has been used in the recent years as a promising method for the removal of toxic organic and inorganic contaminants from industrial wastewater, since it does not only degrade the pollutants but also causes their complete mineralization to CO_2, H_2O and mineral acids (Xu and Langford, 2001).

In general, azo dyes are the most commonly used commercial dyes in the textile industry, accounting for over 50% of all commercial dyes. A large amount of azo dyes, however, remain in the factory effluent after the completion of the dyeing process and represent an environmental danger due to their refractory nature. The removal of azo dyes is important because many azo dyes are toxic to aquatic organisms (Sharma et al., 2003). Many physical and chemical methods including adsorption, coagulation, membrane process, oxidation– ozonation, and biological treatment have been used for the treatment of azo dyes (Walker et al., 2003).

Azo-dyes contain azo groups (-N=N-) mainly bound to substituted benzene or naphthalene rigs (Wu and Wang, 2001). Figure 2.5 shows the chemical structure of an

azo-dye which contains sulphonic acid groups that ensure both its solubility in water and its ability to dye wool, silk, nylon (polymide), cotton, cellulose acetate and other kinds of fibres.

However, the sulphonic acid group deactivates the structure with respect to an electrophilic attack and biological degradation that occur in common waste water treatment techniques (Liakou et al., 1997; Muthukumar et al., 2001). Therefore, the treatment of textile wastewater by conventional methods such as biological, physical and chemical processes or a combination of each is inefficient for colour removal. A direct solution to this problem is the treatment with advanced oxidation processes (AOP), such as O_3, pH>7; O_3/H_2O_2 or O_3/UV (Perkowski et al., 2000; Balcioglu et al., 2001 and Rivas et al., 2003). Studies on the degradation of azo-dyes using AOPs is very important. It is in this wider context that a reactive azo-dye (Reactive orange (RO16: $C_{20}H_{17}N_3Na_2O_{11}S_3$) was chosen in this study (CAS Number: 12225 -831-1 and Colour Index Number. 17757).

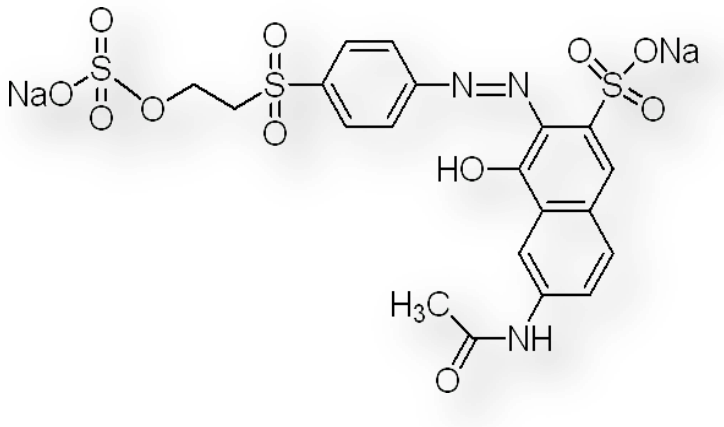

Figure 2.5: Molecular structure of dye (RO16).

2.12 Triclocarban

Triclocarban or 3-(4-chlorophenyl)-1-(3, 4-dichlorophenyl) urea (TCC) is a substance with antibacterial and antifungal properties. Hence it finds applications in disinfectants, detergents, cosmetics, soaps, etc. Although the disinfection mechanism is unknown, TCC may be involved in the inhibition of enzyme Enoyl-acyl carrier protein reductase (ENR). At lower concentrations, TCC provides bacteriostatic effect by binding to ENR. This enzyme is absent in humans but essential in building cell membranes of many bacteria and fungi. The data on the environmental impact of using TCC is very scarce. However, few studies have shown that the chemical is toxic to humans and other animals (Halden and Paull, 2005) since it increases methemoglobinemia. But still the use of TCC is not limited. For example, in 1998 and according to the summary report which was submitted by the US Environmental Protection Agency (EPA) estimated TCC production for the US market to approach one million pounds or about 454 metric tons per year, and the same report evaluates the maximum current use is estimated to about 750 metric tons per year (Sapkota et al., 2007).

Researchers have already found that 75 percent of Triclocarban originate from anti-microbial soaps which had been washed down from household drains persists during waste water treatment. The worse part is the accumulation of TCC at remarkable concentrations in the municipal sludge which may be used as a fertilizer and soil conditioner for crops. It is already known from literature that TCC-contained sludges treated biologically for an average period of three weeks showed negligible degradation. The continuous persistence of TCC in rivers and streams is really a major issue to the environment and mankind. TCC is a topical antiseptic but can end up in the food chain which is neither regulated nor monitored. The molecular structure of TCC is

shown in Figure 2.6. Treatment studies to remove the compound from water are scarce. In order to understand the behavioural degradation of TCC with photocatalysis this study was carried out. This work was thus concerned with the photodegradation of the TCC, which is not currently available in the literature.

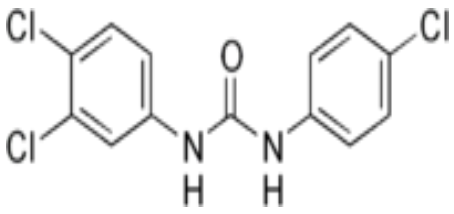

Figure 2. 6: Molecular structure of triclocarban.

2.13 Clopyralid

Clopyralid (3, 6-dichloro-2-pyridinecarboxylic acid, CAS No. 1702-17-6, $C_6H_3Cl_2NO_2$, M = 192 g/mol, its molecular structure is shown in Figure 2.7) is a selective herbicide, from the chemical class of pyridine compounds, used to control broadleaf weeds in certain crops and turf. It derives from the pyridine-carboxylic acid family and presents high solubility in water that increases with pH due to its ionisation. Clopyralid is particularly stable against hydrolysis and photolysis. Its chemical stability along with its mobility enable this herbicide to penetrate through the soil causing a long term contamination of the ground water as well as surface water supplies (Donald et al. 2007, Huang et al. 2004, Sakaliene et al. 2009). Due to these properties, clopyralid is one of the herbicides often reported to occur in drinking water. In a recent research, levels as high as 0.23 μg/L clopyralid in the final water have been reported in the UK, vastly exceeding the Permitted Concentration Value (PCV) for an individual pesticide of 0.1 μg/L (EU directive 98/83/EC). In North America, clopyralid has been detected in

reservoirs that received water from snowmelt and rainfall runoff from agricultural crop lands. It reached concentrations as high as 1050 ng/L (Donald et al. 2007). The mean annual concentration of clopyralid in drinking water was 24 ng/L and the maximum concentration detected in drinking water reached 393 ng/L (Donald et al. 2007). Because it is easily transported in the environment, clopyralid is of special interest since it presents potential for threatening the aquatic environment and human health. Moreover, the transport of clopyralid to agricultural areas sensitive to this herbicide, such as potato (Wall 1994), can lead to losses in the production yield causing economical losses. Clopyralid is also hazardous to certain endangered plant species and beneficial insects (Hassan et al. 1994).

Although the occurrence of clopyralid in surface, ground and drinking water is widely reported, there is only very few studies concerned with its removal in water (Ozcan et al. 2010, Sojic et al. 2009). Hence there is a need to develop effective purification methods for eliminating this herbicide from water. This study was therefore carried out to determine experimentally the effectiveness of three oxidation techniques namely: photocatalysis (UV/TiO_2), UV/H_2O_2 and ozone on the degradation of clopyralid in water. These oxidation techniques are generally characterised by a common factor, which is the generation of powerful oxidising species including hydroxyl radicals ($^{\bullet}OH$). Hydroxyl radicals, which are unselective, are powerful enough to oxidise almost all organic compounds in water. Several studies have already shown that a range of herbicides and pesticides can be degraded effectively, though at various rates, by ozonation (Benitez et al. 1994, Broseus et al. 2009, Hua et al. 2006, Ikehata and El-Din 2005a, Xiong and Graham 1992), photocatalysis (Muneer and Boxall 2008, Rajeswari and Kanmani 2009) and UV/H_2O_2 (Kruithof et al. 2002, Wu and Linden 2008).

The oxidation by ozone occurs generally through two possible mechanisms that depend on the operating conditions (e.g. pH; presence of radical scavengers such as carbonates and bicarbonates): (i) a direct mechanism, which is selective, involves reactions with molecular ozone and (ii) an indirect mechanism, which is unselective, involves reactions with hydroxyl radicals produced as a result of the decomposition of ozone in water by for example hydroxide ions (OH^-). On the other hand, photocatalytic reactions are based on the interaction between a photocatalyst (generally TiO_2) and the UV irradiation to produce electron-positive hole pairs on the surface of the photocatalyst. The organic compound reacts either directly with the positive hole or with the potent hydroxyl radicals produced by reactions between the positive holes and water or OH^- (Andreozzi et al. 1999). The mechanism of the UV/H_2O_2 system also involves hydroxyl radicals produced as a result of photolytic decomposition of hydrogen peroxide.

Daniela et al., (2009) identified the intermediates and reaction pathways of the photocatalytic degradation of clopyralid in the UV-illuminated aqueous suspensions of TiO_2 (Degussa P25) (Figure 2.8). They studied the effects of the substrate and catalyst concentrations, pH, temperature, hydroxyl radical ($OH^{\bullet}$) scavenger, as well as the effect of several electron acceptors on the rate of this degradation reaction. They also observed that the photodegradation of clopyralid was fastest at pH 3.2 because of the influence of various factors at the different pHs of the system. They found that the presence of ethanol as a scavenger of hydroxyl radicals inhibited the clopyralid photodecomposition, suggesting that the reaction mechanism involved free hydroxyl radicals.

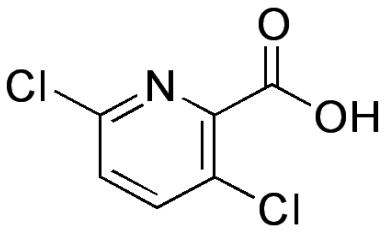

Figure 2. 7: Molecular structure of clopyralid.

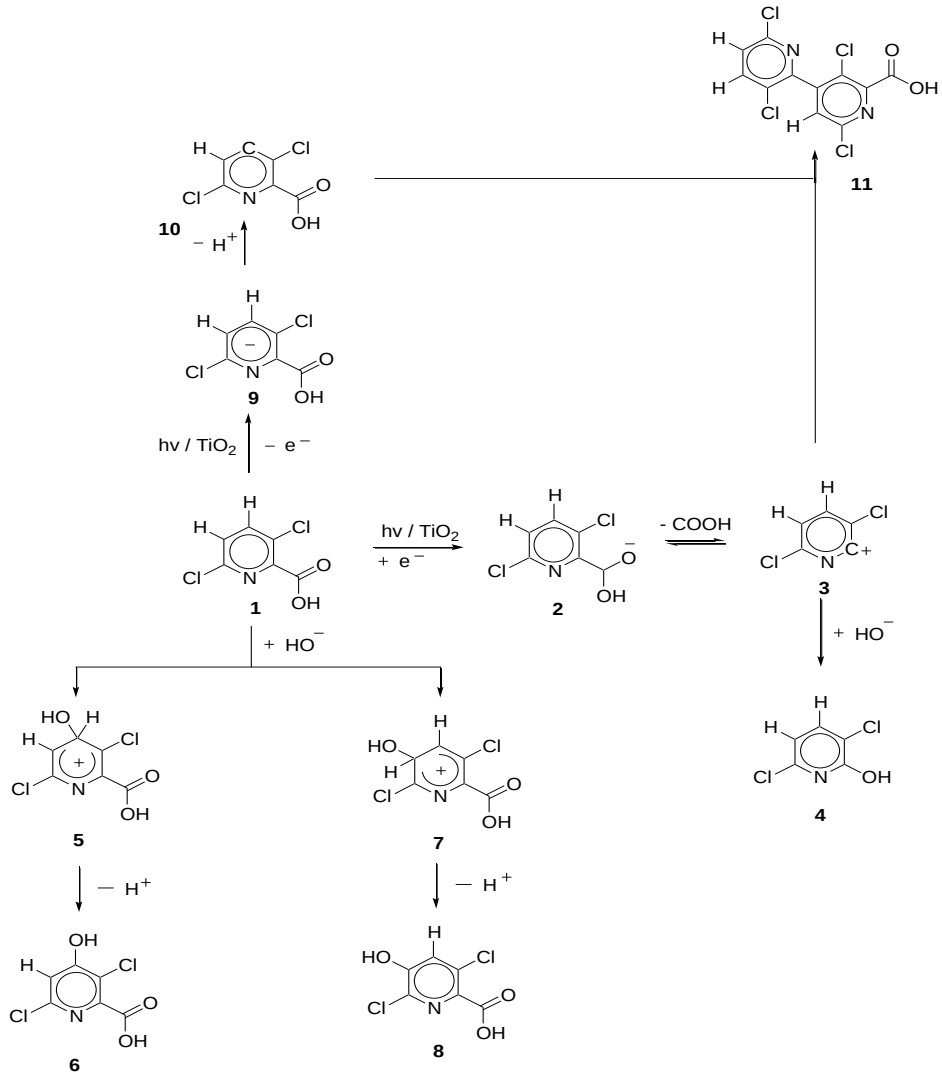

Figure 2. 8: Tentative pathways for photocatalytic degradation of clopyralid.

2.14 Endocrine Disrupting Chemicals (EDCs)

2.14.1 Nature of steroid estrogens

2.14.1.1 Natural estrogens

Although natural EDCs are present in both male and female organisms, they are usually present at considerably higher levels in females of reproductive age. EDCs play an important role in growth, development and puberty, and influence many body parts (skin, bones, arteries, brain) (Hess et al., 1997). In females, EDCs are involved in the development of secondary sex characteristics and in regulating the menstrual cycle and pregnancy. In males, the purpose of estrogen is to control certain functions of the reproductive system (maturation of sperm); it is also required for healthy libido (Stryer, 2000).

The amounts of natural EDCs vary depending on species, age, sex or reproductive stage. The three major naturally occurring estrogens in women are estrone (E1), 17β-estradiol (E2), and estriol (E3). E2, referred to as a “female” hormone but present in both females and males, is a most important estrogen in humans. It does not only have a vital impact on reproductive and sexual functions, but also affects other organs. In a female organism E2 is secreted by the ovaries and it is the primary estrogen until menopause. E2 levels vary through the menstrual cycle, with levels highest just before ovulation. E1 is formed from E2 and represents a weaker estrogen; it is predominant in postmenopausal women. There is also a group of compounds called phytoestrogens, natural plant chemicals generally found in food, which can have "estrogen like" effects in the body (Dictionary of Science and Technology, 1992).

2.14.1.2 Synthetic estrogens

Synthetically produced EDCs are used in pharmaceutics as part of birth control pills and other contraceptives and in some countries also for cattle hormonal growth promotion in farming. 17α-ethinylestradiol (EE2), a synthetic form of E2, is a main active component of hormonal contraceptives to prevent ovulation and, thus, pregnancy. Oral contraceptives contain between 30 and 50 μg of EE2 per pill (Desbrow et al., 1998). Synthetic EDCs are among the major types of hormones involved in hormone replacement therapy (Handbook of Chemistry and Physics, 1976).

2.14.2 Occurrence of EDCs in the aquatic environment

There are several sources and pathways for the exposure of EDCs to the environment, for example, wastewaters from production of synthetic EDCs in pharmaceutical industry and runoff waters from agriculture. Intensive farming with both natural and synthetic EDCs in its runoff waters also acts as a steroid estrogens contributor to environmental contamination with EDCs. However, the most important source of EDCs in the environment is domestic sewage. Natural EDCs together with the residues of synthetic ones, originating from contraceptives and other pharmaceuticals, are excreted by humans mainly through urine. Table 2.4 represents the approximated daily amounts of human excreted EDCs. The increasing amount of EDCs in domestic sewage is due to the growing world population and the increasing urbanisation and consequently consumption of synthetic EDCs.

Table 2. 4: Daily excretion (μg) of EDCs in humans (Johnson et al., 2000).

Category	E1	E2	EE2
Males	3.9	1.6	-
Menstruating females	8	3.5	-
Menopausal females	4	2.3	-
Pregnant women	600	259	-
Women (contraceptive)	-	-	35

The chemical structure of E1, E2 and EE2are presented in Table 2.5.

Table 2. 5: Structure and molecular mass of the EDCs studied in this project.

EDC	Structure	Molecular mass (g/mol)
Estrone (E1) - secreted by the ovary	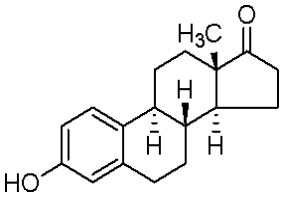	$C_{18}H_{22}O_2$ M=270.366
17β-estradiol (E2)	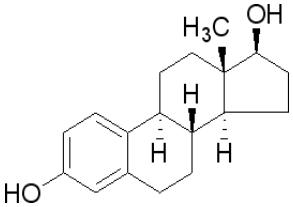	$C_{18}H_{24}O_2$ M=272.39
17α-ethinylestradiol (EE2) – synthetic	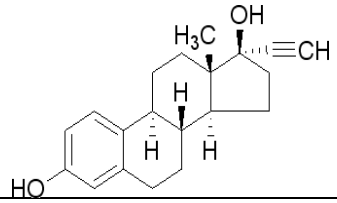	$C_{20}H_{24}O_2$ M=296.403

2.14.3 Health effects

The effects of EDCs on the endocrine system can result in health changes of the organism itself or might not be seen until the next generation. The development of embryos and foetuses are especially sensitive to disruption. Although trace amounts of EDCs do not affect adults, they can have a crucial impact on the developing embryo. The time of exposure is assumed to be more important than the dose (Ying et al., 2004). The observed impacts of EDCs on wildlife include hermaphrodite fish and polar bears, reproductive failure in birds and abnormalities in the reproductive organs of reptiles, amphibians and non-vertebrates (Jobling et al., 1998; Ahmed, 2000). The health effects on humans include reproductive abnormalities, effects on male to female ratio, decreased sperm counts and quality, both male and female fertility problems (reproductive function, miscarriage, ectopic pregnancy, stillbirth, premature birth), and an increase in certain types of male and female cancers (testicular cancer, prostate cancer, breast cancer), effects on brain and behaviour (Mendes, 2002;Ferguson, 2002).

2.14.4 Treatment of EDCs by advanced oxidation processes

While other treatment methods, particularly membranes, have been the focus of numerous studies regarding EDCs, the use of advanced oxidation processes (AOPs) involving ozone, hydrogen peroxide and ultraviolet radiation has gained attention in recent years; AOPs are felt to be particularly applicable to the treatment of micro-pollutants (such as EDCs) owing to their potential for complete degradation of the parent compound and its degradation products. As has been well established, the combination of O_3 with either H_2O_2, or UV, and H_2O_2 with UV, can provide very powerful oxidizing conditions as a consequence of the generation of OH radicals.

One study investigated the use of UV/H_2O_2 treatment to degrade EE2, and E2 (Rosenfeldt and Linden, 2004). It was found that an H_2O_2 dose of 15 mg L^{-1} and a UV fluence of 1000 mJ cm^{-2} degraded more than 95% of EE2, and E2, for both low- and medium-pressure lamps. Low-pressure UV lamps alone degraded 2% and 5% of EE2, and E2, respectively, while medium-pressure lamps alone degraded 21% and 18% of EE2, and E2, respectively. Hydroxyl radical rate constants for EE2 and E2 were found to be (1.02 - 1.08) $\times 10^{10}$ and 1.41 $\times 10^{10}$ M^{-1} s^{-1}, respectively. Quantum yields for the aforementioned compounds were 0.026 and 0.043 mol Es^{-1} respectively with low-pressure lamps, and 0.061 and 0.10 mol Es^{-1} respectively with medium-pressure lamps.

2.14.4.1 Photocatalytic degradation of EDCs

Many pharmaceuticals and EDCs undergo photolysis under typical sunlight conditions. Photolysis rates can sometimes be increased by exposing the contaminants to a UV light source; thus providing greater UV radiation intensity, or light at a shorter wavelength and higher energy. While the removal of micro-contaminants with UV-based treatment technologies has been studied for application in the treatment of drinking water, there have been few studies on the use of these technologies for the treatment of wastewater.

Liu and Liu (2004) found that direct photolysis with UV at 254 nm and >365 nm were effective at degrading natural estrogens (i.e. 17-β-estradiol, estrone) in water.

Poulopoulos et al. (2006) monitored the degradation of phenol under direct photolysis at 254 nm and by treatment with UV/H_2O_2, and observed that addition of H_2O_2 produced 50% removal after 10 minutes and total removal after 30 minutes. Rosenfelt and Linden (2004) found that bisphenol A, ethinylestradiol and estradiol were removed at efficiencies of less than 5% with UV irradiation at 254 nm, but removals were increased to 90-99% when the water was irradiated with addition of 15 ppm H_2O_2. Vogna et al. (2004a) reported that the anti-epileptic drug, carbamazepine is completely removed

from water within 4 minutes under UV light (254 nm) with addition of H_2O_2 and Vogna et al. (2004b) found nearly complete removal of the anti-inflammatory drug, diclofenac from water within 90 minutes using irradiation with UV light (254 nm) and H_2O_2. Andreozzi at al (2003) observed 93% removal of clofibric acid (i.e. lipid regulating drug) from water after 60 minutes under UV light (254 nm) with H_2O_2. Thus, UV irradiation with the addition of H_2O_2 appears to be a promising technique for removal of micro-contaminants from water, but the efficacy of these technologies has not been fully investigated for the treatment of wastewater.

Mazellier et al. (2008) studied the photochemical transformation of natural estrogenic steroid 17β-estradiol (E2) and the synthetic oral contraceptive 17α-ethinylestradiol (EE2) in dilute non buffered aqueous solution (pH 5.5 – 6.0) upon monochromatic (254 nm) and polychromatic (k > 290 nm) irradiation. Upon irradiation at 254 nm, the quantum yields of E2 and EE2 photolysis were similar and evaluated to be 0.067 ± 0.007 and 0.062 ± 0.007, respectively. Upon polychromatic excitation, and by using phenol as chemical actinometer, the photolysis efficiencies have been determined to be 0.07 ± 0.01 and 0.08 ± 0.01 for E2 and EE2, respectively. Most of these studies focused on the photodegradation of one component in water and studies on multicomponents are almost nonexistent. This work was thus concerned with the photodegradation of a multicomponent system of EDCs involving E1, E2 and EE2, which is not currently available in the literature.

2.14.4.2 Ozonation of EDCs

For comparison purposes, the ozonation of multicomponent EDCs was also studied in this project. Background information on the ozonation of EDCs is presented in the following paragraphs.

Recently numerous studies have been carried out for the removal of EDCs using ozonation (Feng 2005; Yue 1992; Chu 2007; Bila 2007; Auriol 2006; Ning 2007; Deborde 2005; Kim 2008; Nakonechny 2008 and Irmak 2005). The rates of reaction of E2, EE2 and E1 with ozone are investigated by Deborde (2005) and Nakonechny (2008). It was found that at a pH range of 2.5-10.5 and 20 ^{o}C with t-butanol alcohol as a radical scavenger, the second order rate reaction of ozone with ionised EDCs was almost 10^{9} (mol/L.s) but was found to be 10^{4}-10^{5} times higher than with neutral EDCs. The observed pseudo-first order reaction kinetics was justified through combined direct ozone and indirect radical oxidation mechanisms. The degradation of EDCs increased with the increase of the solution pH (Chu, 2007). The pH effect on ozonation is considered to be responsible to the observed difference in rate constants. It was also noted that both direct and indirect ozone reactions are dependent on pH (Hai-yan 2006).

The degradation products following oxidation of E1 and E2 by ozone has been reported by Ning (2007). By analysis, two products were identified (Product 1 and 3), which are shown in Figure 2.9 (Huber et al., 2004). Product 3 was expected to be a decomposition product of the intermediate Product 2, and the cyclohexanedione moiety could be reduced to form Product 4.

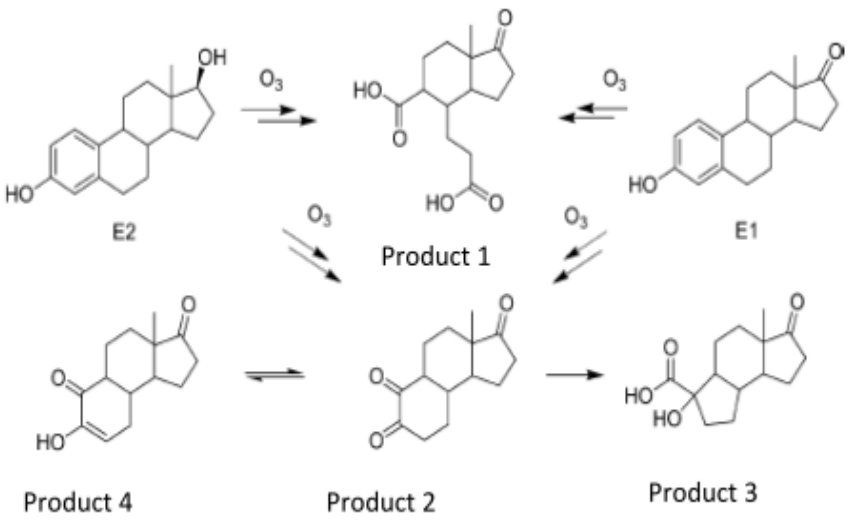

Figure 2. 9: Ozonation products of estrone and 17β-estradiol (Huber et al., 2004).

Chapter Three

Materials and Experimental Methods

3.1 Introduction

In this chapter the experimental methods used are described. The chapter also outlines the chemicals and reagents used in the study as well as their origin and purity together with the analytical instruments used. The solvents used in this study are hazardous by inhalation and skin/eye contact. Hence at all stages, solution preparations were carried out in fume cupboard. Moreover ozone experiments were also carried out in fume cupboard.

3.2 Chemicals and Reagents

Chemicals used in this research work include HPLC grade Acetonitrile 99.99% (Fisher Scientific UK Limited, England); Reactive Orange 16 50% ,Triclocarban 99% , Gold (III) chloride hydrate, Silver nitrate 99.9999% , 17β-Estradiol 98% , 17α- Ethynylestradiol 98%, Estrone 99%, Sodium Hydroxide, Sulphuric acid 99%, Hydrochloric acid, Hydrogen peroxide 30%, Ethanol 99.5%, Methanol 99.9%, Tin oxide, Zinc oxide 99.5%, Ferric oxide 97% and Formic acid 98% (Sigma-Aldrich Chemie, UK); Clopyralid (Dow AgroSciences, UK); Titanium dioxide (Degussa P25 and Hombifine) (Germany); Sodium thiosulphate 99.5%, (BDH chemicals ltd, England); Synthetic Air 100%, Nitrogen 100% and Oxygen 100% (BOC Gases, UK).

3.3 Equipment

Photocatalytic Reactor (manufactured in-house), Oriel power supply (Oriel Corporation of America, USA), Mercury arc lamp Model 66011 (Oriel Instruments, USA), Bentham M300 monochromator (Bentham Instruments Limited, USA), High performance liquid chromatograph (Waters 2695, Waters, England), Agilent 8453 UV-visible Spectrophotometer (Agilent, Germany), inolab pH/oxi pH meter (England), Millipore Direct-Q3 (Millipore, France), Ozone generator (BMT 813, BMT-Messtechnik Germany), Ozone Analyzer (BMT 963, BMT-Messtechnik Germany), Scanning electron microscope (C900, EPSON Aculaser, England), Mistral 1000 Centrifuge (MSE, England), Micro Centaur MSE (Sanyo, England), Hotbox Oven (Gallenkamp, England), WhirliMixer CE Mixer (Millipore, England), , Micromeritics ASAP 2000 Particle size analyzer (Micromeritics, USA),. Membrane filter Miliex GP 0.22µm (Millipore, Ireland), BD Microlance needle (Becton Dickson Limited, Ireland), UAF 14/5 Furnace (Lenton thermal designs Limited, Thailand), 10 mL Syringe (Becton Dickson Limited, Belgium), Filter paper (Whatman International Limited, England), HI 190M Magnetic stirrer (Hanna Instruments, Singapore), Mettler AE200 Digital mass balance (Mettler Toledo, Switzerland), Comark 314 Digital thermometer (Comark Instruments, Korea), Stop watch.

3.4 The photocatalytic system

3.4.1 The reactor

The photocatalytic reactions were studied in a Pyrex glass reactor (200 cm^3) Figure 3.1 into the wall of which two diametrically opposite circular holes, centred along a

horizontal axis, were sealed with optical quality quartz circular windows (35 mm diameter) using a cyanoacrylate-based polymer adhesive. This arrangement provides a horizontal cylindrical irradiated volume of 47.6 cm^3 with a path length of 5.9 cm. The UV light focused in parallel beams was produced by a 500-W medium pressure mercury lamp housed in a point source (Oriel, Model 66011). All of the components of the assembly were mounted rigidly upon a linear steel optical rail.

The glass reactor, constructed in two halves, was joined by a gas-tight flat circular gasket of PTFE pressed between the surfaces of two ground-glass flanges with the aid of push-fitting clamps. The lower half of the reactor possesses a well containing a cylindrically-shaped (poly tetrafluroro ethene) (PTFE) coated magnetic impeller. The reactor contains ports through which sensors, or septa, can be inserted when required, and two PTFE stopcocks, through one of which, gases (oxygen, dry air, or nitrogen) can be sparged into the liquid contents of the reactor via a fine sintered glass frit, while the second stopcock acts as the outlet for flowing gases. In normal use, the liquid contents of the reactor (200 cm^3) occupy most of the volume below the flange, while the volume above the liquid surface forms a headspace containing the required gas at atmospheric pressure.

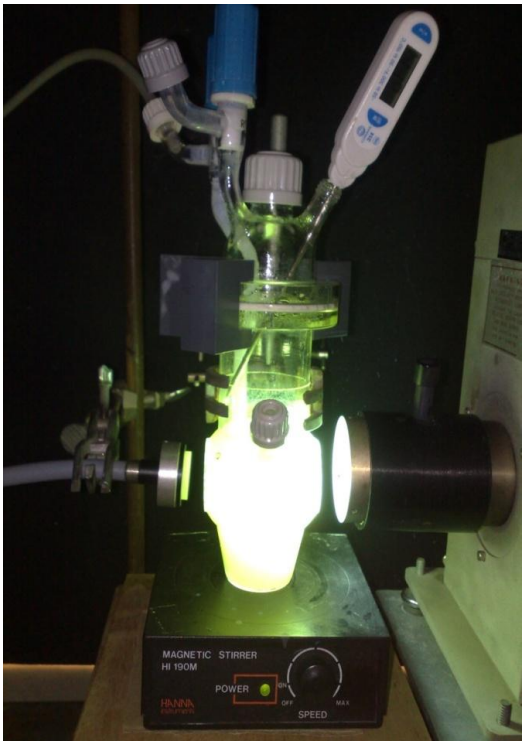

Figure 3.1: The photocatalytic Reactor.

3.4.2 The Mercury Arc Lamp

The light source used in the present study was an Oriel Medium pressure mercury arc lamp as shown in Figure 3.2 inset. The spectral distribution of this type of lamp was measured at a wavelength of 365 nm (the wavelength at which the lamp emits the highest intensity of light) shown in Figure 3.2. The quartz arc tube used was (500 W, Osram), was typical of the medium pressure mercury arc lamps. It contained a small droplet of high purity mercury, together with a small pressure of the inert gas argon (Oriel Products Catalogue).

The power supply used was an Oriel constant voltage supply with a built- in high voltage starter. Upon energising the striking circuit, the high voltage is impressed across the gap between the two electrodes creating an argon arc. The current is limited to a

very low value by a resistor. The heat generated by the argon arc causes the mercury to vaporise and the resistance between the two electrodes begins to drop until the main mercury arc is able to strike, resulting in vaporisation of more mercury. Eventually, all of the mercury vaporised and the lamp attains a steady state condition.

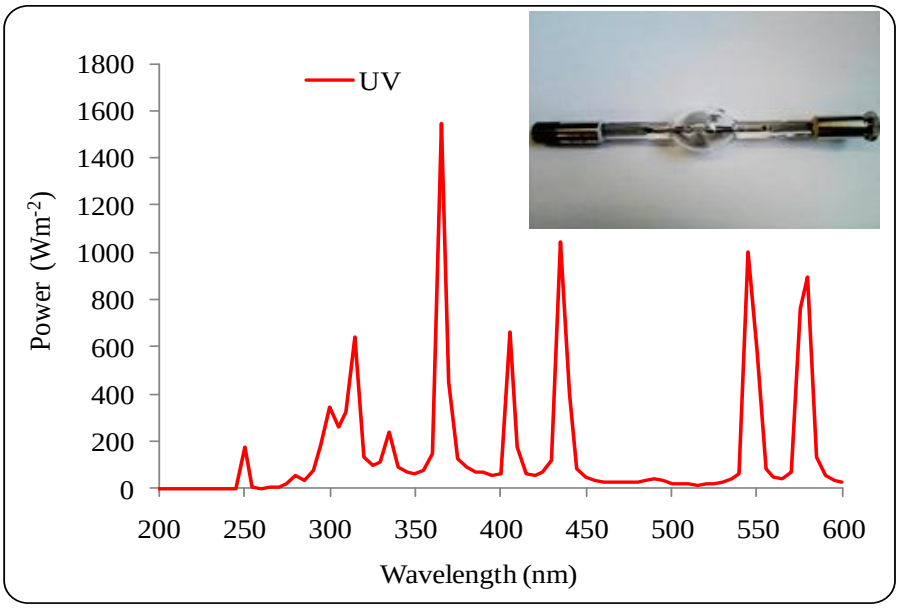

Figure 3.2: Spectral distribution of medium pressure lamp.

3.4.3 Measurement technique for light intensities in this research

A Bentham spectroradiometer system was employed to measure the light intensities for the UV lamp. It consists of five units:

1. Input optics.

2. DM150 Double Monochromator.

3. Detector (Dh-Si).

4. 217T Control and logging bin (267 DC current amplifier and 228A integrating ADC).

5. Computer with BENTHAM software.

The input optics gather radiation from a specified field of view and deliver it to the Monochromator that separates the radiation into its component wavelengths. The detector measures the radiation at each wavelength and sends a signal to the control and logging bin. The computer uses installed software to control various hardware configurations, collects data and performs data manipulation. Fig.3.3 shows a schematic diagram of the spectroradiometer.

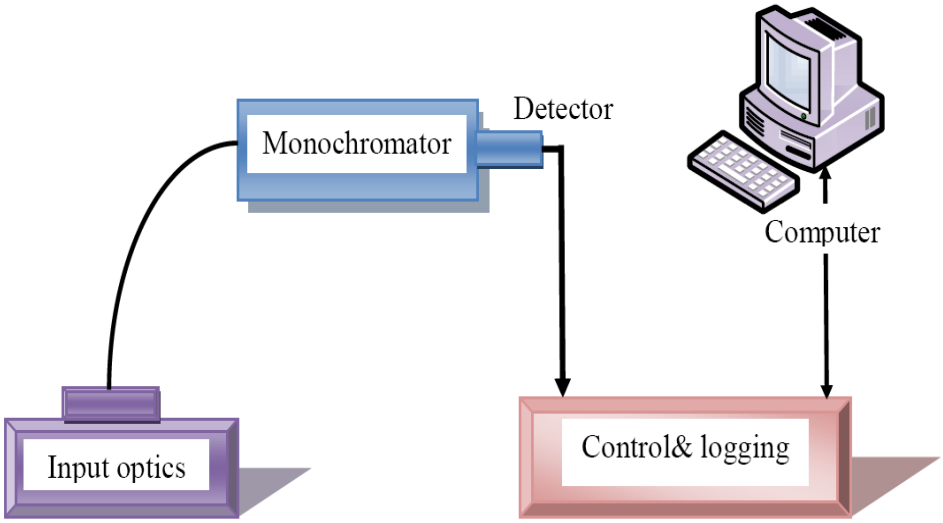

Figure 3.3: Diagram showing the units of a spectroradiometer.

3.5 UV/VIS Spectroscopy

3.5.1 Principles of the UV/Vis spectrophotometer

The UV/Vis spectrophotometer is used to measure the absorbance of light of a chemical at a given wavelength. The value of the absorbance is proportional to the chemical concentration (Beer Lambert law), thus concentrations may be measured through absorbance measurements and a calibration curve. In this study, a diode array Agilent 8453 UV- visible Spectrophotometer (190 to 1100 nm) was used. It is fitted with a

general purpose Agilent ChemStation software for UV- visible spectroscopy running on PC with the supported Microsoft operating system. These two components are linked together by a network connection. All of the data display, evaluation and long-term storage are done under software control on the PC Figure 3.4.

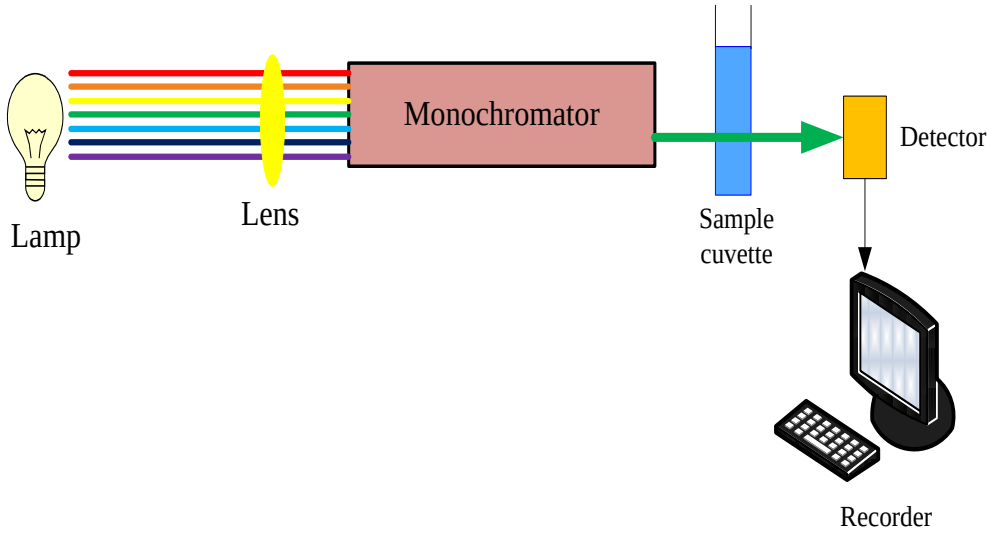

Figure 3.4: Schematic of UV- visible spectroscopy.

3.5.2 Beer-Lambert Law

In optics, Beer-Lambert Law defines as a relationship between absorbance of light and concentration of liquids or solutions (e.g. dye) when light passes through a cell containing the solution, Figure 3.5 (Bickley et al., 2005). The general Beer-Lambert Law could be written as the following:

$$Abs = \varepsilon lC \tag{3.1}$$

where:

Abs = Absorbance

ε = The absorption coefficient or the molar absorptivity of the absorber

l = Length of the light travel through path

C = Concentration of liquids or solutions (dye)

The Beer-Lambert Law can be written in a logarithm form as following:

$$\ln_e\left[\frac{I_o}{I}\right] = \varepsilon l C$$

where:

I_o = The intensity of the incident light

I = The intensity after passing through the material

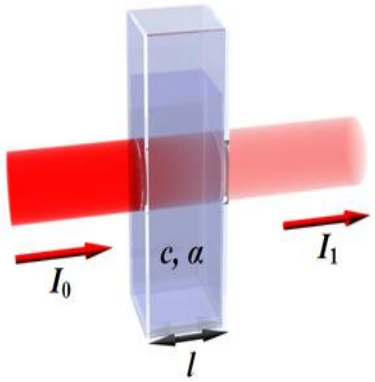

Figure 3. 5: Diagram of Beer-Lambert Law when light travels through a liquid cell.

3.6 High-performance liquid chromatography (HPLC)

High-performance liquid chromatography (HPLC) is a separation technique which has the facility to separate highly complex mixtures. HPLC (Waters 2695) with UV detection (Waters 2487 Dual λ) was used in this work to analyse triclocarban, clopyralid and estrogens. The mobile phase used for triclocarban analysis was 70% acetonitrile + 30% water mixture, for clopyralid was 70% acetonitrile + 30% water mixture and for estrogens was 50% acetonitrile + 50% water. The sample was injected at one end of the

column [C18 Hypersil Gold column (150 × 4.6*mm*, 5μm Thermo Scientific)], and carried through the column by a continuous flow of the mobile phase.

3.6.1 Principles of HPLC

The principle of HPLC is that a liquid mobile phase transports a sample through a column containing a liquid stationary phase Figure 3.6. The interaction of the sample with the stationary phase selectively retains individual compounds and permits separation of sample components. Detection of the separated sample compounds is achieved mainly through the use of absorbance detectors for organic compounds and through conductivity and electrochemical detectors for metal and inorganic components

$$A_{mobile} \leftrightarrow A_{stationary}$$

Equilibrium constant $K = \frac{[A]}{[A]} \frac{stationary}{mobile}$

The chromatogram is a record of the detector response as function of time and indicates each separate eluted component as a peak. In quantitative measurement, the area under each peak is directly proportional to the amount of sample. With the integrator calculating the area under each peak a calibration plot can be achieved by measuring the different areas of the same compound at different concentrations.

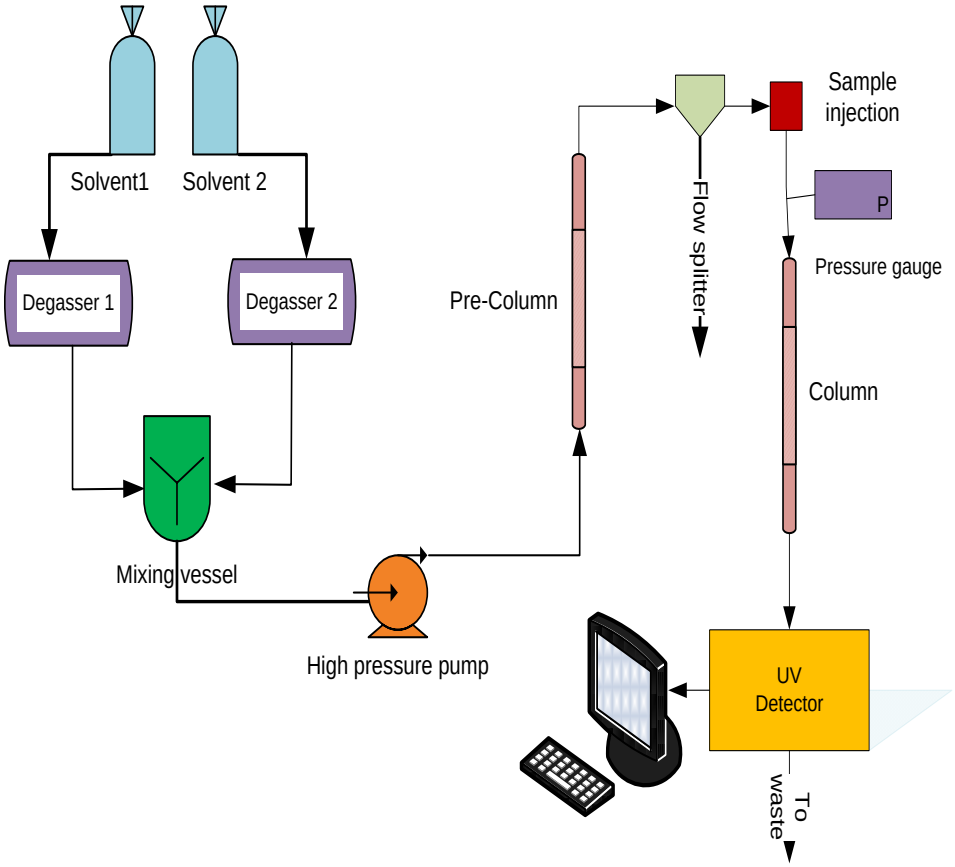

Figure 3.6: Schematic of High performance liquid chromatography.

The HPLC analytical conditions used in this study for each compound are shown in Table 3.1.

Table 3.1: Data of HPLC analytical conditions of substances.

Compound	HPLC analytical conditions					
	Analysis method	Mobile phase ACN%, W%	Wavelength (nm)	Injection volume (µL)	Flow rate ml/min	Colum type
TCC	Isocratic	70 : 30	265	20	1	C18 Hypersil Gold (150 × 4.6*mm*)
Clopyralid	Isocratic	70 : 30	225	20	1	C18 Hypersil Gold (150 × 4.6*mm*)
EDCs	Isocratic	50 : 50	205	20	1	C18 Hypersil Gold (150 × 4.6*mm*)

3.7 Experimental Set ups

3.7.1 UV/TiO_2

A commercial titanium dioxide TiO_2 (Degussa P25) was used as photocatalyst. Different concentrations of the organic compounds (i.e. Reactive orange, Triclocarban, Clopyralid and Estrogens) were used with the different concentrations of catalyst to monitor the activity of UV/TiO_2 on degrading these compounds. All experiments were carried out under the same conditions (at room temperature, pressure 0.1 bar, power of light 200 W and a given pH). All experiments were carried out in a dark chamber as shown in Figures 3.7 and 3.8 to prevent interferences and for health and safety purposes.

The mercury arc lamp was switched on and allowed to warm up for one hour. During this time, the power supply was monitored using the multimeter provided on the power supply, which displayed both the current drawn (amperes), and the potential applied (volts). The light source was temporarily blocked with a silvered shutter. The photocatalyst was stirred with a magnetic stirrer while the reactor was sealed with the head-space volume containing pure oxygen (or synthetic air). Then the shutter was opened to allow irradiation to begin. Liquid samples 3mL were removed at regular intervals of time and the solid titanium dioxide separated by (Millex GP 0.22μm). Analysis of the clear liquid was then performed by Ultraviolet/Visible (UV/VIS) spectroscopy for RO16 and using HPLC for TCC, Clopyralid and the estrogens.

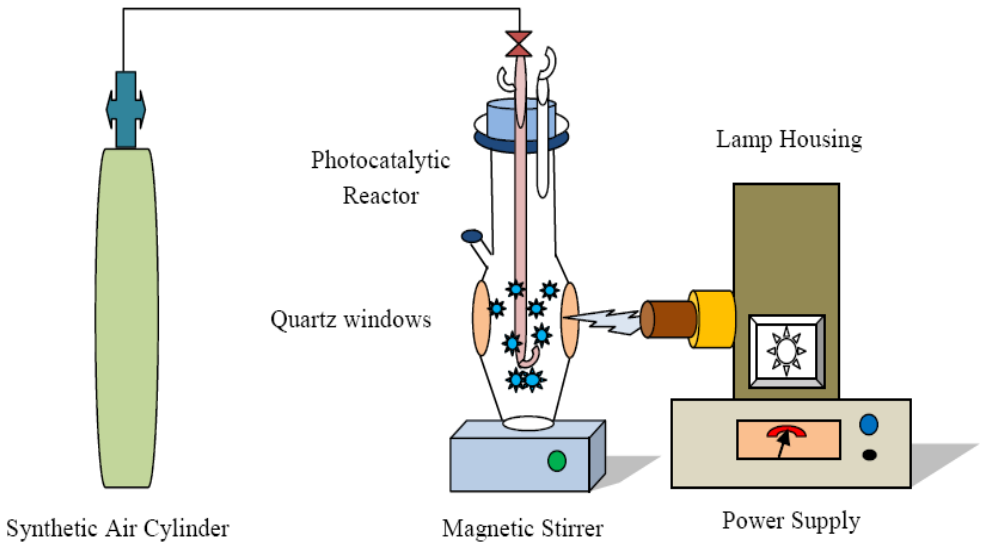

Figure 3.7: Schematic of the photocatalytic system.

Figure 3.8: The Photocatalytic experiment.

3.7.2 UV/H_2O_2

The UV/H_2O_2 experiments followed the same procedure as for UV/TiO_2 with the exception that H_2O_2 was added to the solution instead of TiO_2. In a typical run, after the UV system reached thermal equilibrium, a given volume of hydrogen peroxide (30%) was added to the solution to make a desired concentration of 1g/L or 2 g/L H_2O_2.

Samples of the solution (~2mL) were collected at given times using a glass syringe. Immediately after sampling, the sample aliquot was subjected to a 0.005M sodium thiosulphate solution to quench any remaining H_2O_2 in the solution, which stops the reaction, before analysis in the HPLC. In the case of RO16 solutions, the analysis was made immediately after sampling with the UV/VIS spectrophotometer without adding sodium thiosulphate.

3.7.3 Ozone

Ozone experiments were carried out in a semi-batch gas/liquid glass reactor filled with 200 mL of clopyralid and estrogens solution of known initial concentration (15, 50, 100 and 20 mg/L) respectively. Pure oxygen was used to generate ozone with a lab ozone generator (Triogen LAB2B) Figure 3.9. The gas flow rate was 200 mL/min and the ozone gas concentration was 60 g/m^3 NTP. Ozone gas concentration was measured using a BMT 963 ozone analyser that automatically converts ozone concentrations to NTP conditions (i.e. 0°C, 1atm) and displays them in g/m^3 NTP. The gas mixture of O_3+O_2 was introduced to the reactor through a sintered glass diffuser and further dispersed in the solution by stirring the entire gas/liquid mixture with a magnetic bar stirrer. Samples of the solution were collected at given times using a glass syringe. Immediately after sampling, the sample aliquot was subjected to a 0.005M sodium thiosulphate solution to quench any remaining ozone in the solution, which stops the reaction, before analysis.

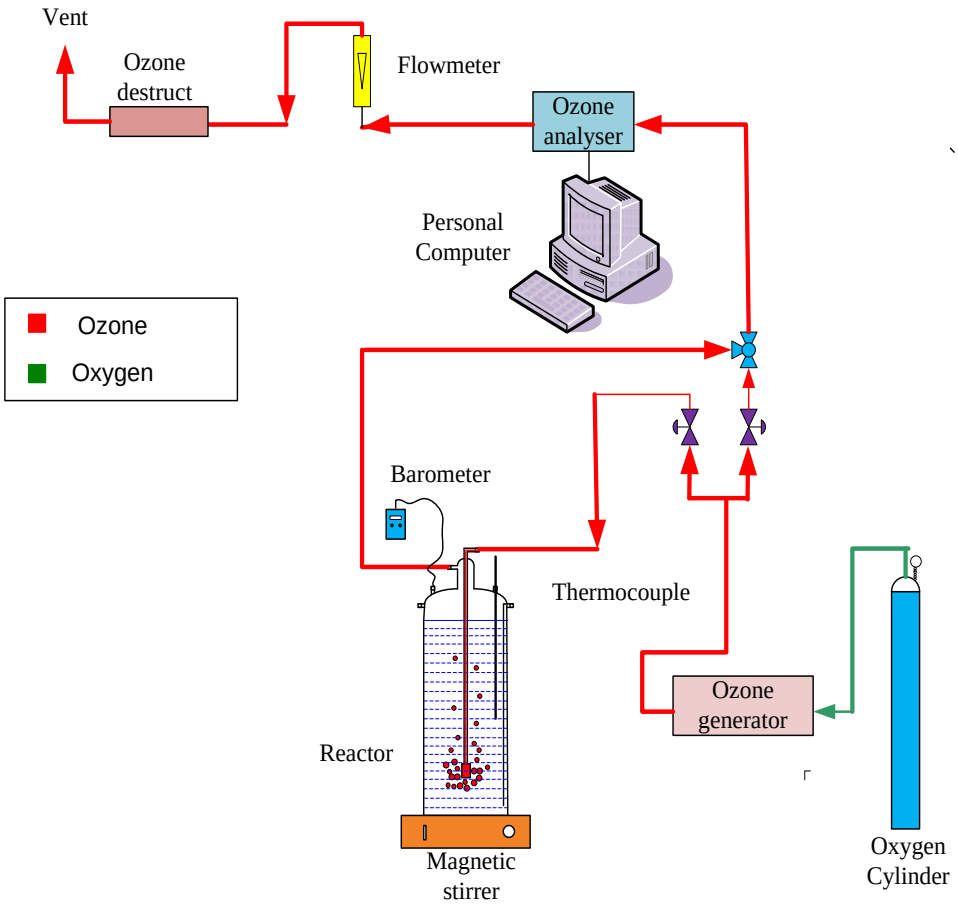

Figure 3.9: Schematic of the ozonation experimental set up.

Table 3.2 shows the different initial concentrations of organic compounds used in this work.

Table 3. 2: Data of substances concentrations used in this work.

RO16 (mg/L)	TCC (mg/L)	Clopyralid (mg/L)	EDCs (mg/L)
20	15	15	0.5
40	20	50	1
60	50	75	5
-	-	100	20

3.8 Adsorption properties of TiO_2

Adsorption is the accumulation of substances at the interface between two phases, such as a liquid and a solid or a gas and a solid. Adsorption equilibrium is reached when the number of molecules leaving the surface of the adsorbent is equal to the number of molecules being adsorbed on the surface.

It is generally agreed that adsorption is one of the steps in heterogeneous photocatalytic reactions; however, there is lack of convincing interpretation of the role of solute adsorption onto surfaces of the photocatalyst. Surface area and pore size distribution are important adsorbent characteristics that affect the isotherms, and the maximum amount of adsorption is proportional to the amount of surface area within pores which is accessible to adsorbent. The influence of such adsorption on reaction kinetics has not been explored thoroughly. It is proposed that for specific photocatalytic reactions, the role of adsorption may vary. For example, if the adsorption process is very fast as compared to the whole reaction process, adsorption is unlikely to be a rate-limiting step. On the other hand, if the adsorption process is slow as compared to the whole reaction process, it is possible that adsorption is rate-controlling. Different combinations of certain chemicals catalyst may therefore have different adsorption characteristics.

3.8.1 Adsorption experimental method

Table 3.4 shows the experimental data performed in four 0.5 litre glass bottles which was covered by aluminium foil to prevent radiation absorption from outside, which had a magnetic stirrer to stir the solution. Figure 3.10 shows the experimental set up. All the experiments were carried out at an approximately constant room temperature at 294±2 K for 24 hrs and allowed the suspension to

achieve physical and chemical equilibrium. At specific time intervals, samples of 10 *mL* were withdrawn. The samples were filtered immediately through a (Cellulose Nitrate Membrane Filters 0.45μm). The liquid samples were then analysed either using UV/VIS spectrophotometer for the dye or the HPLC system for the other compounds.

Table 3. 3: Experimental data of RO16 adsorption on TiO_2.

Experimental duration time (h)	Volume of dye solution (mL)	RO16 dye concentration (mg/L)	Catalyst TiO_2 concentration (g/L) at 294 °K
24	200	20	0.5
			1.0
			1.5
			2.0
24	200	50	0.5
			1.0
			1.5
			2.0
24	200	100	0.5
			1.0
			1.5
			2.0

Figure 3.10: Equipment of adsorption equilibrium coefficient.

3.9 Safety

Before the experimental work has started in the lab, COSHH forms have been completed to assess the health and safety related to the chemicals used in this project. Personal protective equipment, which involved gloves, goggles (Figure 3.11) and lab coat are always worn. A UV-Protective wraparound face shield (Cole-Parmer, UK) was also used when working with the photocatalytic reactor.

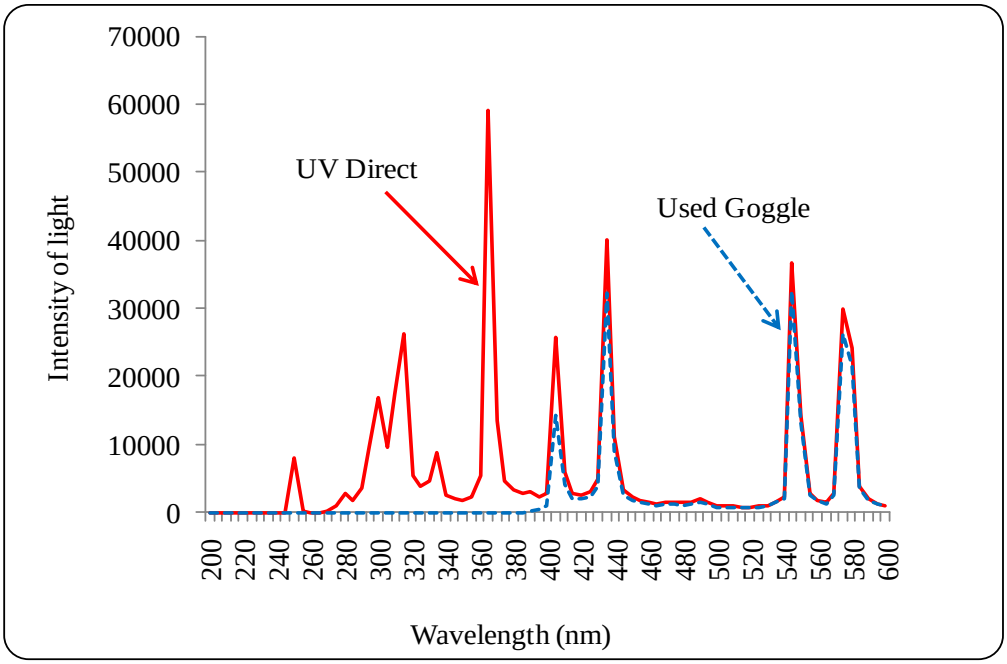

Figure 3. 11: UV-Protective.

3.10 Summary

The materials and methods used for the study were described in this chapter. The UV/Vis spectrophotometer was used to measure the concentration of RO16 while an HPLC system coupled with a UV detector was used for the analysis of triclocarban, clopyralid and the endocrine disrupting chemicals.

Chapter Four

Analytical Results

Results related to calibration and determination of conditions used for the analytical methods for each compound, are presented in this chapter.

4.1 Orange reactive 16 (RO16)

4.1.1 UV/Vis Spectrum of RO16 dye

Figure 4.1 shows a full spectrum of the dye RO16. From this spectrum, it can be seen that the maximum absorbance of RO16 takes place at λ_{max} = *494nm.* Thus, all subsequent analyses of the dye were made by measuring the absorbance at λ_{max} = *494nm.*

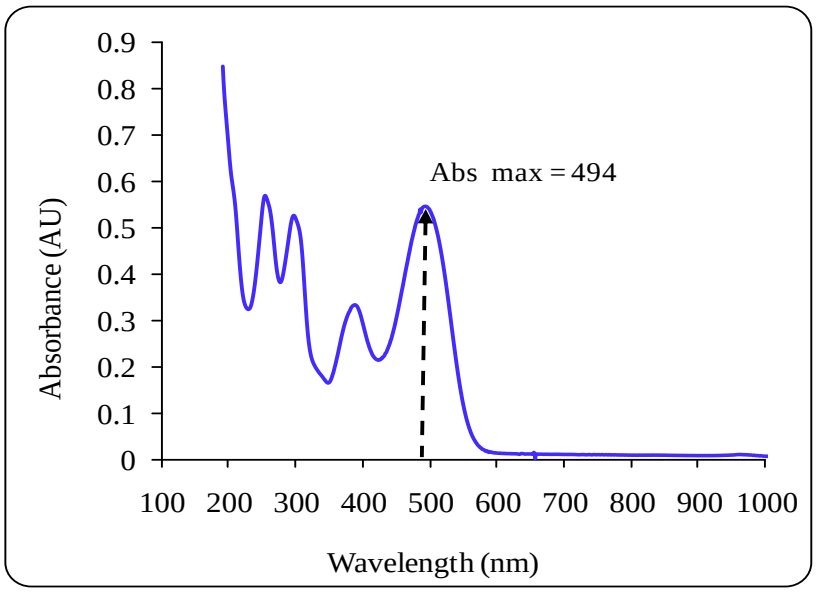

Figure 4.1: Full spectrum of 20 mgL^{-1} RO16.Calibration curve of RO16 dye

Figure 4.2 shows that the Beer-Lambert law is valid since good linearity between absorbance and concentration was obtained and the determination factor R^2 was 0.999.

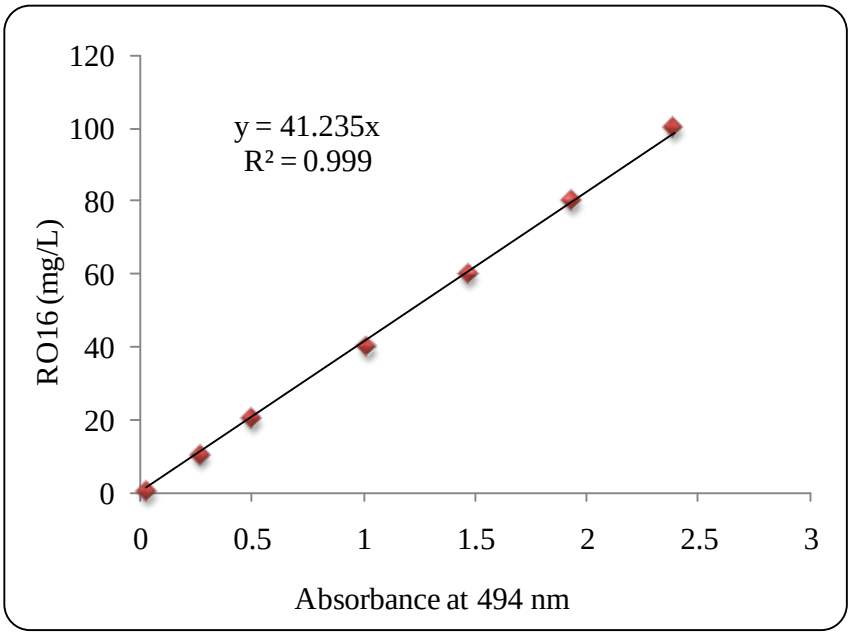

Figure 4.2: Calibration curve of RO16 solution at 494 nm.

4.2 Triclocarban (TCC)

4.2.1 UV/Vis Spectrum of TCC

The full spectrum of a TCC solution at 25 mg/L is presented in Figure 4.3, the maximum absorbance for TCC occurred at almost 265 nm. Based upon this result, subsequent analysis of TCC using the HPLC/UV detector was carried out at a wavelength of 265 nm.

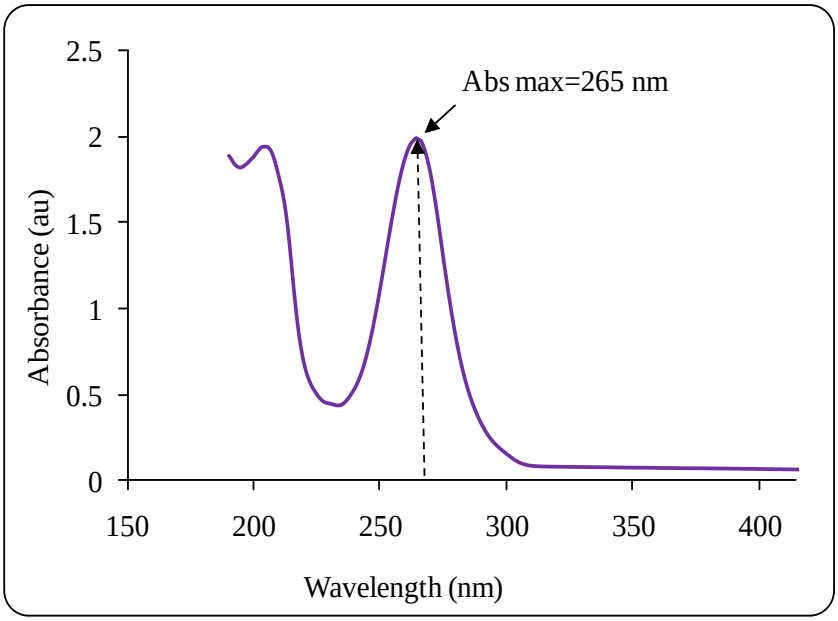

Figure 4.3: Full spectrum of 25 mgL^{-1} TCC.

4.2.2 Calibration curve of TCC

Good peak separation was obtained as shown in Figure 4.4 and the retention time for TCC was 4.84 minutes. The peak was integrated and its area was correlated to each TCC concentration using a developed calibration curve. Good linearity between peak areas and concentrations was obtained as shown in Figure 4.5 with correlation coefficients R^2 higher than 0.999.

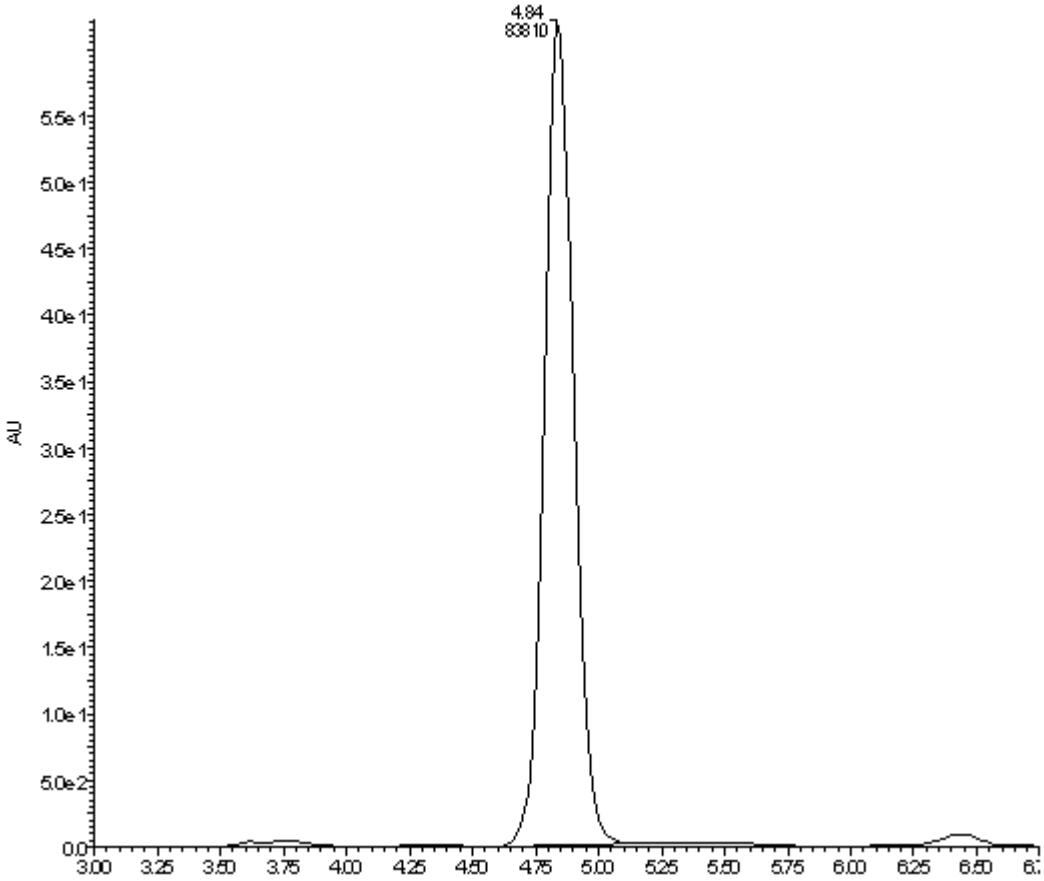

Figure 4.4: Peak and retention time of TCC.

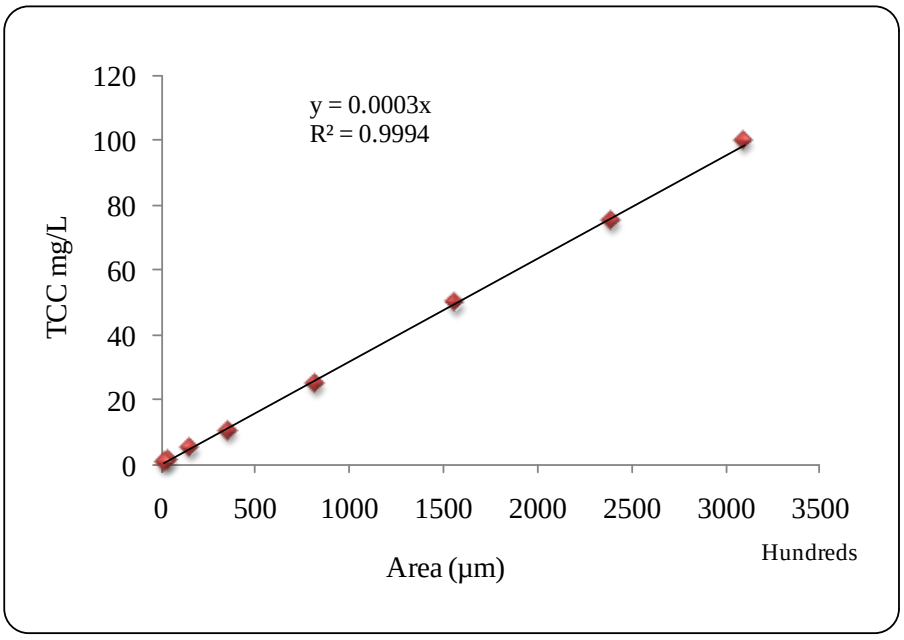

Figure 4.5 Calibration curve for HPLC analysis of TCC

4.3 Clopyralid

4.3.1 UV/Vis Spectrum of Clopyralid

The full spectrum of a clopyralid solution at 25 mg/L is presented in Figure 4.6, the maximum absorbance for clopyralid occurred at almost 225 nm. Based upon this result, subsequent analysis of clopyralid using the HPLC/UV detector was carried out at a wavelength of 225 nm.

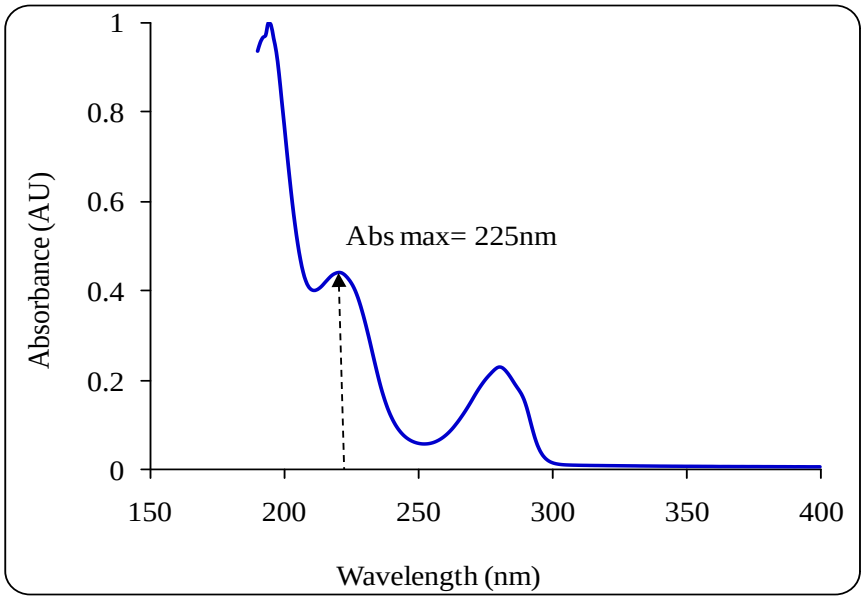

Figure 4.6: Full spectrum of 25 mgL^{-1} Clopyralid.

4.3.2 Calibration curve of Clopyralid

Good peak separation was also obtained as shown in Figure 4.7 and the retention time for clopyralid was 1.22 minutes. The peak was integrated and its area was correlated to clopyralid concentration using a developed calibration curve. Good linearity between peak areas and concentrations was obtained as shown in Figure 4.8 with correlation coefficients R^2 higher than 0.999.

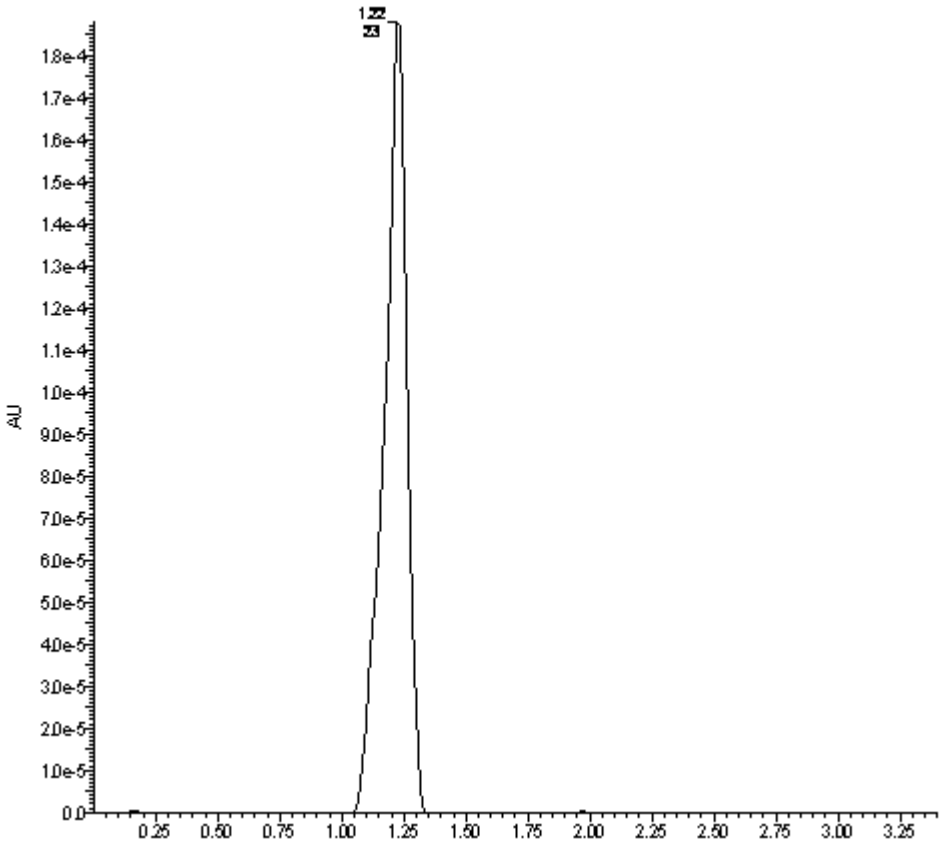

Figure 4.7: Peak and retention time of Clopyralid.

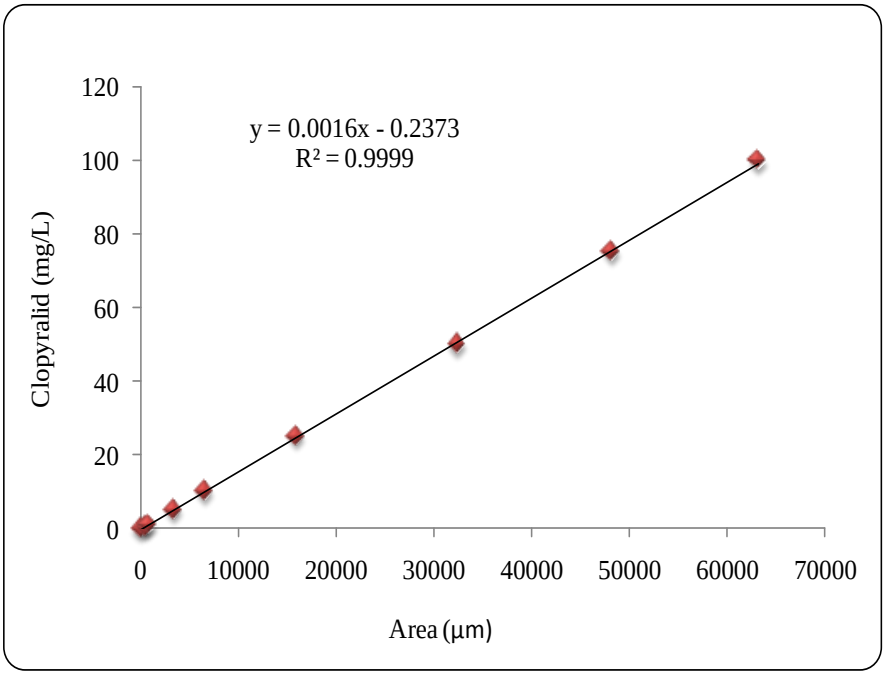

Figure 4.8: Calibration curve for HPLC analysis of clopyralid.

4.4 Endocrine disrupting chemicals (EDCs)

4.4.1 UV/Vis Spectrum of EDCs

The analyses of EDCs were made using the HPLC/UV methodology. The maximum absorbance wavelengths of the compounds used in this study estrone (E1), 17β-estradiol (E2) and 17α-ethinylestradiol (EE2) were determined with the UV/Vis spectrophotometer (HP8453). Water was used as blank solution and E1, E2 and EE2 have been used at concentrations of 25 mg/L (E1= 9.25×10^{-2}, E2= 9.18×10^{-2} and EE2= 8.43×10^{-2} mM) each in water. The full spectrum for each EDC is presented in Figure 4.9, which shows that a wavelength of 205 nm is suitable for UV detection of the three compounds. Bila et al., (2004) used 203 nm to analyse E2. Based upon this result, subsequent analysis of E1, E2 and EE2 using the HPLC/UV detector was carried out at a wavelength of 205 nm.

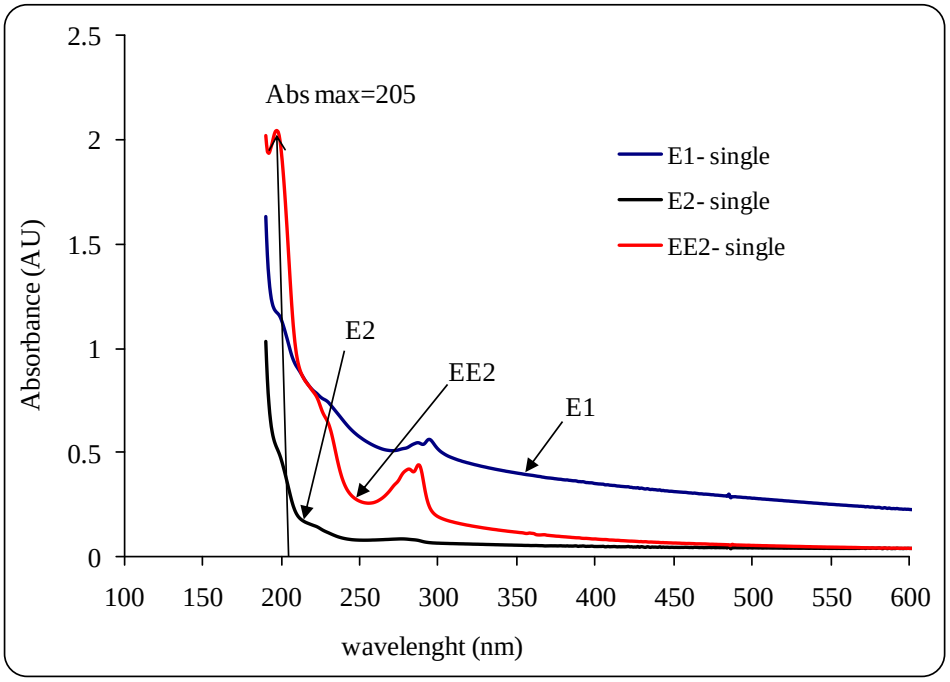

Figure 4.9: UV absorption spectrum of 25 mgL^{-1} E1, E2, and EE2.

4.4.2 Calibration curve of E1, E2 and EE2

Peak separations were also obtained as shown in Figure 4.10. The retention times for E2, EE2 and E1 were 4.25, 4.87 and 5.57 minutes respectively. The peaks were integrated and their areas were correlated to each EDC concentration using developed calibration curves. Linearity between peak areas and concentrations was obtained as shown in Figure 4.11.

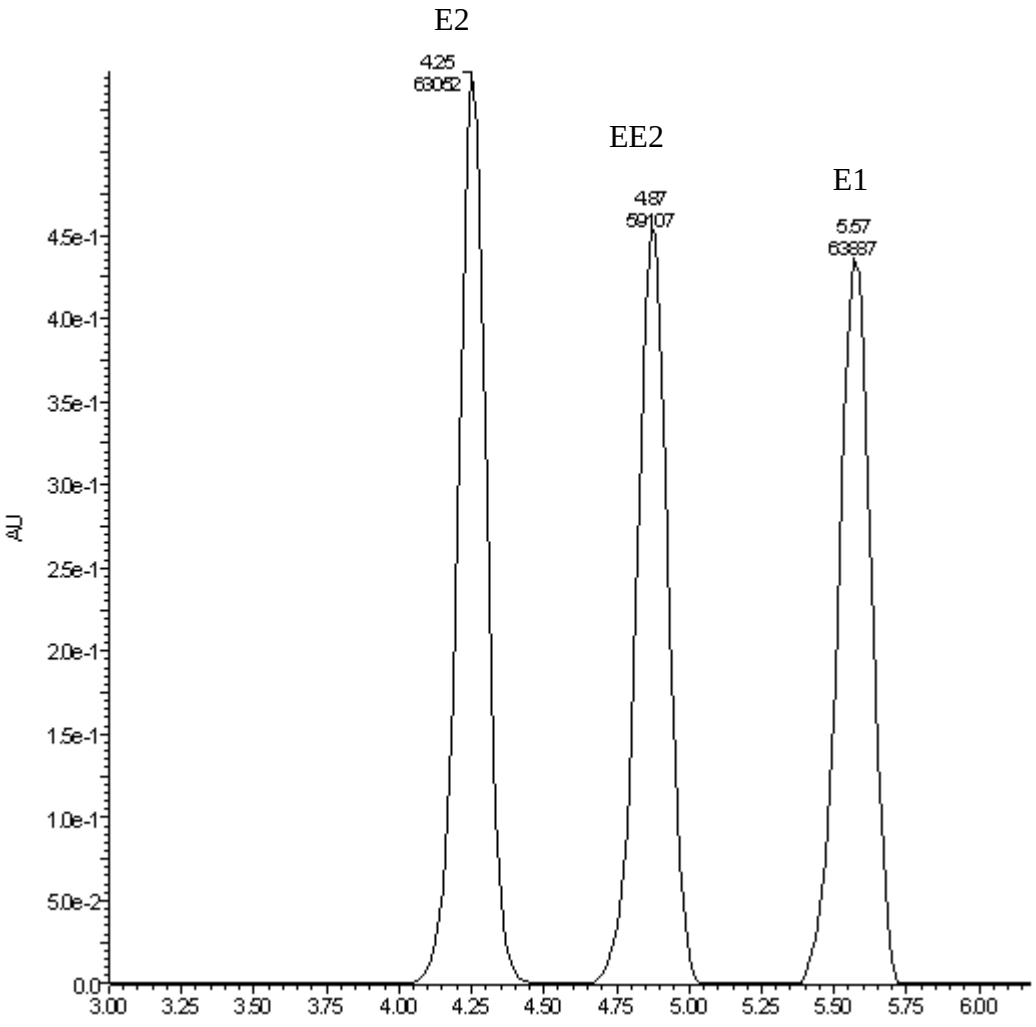

Figure 4. 10: The peaks and retention times of the three EDCs mixture.

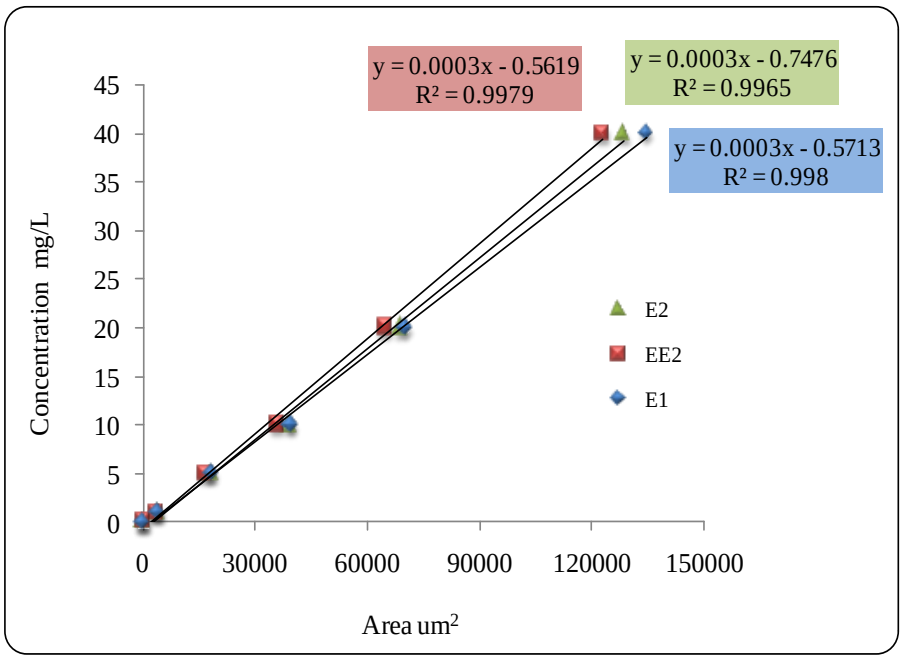

Figure 4.11: Calibration curves for E1, E2 and EE2 (mixture) at 205 nm.

4.5 Summary

In this chapter the analytical results related to calibration curves obtained for RO16, TCC, clopyralid and the EDCs have been presented. Absorbance at 494 nm is used to determine the concentrations of RO16 samples while the retention times and the areas under the peaks obtained during the HPLC analysis of the compounds are used to calculate the sample concentrations.

Chapter Five

Results and Discussions

Results of this research are summarised and discussed in this chapter. The chapter starts with discussing the results of RO16 followed by TCC, 3,6-DCP and EDCs.

5.1 Photocatalytic degradation of RO16

Table 5.1 shows the dye concentrations and catalyst concentrations used in this study. The pH was 5.5 and the lamp power was 200 W.

Table 5. 1: Data of experimental conditions, pH=5.5, power =200 W.

RO16 concentration (mgL^{-1})	TiO_2 concentration (g/L)				
20	0.3	0.5	1.0	2.0	2.5
40	0.1	0.5	1.0	2.0	3.0
60	0.5	1.0	2.0	3.0	4.0

This section will discuss the effect of the operating parameters on the photocatalytic degradation of a 20 mg/L (3.24×10^{-2} mM) RO16 solution.

5.1.1 Photodegradability of RO16

In order to investigate the effect of the presence of the photocatalyst, the decolorization of RO16 dye in aqueous solution was studied using different experimental sets: (i) UV irradiation only (ii) TiO_2 photocatalyst only in the dark (iii) UV in the presence of TiO_2. The results are shown in Figure 5.1.

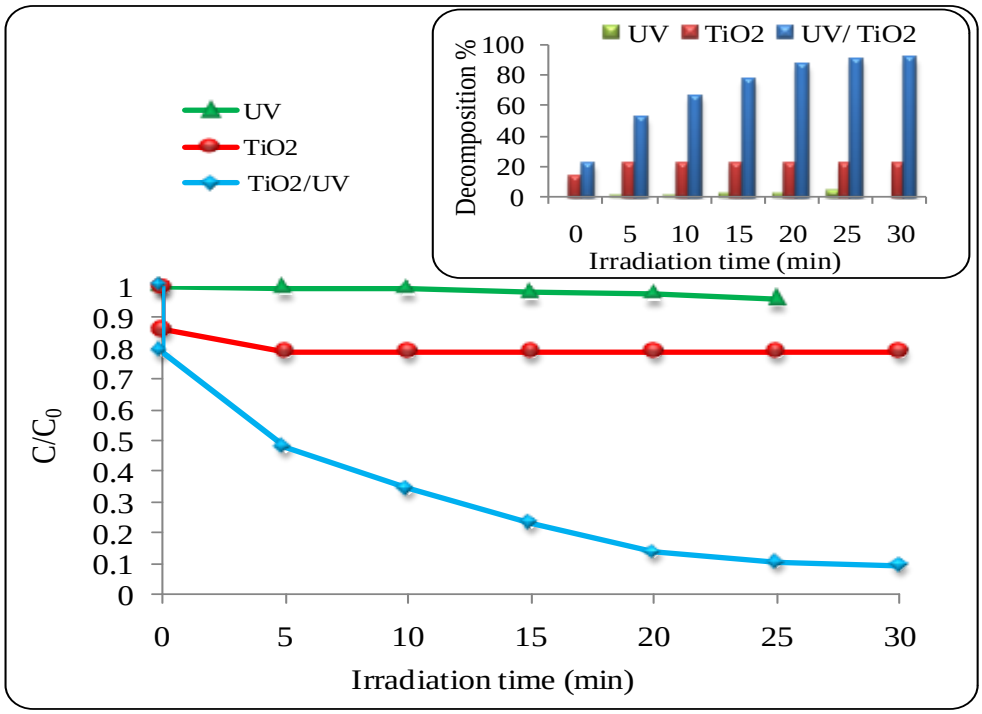

Figure 5.1: Photodegradability of RO16 [C_0=20 mg L^{-1} (3.24×10^{-2} mM), Ccat=1gL^{-1}, pH=5.5, Power=200W].

Figure 5.1 shows that no significant degradation occurred when either the photocatalyst or UV irradiation were used alone. However, when UV irradiation was combined with the photocatalyst, a clear decolourisation of the dye took place. In this condition 90% of the colour was removed in only 30 minutes. This shows that the decomposition of RO16 is attributed to photocatalytic reactions that can effectively decolorize and degrade this dye. The rapid decolorization of dye may be due to the initial electrophilic

cleavage of its chromophoric azo (-N=N-) bond. Azo bonds are more reactive in azo-dyes and can be oxidized by positive holes or hydroxyl radicals; they can also be reduced by electrons in the conduction band (Ganesh el at., 1994). Additionally, Ganesh el at., (1994) showed that the decolorization of a related chromophoric azo bonds bearing dye molecule, Yellow 12, to proceed as a result of cleavage of these azo bonds.

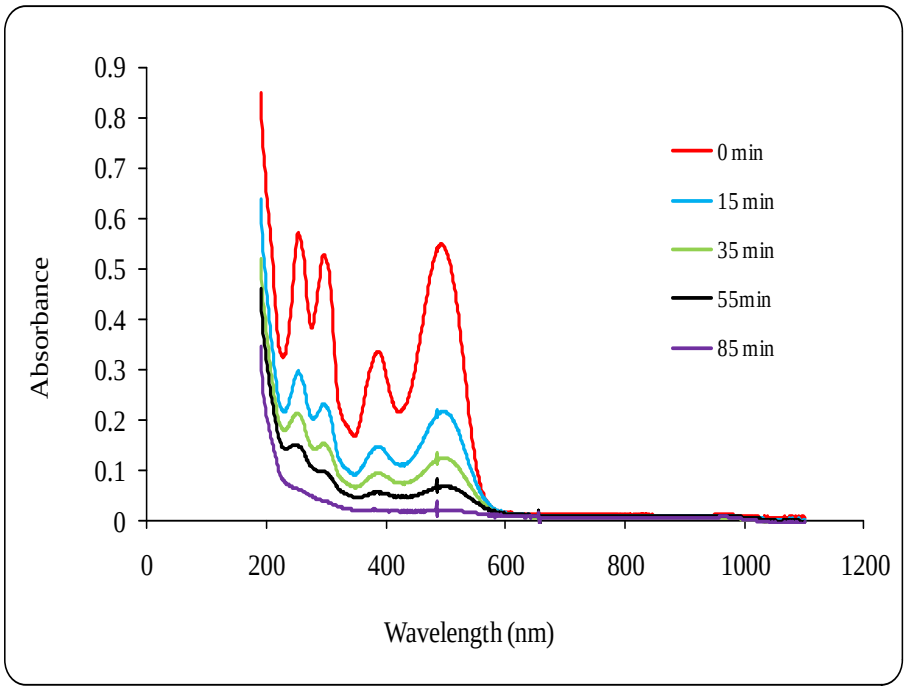

Figure 5.2: Changes of the UV/Vis spectra as function of irradiation times [C_0=20 mg L^{-1} (3.24×10^{-2} mM), Ccat=1gL^{-1}, pH=5.5, Power=200W].

The formation of reaction products can be characterised by measurements of the absorbance in the UV region (Figure 5.2). In this study the wavelengths of 253, 296 and 388 nm were used for this purpose. The measured absorbance at a particular wavelength is the sum of absorbances due to all molecules present in solution (Beer-Lambert law). If it is assumed that only the parent molecule RO16 and a product formed as a result of the photocatalytic reaction absorb light. Hence the product absorbance can be calculated by:

$$Abs_{product}(\lambda_{UV}) = Abs_{meas}(\lambda_{UV}) - Abs_{RO16}(\lambda_{UV})$$

The absorbance due to RO16 (i.e. Abs_{RO16}) can be calculated from a relationship between the absorbance at the given UV wavelength and the RO16 maximum absorbance wavelength in the visible region (i.e. λ_{max}=494nm) determined from measurements made for RO16 solutions at different concentrations. From Beer-Lambert law this relationship in dilute solutions should be linear of the form: $Abs_{RO16}(\lambda_{UV}) = \alpha Abs_{RO16}(494)$. For the three wavelengths above, the relationship was linear, as expected, and the results are shown in Figure 5.3 and Table 5.2.

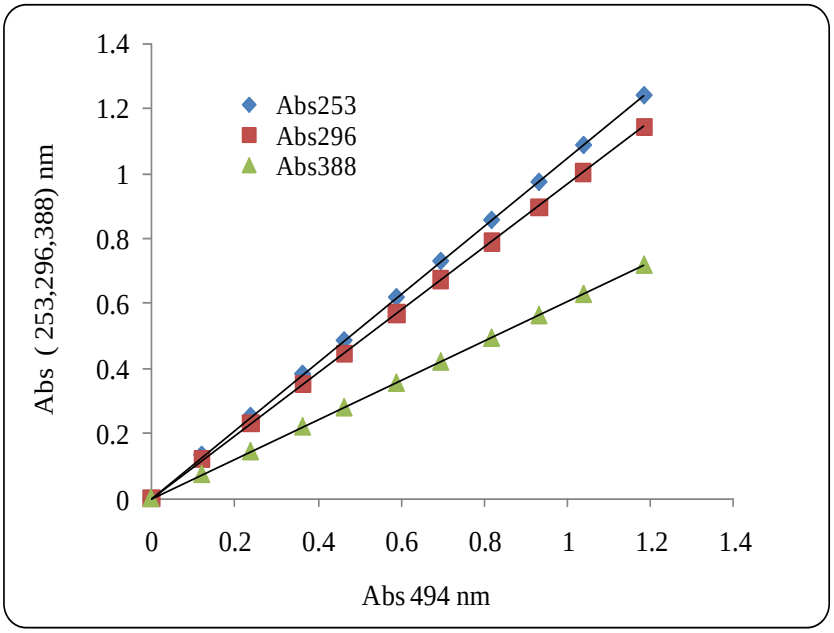

Figure 5.3: Relationship between selected UV wavelengths and maximum absorbance wavelength.

Table 5. 2: Values of α.

α_{253}	α_{296}	α_{388}
1.052768	0.969371	0.60457

The change of absorbance due to product formation measured at 253, 296 and 388 nm relative to the initial absorbance at these wavelengths is shown in Figure 5.4. The figure shows that all three wavelengths gave similar trends though at different values, possibly due to different extinction coefficients at the different wavelengths. Clearly the concentration of reaction products increases with time to reach a maximum after about 40 min of irradiation. This maximum is sustained for about 10 min followed by a clear decrease that is most probably due to photocatalytic degradation of the reaction products. On the other hand, the concentration of the parent molecule decreases continuously up to about nil concentration after 100 min irradiation.

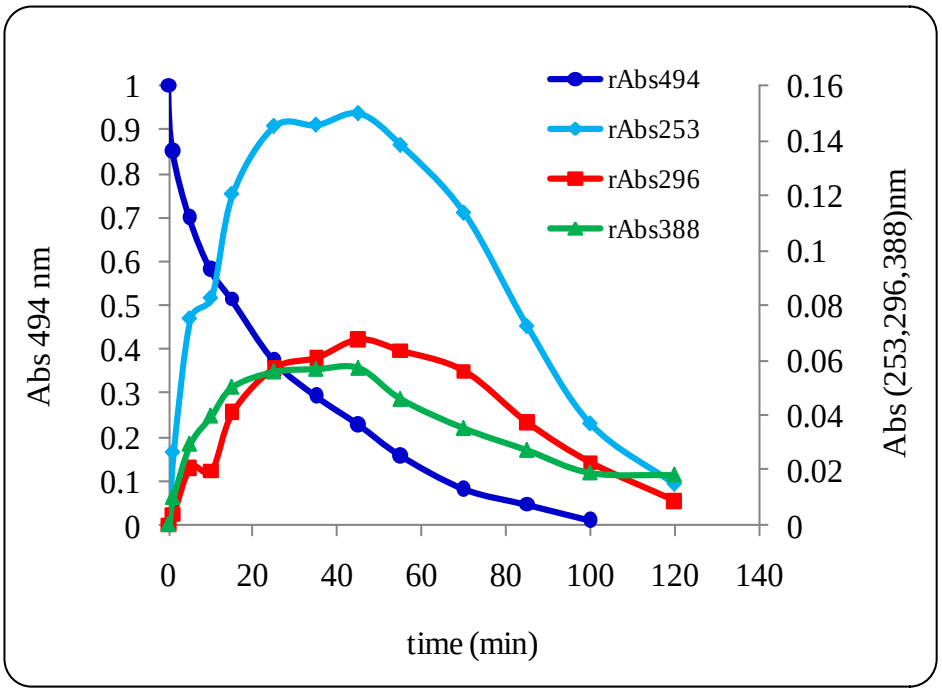

Figure 5. 4: Change of absorbance due to product formation.

5.1.2 Adsorption isotherm

Adsorption experiments in dark were carried out at a temperature of 294±2K. Freundlich's isotherm (Equation 5.1) gave good fitting of the experimental data, which clearly reveals the higher adsorption capacity of Degussa P25 for RO16 dye.

$$q^* = Kc^{1/n} \tag{5.1}$$

$$\ln(q^*) = \ln(K) + \frac{1}{n}\ln(C_f) \tag{5.2}$$

where q^* = the mass of solute adsorbed per gram of TiO_2, mg g^{-1} catalyst.

C_f = equilibrium concentration of adsorbate in solution mg/L.

K and 1/n are constants for a given adsorbate and adsorbent at a particular temperature.

The equilibrium curve between q^* and C_f is shown in Figure 5.5.

Figure 5.6 below shows good agreement between experimental data and Freundlich equation ($T=294\pm2K$) see Equation 5.2.

The values of K and n were 2.24 mg/g*$(mg/l)^{-1/2.76}$ and 2.76 respectively.

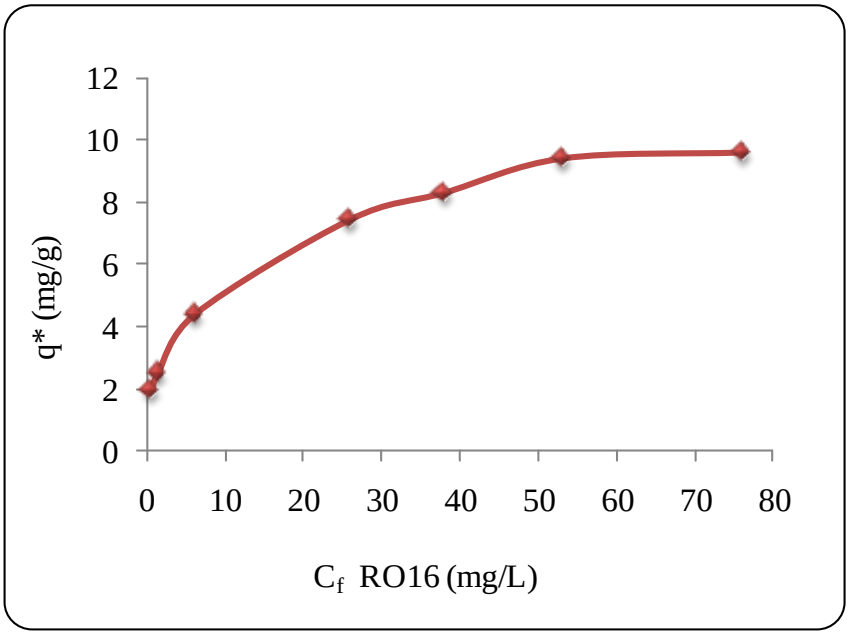

Figure 5.5: Isotherm of adsorption onto TiO_2 from aqueous solutions for RO16.

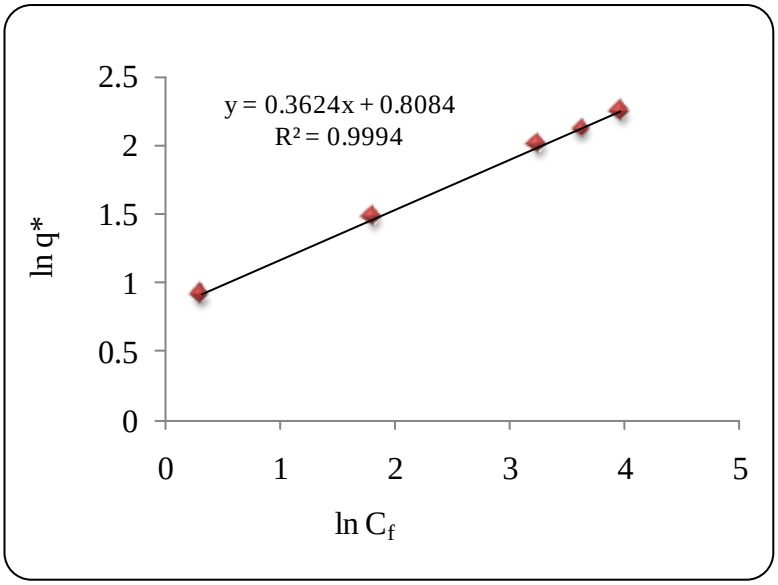

Figure 5.6: Determination of Freundlich equilibrium coefficients at 294 K.

5.1.3 Photocatalyst selection

The degradation of RO16 dye at pH 5.5 at initial concentrations of 20 mgL^{-1} (3.24×10^{-2} mM) was examined using different photocatalysts including TiO_2 Degussa P25, TiO_2 Hombifine N, ZnO, Fe_2O_3, and SnO_2. Figure 5.8 clearly shows that the UV/TiO_2 Degussa P25 system is more efficient in decolorizing RO16. Further the UV/ZnO was also found to have high efficiency in RO16 decolorization. The decolorization percentages with UV/TiO_2 Degussa P25 after 15 and 20 minutes were 97.45% and 100% respectively. Whereas with the UV/ZnO at the same periods of time were 93.92% and 99.08% respectively. But the RO16 decolorization percent with UV/Hombifine at the same periods of time were 62.45% and 69.58% respectively. However the results with UV/SnO_2 and UV/Fe_2O_3 indicated that these catalysts were not effective in decolorizing RO16. The percentage degradation with UV/SnO_2 and Fe_2O_3 at 15 and 20 minutes were only 16.82%, 19.29% and 7.25%, 10.29% respectively. The wide difference between band-gap energies of these semiconductors is the main reason for this wide difference in performance. Indeed, TiO_2 has suitable band gap energy of 3.17 eV requiring a UV light of a wavelength of 390 nm or less. The spectral irradiance of the lamp used in this study (Figure 5.7) gives a maximum light irradiance at 365 nm which is very suitable for photoexcitation of TiO_2. Hence with TiO_2, rapid generation of electron-hole pair occurs after UV irradiation and their recombination is slow (Weller and Angew 1993). However, since the band gap energy of SnO_2 (4.13 eV) is larger than TiO_2 a light with a wavelength less than about 300 nm is required to activate this catalyst. Figure 5.7 shows that the lamp irradiance at 300 nm or less is low, which explains the low performance observed when SnO_2 was used. Although Fe_2O_3 have small band gap energy of 2.3 eV, which requires a light of 539 nm or less to activate,

the recombination of hole and electron is so rapid to the point that the photocatalytic activity of this catalyst is almost negligible (Muruganandham et al., 2004), which explains the results obtained in this study. ZnO has a band gap energy similar to TiO_2 (3.3 eV), which explains its similar performance to Degussa P25. However ZnO has disadvantage of undergoing photocorrosion under illumination as mentioned by (Muruganandham et al., 2004). Although Hombifine N presents the largest surface area, its poor light absorption capability seems more significant in terms of photocatalytic degradation of RO16. This is clearly in agreement with the fact that even though Degussa P25 has low surface area, it showed high degradation rates due to its high capability to absorb UV light. Therefore it can be concluded that photocatalytic degradation of RO16 is more prone to the photocatalyst efficiency of absorbing light than its surface area. In this respect, it is also important to point out that the crystallinity of the photocatalyst plays equally an important role. Moreover, Figure 5.8, shows that at t=0 and due to adsorption, TiO_2 Degussa P25 removes RO16 at much higher rates than the other catalysts, which further highlights the effectiveness of this catalyst. Due to its high performance, Degussa P25 TiO_2 was selected to carry out this study

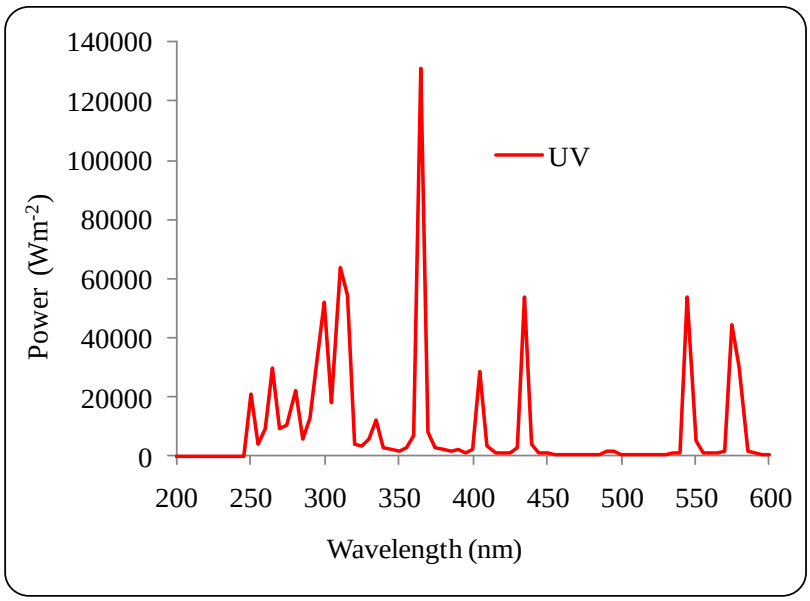

Figure 5.7: Full spectrum of UV lamp used.

.

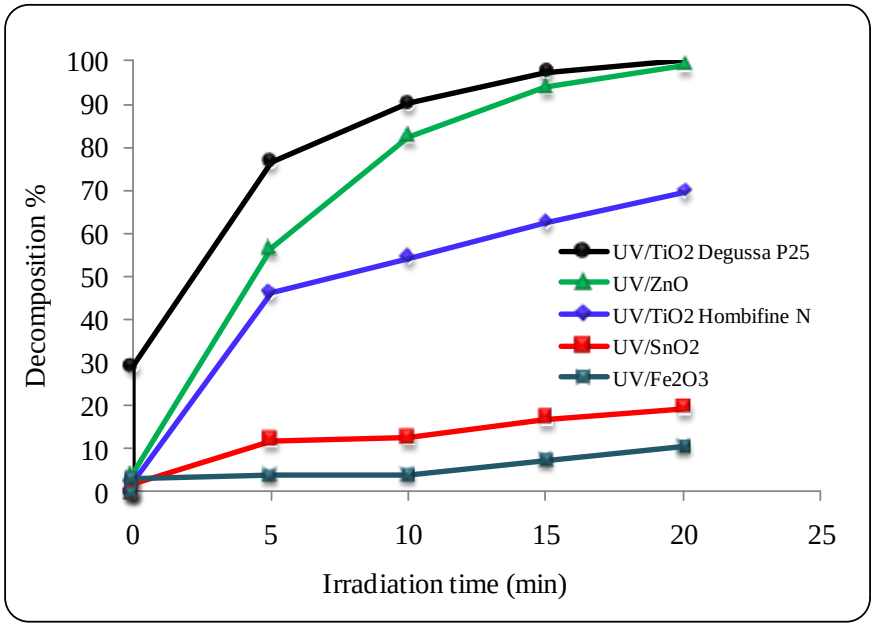

Figure 5.8: Performance of different catalysts on the decolourisation of RO16.

5.1.4 Kinetics of photodegradation

The trends of concentration changes as function of time discussed in previous sections reveal that the decolourisation of RO16 followed a first-order kinetics with a rate constant that depended on catalyst concentration. As expected, the effect of the TiO_2 concentration on the degradation kinetics was significant, confirming the positive influence of the increased number of TiO_2 active sites on the process kinetics. The photocatalytic degradation of various organic compounds by means of illuminated TiO_2 can be formally described by the Langmuir-Hinshelwood (L-H) kinetics model (Equation 5.3), (Bahnemann el at., 1999). In this model d*c*/d*t* is the rate of degradation, k is the apparent reaction rate constant, K is the adsorption coefficient of the substance to be degraded and *c* is its concentration at a time *t*.

$$-\frac{dc}{dt} = \frac{kKc}{1+Kc} \tag{5.3}$$

The L-H equation simplifies for low concentrations of pollutants ($Kc << 1$) to a pseudo-first-order kinetic equation (Equation 5.4) where *k* is the pseudo-first-order rate constant and c_0 is the initial dye concentration at t=0.

$$-\frac{dc}{dt} = kc \quad \text{or} \quad c_t = c_0 e^{-kt} \tag{5.4}$$

A linear form of (Equation 5.4) is given by:

$$Ln(c) = Ln(c_0) - kt \tag{5.5}$$

According to (Equation 5.5), plots of Ln(C) as function of t were made and straight lines were obtained, which confirms the validity of the proposed first-order kinetics model Figures (5.9, 5.10 and 5.11).

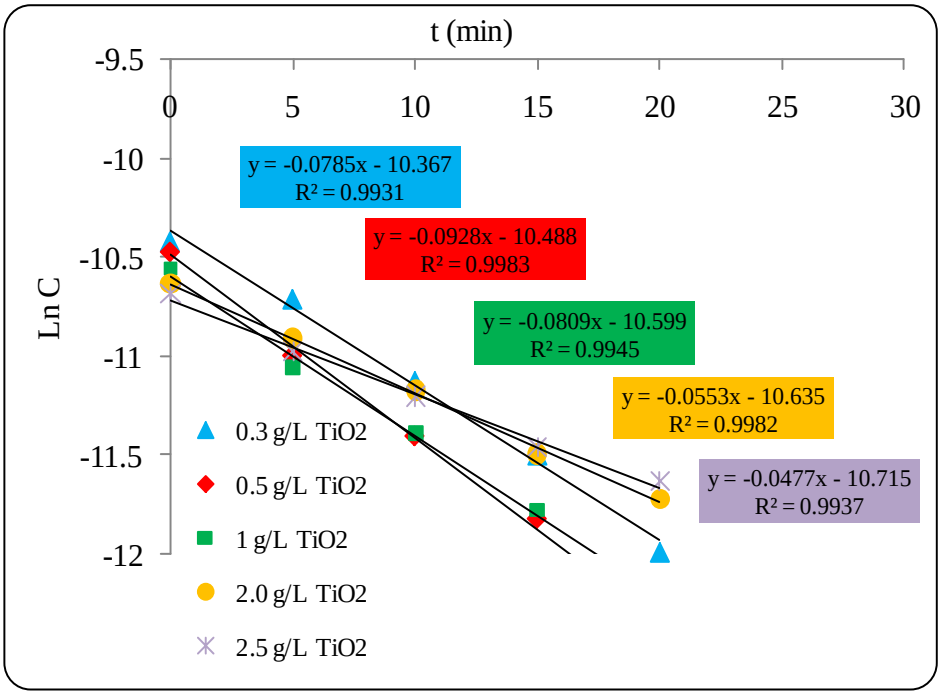

Figure 5.9: kinetic plot of the photodegradation of RO16 [C_0=20 mg L^{-1} (3.24×10^{-2} mM), pH=5.6 Power=200W].

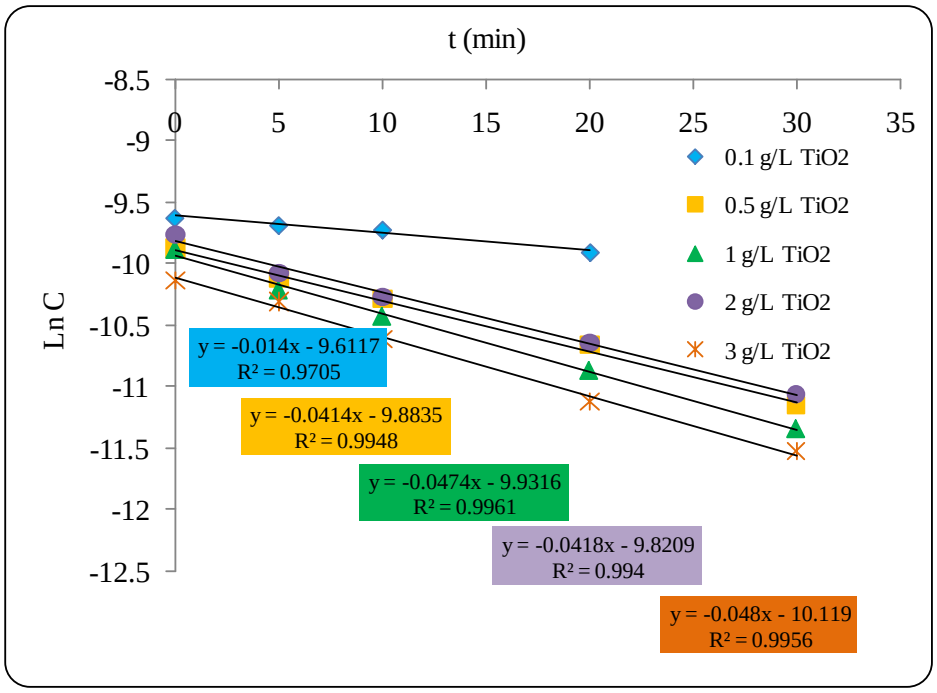

Figure 5.10: kinetic plot of the photodegradation of RO16 [C_0=40 mg L^{-1} (6.48×10^{-2} mM), pH=5.5 Power=200W].

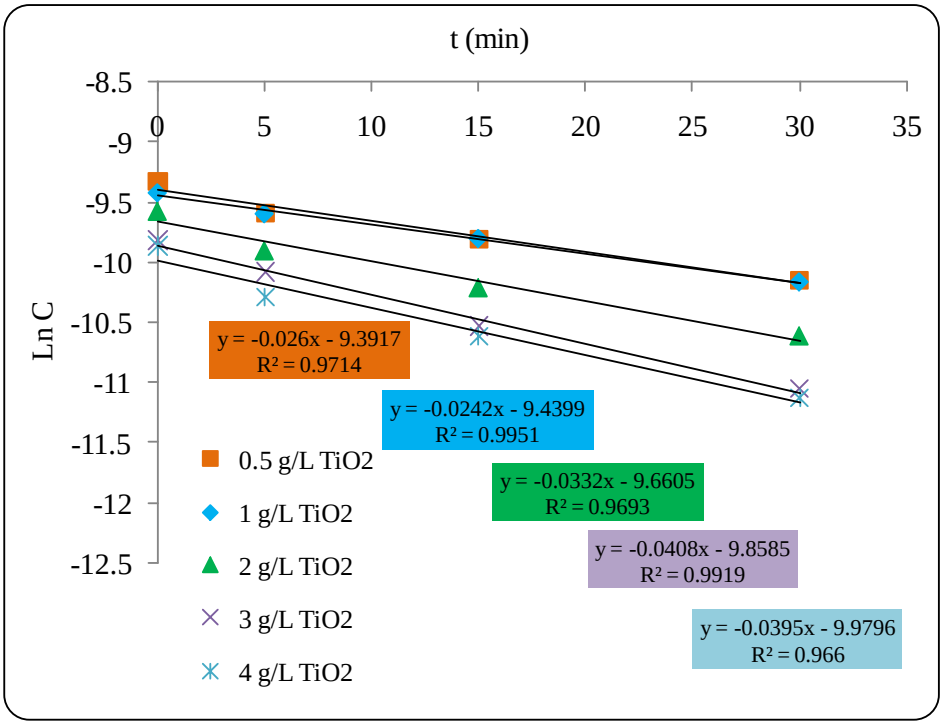

Figure 5.11: kinetic plot of the photodegradation of RO16 [C_0=60 mg L^{-1} (9.72×10^{-2} mM), pH=5.5 Power=200W].

Table 5.3 shows rate constant versus different concentrations of TiO_2.

Table 5.3: Values of rate constant at 20, 40 and 60 mg/L (3.24×10^{-2}, 6.48×10^{-2} and 9.72×10^{-2} mM) RO16 with different concentrations of TiO_2.

Dye concentration (mg/L)	TiO_2 (g/L)	Rate constant k (min^{-1})
20	0.3	8.4×10^{-2}
	0.5	9.3×10^{-2}
	1.0	7.3×10^{-2}
	2.0	5.7×10^{-2}
	2.5	5.7×10^{-2}
40	0.1	3.9×10^{-2}
	0.5	5.3×10^{-2}
	1.0	4.3×10^{-2}
	2.0	4.4×10^{-2}
	3.0	3.7×10^{-2}
60	0.5	3.8×10^{-2}
	1.0	5.0×10^{-2}
	2.0	3.7×10^{-2}
	3.0	3.2×10^{-2}
	4.0	3.4×10^{-2}

The results sketched in Figure 5.12 indicate that the rate constant *k* increases up to a maximum as a function of catalyst concentration and tends to decrease upon further increase in catalyst concentration. The increasing trend of *k* with catalyst concentration is related to the facts that (a) catalyst loading increases the total surface area of the catalyst for RO16 to be adsorbed (b) the increased amount of catalyst produces proportional amount of $^{\bullet}OH$ radicals by absorbing increased numbers of photons which are sufficient and readily accessible to nearby RO16 to decolorize (Garcia and Takashim 2003). The optimum catalyst loading was found to be 0.5 g/L. Consequently, loadings higher than 0.5 g/L, could not further accelerate the decolorization efficiency because (i) agglomeration might have taken place which must reduce the total active surface area to adsorb RO16 and to absorb UV radiation in order to promote the degradation of RO16 (ii) higher concentrations of catalyst create turbidity. Turbidity is capable to reduce the penetration of UV radiation by the scattering effect (Bekbolet and Ozkosemen 1996).

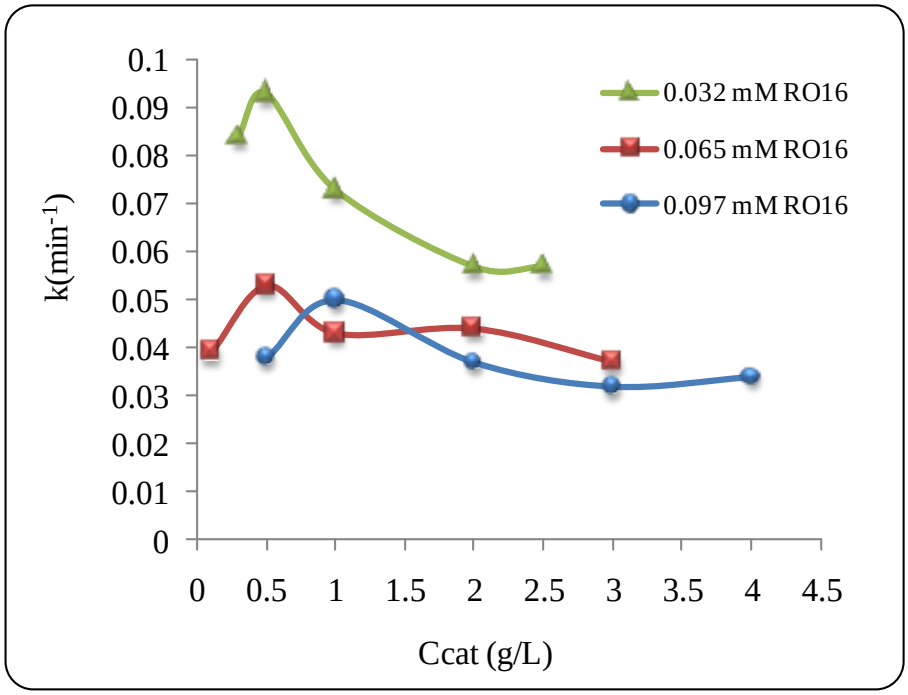

Figure 5.12: Effect of TiO_2 concentration on RO16 degradation rate constant [C_0=20, 40 and 60 mgL^{-1} (3.24×10^{-2}, 6.48×10^{-2} and 9.72×10^{-2} mM), pH=5.5, Power=200W].

5.1.5 Effect of the operating parameters

5.1.5.1 *Effect of pH on RO16 decolourisation*

pH is one of the most important parameters that influences the photocatalytic degradation. Therefore, the degradation of RO16 was studied at different pH values from 3 to 11 and the results are shown in Figure 5.13. For altering pH in the acidic and in alkaline regions H_2SO_4 and NaOH solutions were used respectively.

The results in Figure 5.13 show that as the pH of the dye solution was reduced from 11 to 5.5, the degradation was observed to increase from 82.10% to 91.29% at 30 minutes, but at pH 3.5 the degradation decreased again (75.18% at 30 minutes). Therefore, the highest efficiency of degradation was observed at pH 5.5.

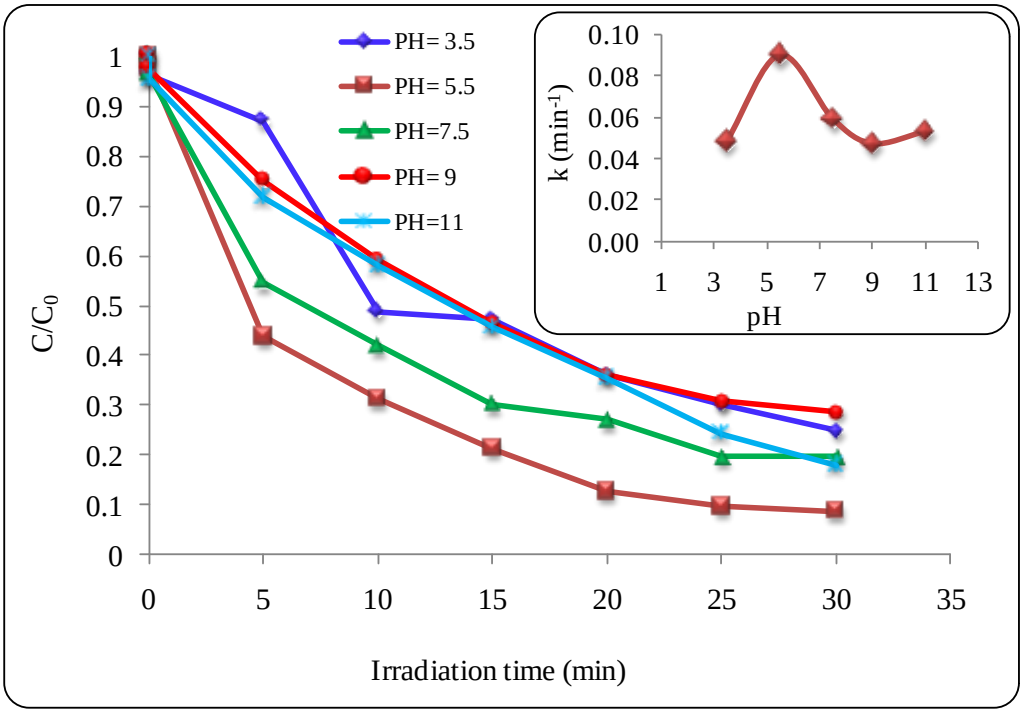

Figure 5.13: Effect of pH on RO16 decolourisation [C_0=20 mg L^{-1} (3.24×10^{-2} mM), Ccat=1gL^{-1}, Power=200W].

Similar observation has been reported by Sohrabi and Ghavami (2010) in their study of photocatalytic degradation of Direct Yellow 12 dye. The effect of the pH of solution on the degradation rate can be explained mainly by the sorption-desorption processes and the separation of the photogenerated electron-hole pairs on the surface of the semiconductor particles. The point of zero charge (pzc) of TiO_2 is around 6, hence in acidic suspensions; the adsorption of dye on the TiO_2 particles is significantly higher than the extent of adsorption in neutral or alkaline suspensions. At high pH, repulsion forces between the negatively charged TiO_2 surface and the negatively charged sulphonate group (SO_3^-) of the RO16 molecule could be the main cause for the observed low rates at high pH. As the pH of solution decreases, particularly beyond TiO_2 pzc, the number of positively charged TiO_2 increases, which leads to increased RO16 uptake and hence its degradation is improved. A further decrease in the pH leads to reduction in the

negatively charged RO16 molecules and as a result the attraction forces may reduce, which explains the lower decolourisation rates observed at pH 3.5.

5.1.5.2 *Effect of catalyst concentration*

The effect of TiO_2 concentration on the photocatalytic degradation of RO16 was studied. Figure 5.15, shows plots of the relative dye concentration as function of irradiation time at different catalyst concentrations. It was observed that direct photolysis had no effect on the degradation of RO16 which was explained early in (section 5.1.1, Figure 5.1) see also (Figure 5.14). But when 0.5 g/L TiO_2 was added, the degradation of the dye increased substantially giving a final concentration of RO16 of less than 2 mg/L after 25 minutes irradiation. A further increase of TiO_2 concentration decreased the degradation reaction. Therefore the optimum amount of catalyst required for the degradation of 20 mg/L (3.24×10^{-2} mM) RO16 was 0.5 g/L TiO_2. Also it was found that increasing the catalyst concentration above the optimum concentration resulted in aggregation of the catalyst particles, hence the available surface area for contact between the reactant and the photocatalyst was reduced. This would result in reduction of the active sites and leads to lower photocatalytic degradation rates.

Also, when TiO_2 was overdosed, the intensity of incident UV light was attenuated because of the decreased light penetration and increased light scattering, which embedded the positive effect coming from the dosage increment and therefore the overall performance has reduced.

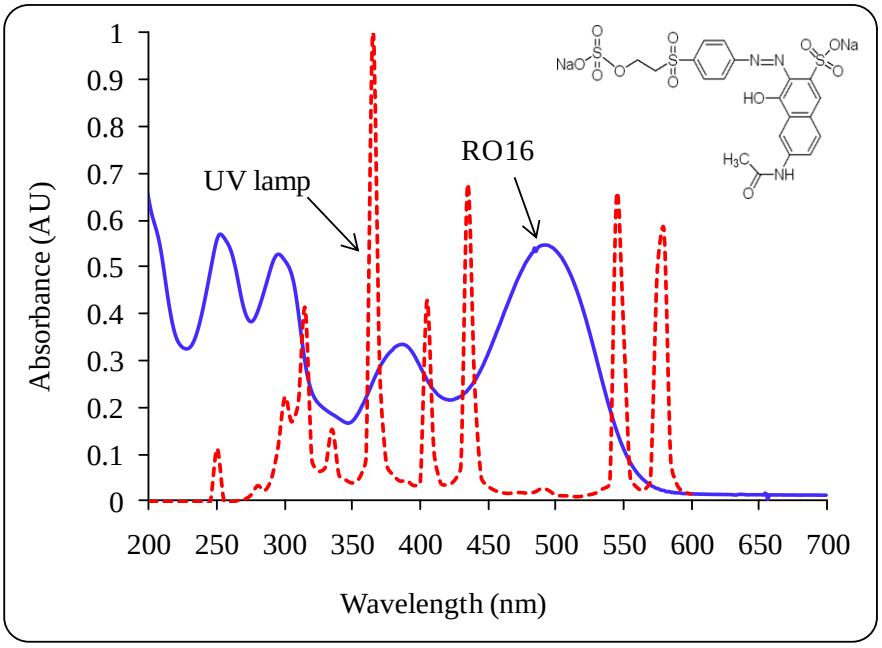

Figure 5.14: Spectral irradiance of the lamp and light absorption spectrum of RO16 [C_0=20 mgL^{-1} (3.24×10^{-2} mM), Power=200W].

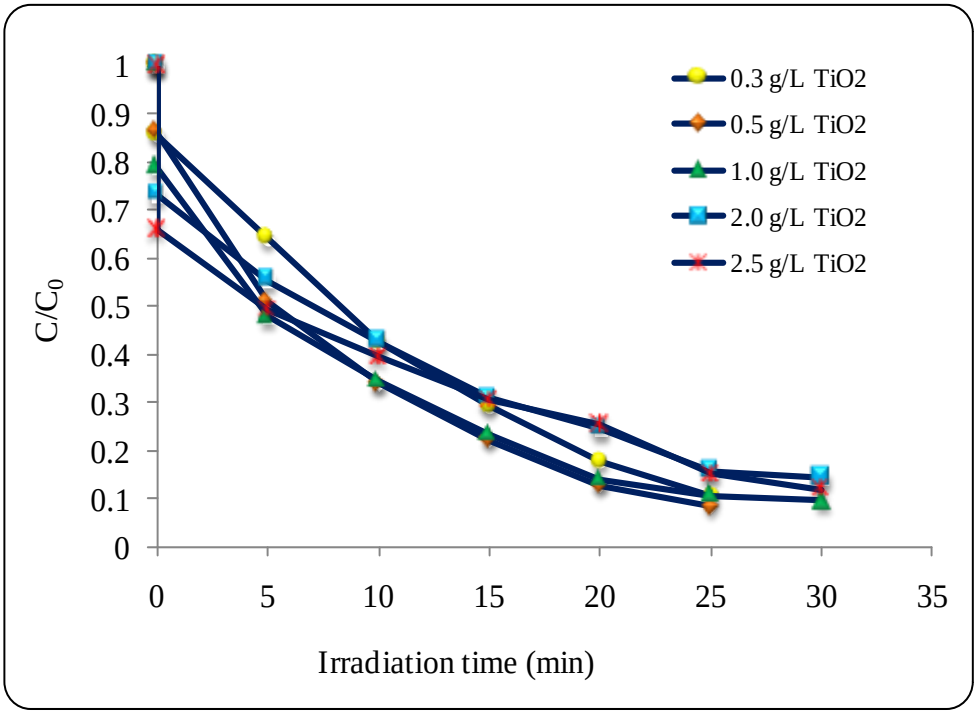

Figure 5.15: Effect of TiO_2 concentration on RO16 decolourisation [C_0=20 mg L^{-1} (3.24×10^{-2} mM), pH=5.5, Power=200W].

Experiments at various catalyst concentrations and an initial concentration of RO16 of 40 mg/L (6.48×10^{-2} mM) were also carried out and the results are shown in Figure 5.16.

As can be seen from Figure 5.16 an initial drop in RO16 concentration due to adsorption on the catalyst has also taken place. The decolourisation rate followed pseudo-first-order kinetic which depended on the catalyst concentration. The removal rate of RO16 reached a maximum in the first 30 minutes (85.42%) when the highest concentration of catalyst was used (3 g/L).

As compared to 0.1 g/L, when 0.5 g/L TiO_2 was added, the degradation of the dye increased substantially giving a final concentration of RO16 of less than 1.5 mg/L after 60 minutes irradiation, with percentage degradation of 96.83%. A further increase of TiO_2 concentration decreased the degradation reaction. Therefore the optimum amount of catalyst required for the degradation of 40 mg/L (6.48×10^{-2} mM) RO16 was also 0.5 g/L TiO_2. Moreover it was found that increasing the catalyst concentration above the optimum concentration resulted in aggregation of the catalyst particles, hence the available surface area for contact between the reactant and the photocatalyst was reduced. This would result in reduction of the active sites and leads to lower photocatalytic degradation rates.

When TiO_2 was overdosed, the intensity of incident UV light was attenuated because of the decreased light penetration and increased light scattering, which embedded the positive effect coming from the dosage increment and therefore the overall performance has reduced.

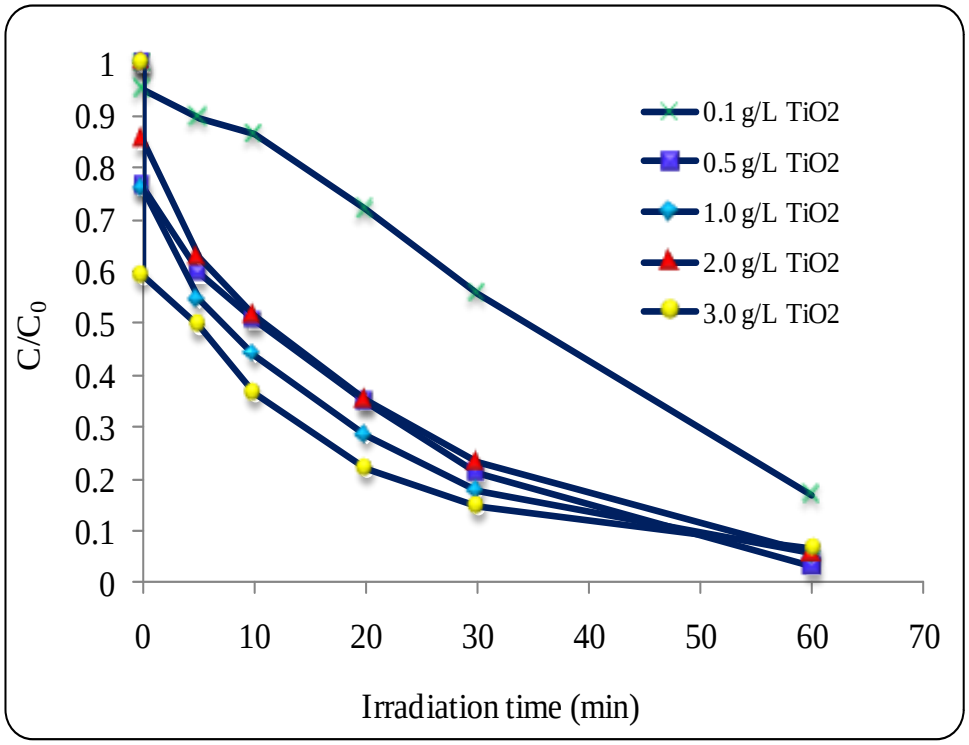

Figure 5.16: Effect of TiO_2 concentration on RO16 decolourisation [C_0=40 mg L^{-1} (6.48×10^{-2} mM), pH=5.5, Power=200W].

Further experiments at an initial concentration of RO16 of 60 mg/L (9.72×10^{-2} mM) were also carried out using various concentrations of catalyst. Figure 5.17 shows the initial drop of RO16 concentration as was observed in the other experiments. As explained earlier this initial drop was caused by adsorption of the dye to the catalyst prior to exposure of the suspension to the UV light. The decolourisation rate followed pseudo-first -order kinetic that depended on catalyst concentration which is similar to the above two cases of 20 and 40 mg/L (3.24×10^{-2} and 6.48×10^{-2} mM) RO16. As the catalyst concentration increased, the removal rate of RO16 reached a maximum at first 60 minutes (94.87%) when the highest concentration of catalyst was used (4g/L). But when 1 g/L TiO_2 was used, the degradation of the dye increased substantially giving a final concentration of RO16 of less than 0.5 mg/L after 90 minutes irradiation, with percentage removal of RO16 (99.34%).

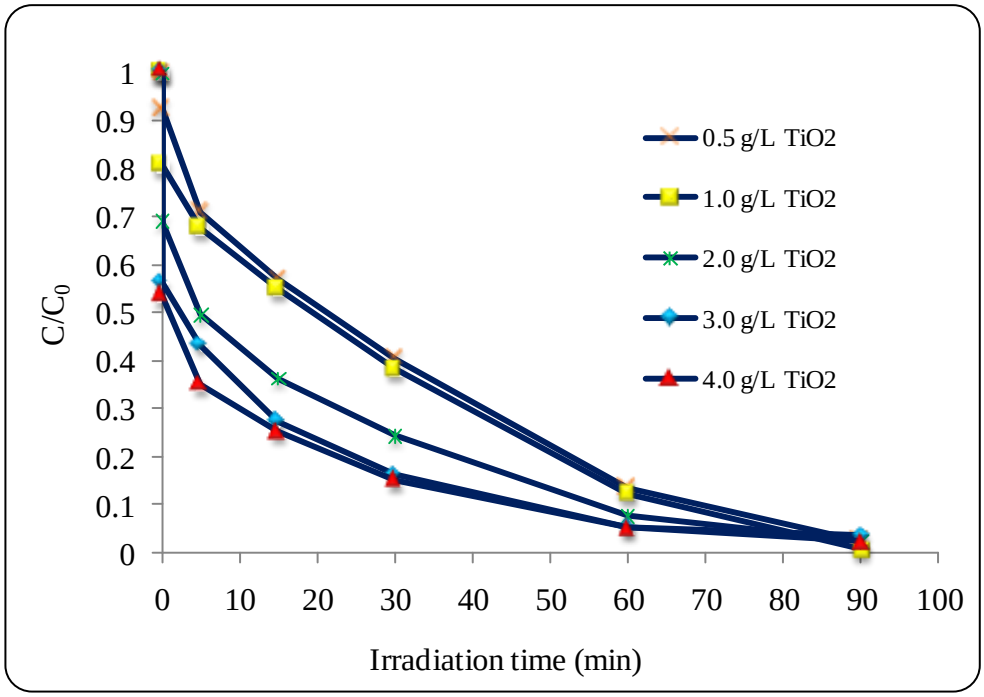

Figure 5. 17: Effect of TiO_2 concentration on RO16 decolourisation [C_0=60 mg L^{-1} (9.72×10^{-2} mM), pH=5.5, Power=200W].

5.1.5.3 *Effect of Initial concentration of RO16*

In photocatalytic oxidation of organic pollutants, reaction rates depend on light intensity, concentration of dissolved oxygen (or any other electron acceptor) and the initial concentration of the organic substrate. In this study, dye concentrations of 20, 40 and 60 mgL^{-1} (3.24×10^{-2}, $6.48\times10^{-2}$and 9.72×10^{-2} mM), were used to investigate the effect of initial dye concentration on the performance of the photocatalytic system. From Figure 5.18, it was observed that initially (i.e. at t=0) the concentration of RO16 drops to below a relative concentration of 1. This drop is mainly due to RO16 adsorption on the catalyst. The decolourisation percentages of the dye after 20 min were 86.2, 71.8 and 61.8% for initial dye concentrations of 20, 40 and 60 mg/L respectively. This result indicates that a further increase in the substrate concentration leads to a decrease in degradation rates and longer times are required to achieve a given

percentage degradation. When the concentration of RO16 was increased, the observed decrease in degradation rates may due to the unavailability of enough active sites since the amount of catalyst was kept constant for all dye concentrations studied. In spite of increasing the dye concentration, the amount of catalyst was kept constant; hence the relative amounts of O_2^- and $^{\bullet}OH$ radicals on the catalyst surface did not increase. As a consequence, the relative degradation efficiency of the RO16 decreased when its concentration increased.

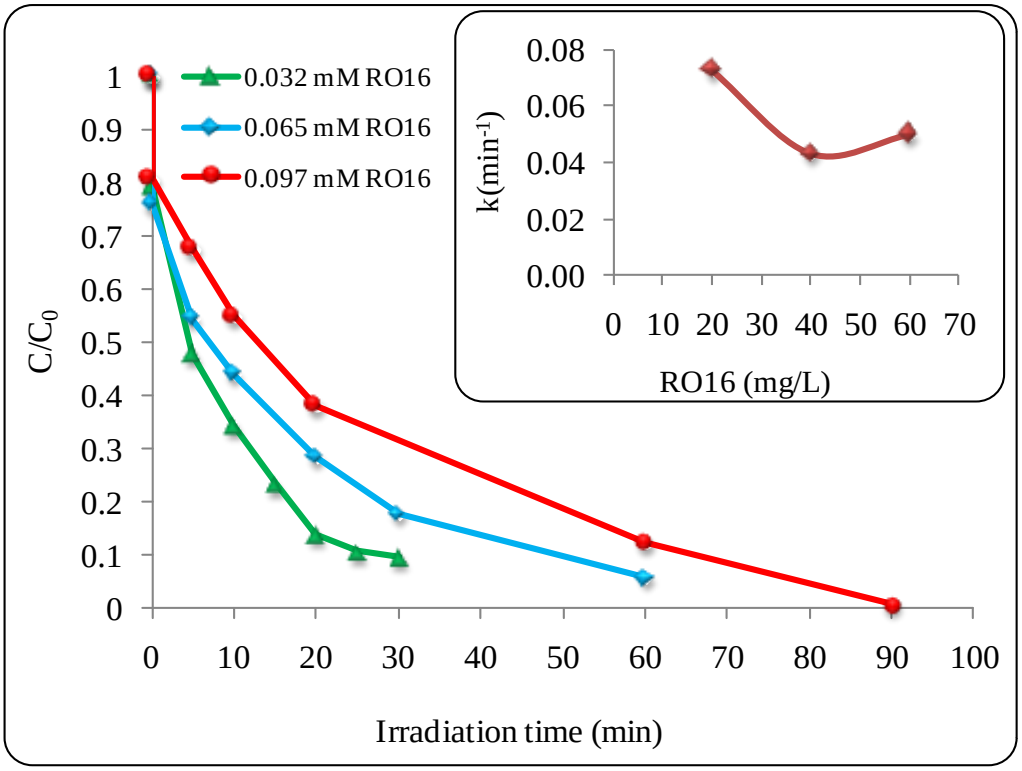

Figure 5.18: Influence of the initial dye concentration on efficiency of UV/TiO_2 photodegradation [Ccat=1.0 gL^{-1} pH=5.5, Power =200W].

5.1.5.4 *Effect of electron acceptors*

One of the more serious problems in using TiO_2 as a photocatalyst is the occurrence of the electron-hole pair recombination, which is very much pronounced in the absence of the appropriate electron acceptor, yielding potentially a lowered efficiency of the

photocatalytic process (Qamar et al., 2006). The most commonly used electron acceptor is molecular oxygen (O_2). Experiment was carried out to investigate the effect of electron acceptors on the degradation of RO16 in this study. Pure oxygen, pure nitrogen and synthetic air were compared. As can be seen from Figure 5.19, the presence of O_2 accelerated the degradation rate slightly more than N_2.

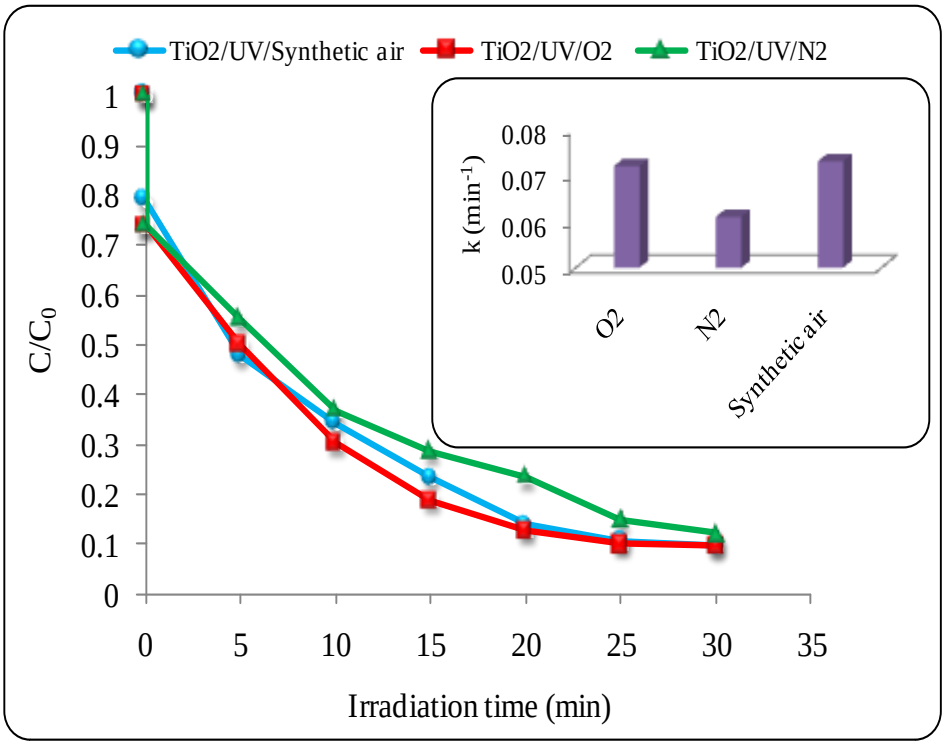

Figure 5.19: Effect of electron acceptor on the degradation of RO16 [C_0=20 mg L^{-1}, Ccat=1gL^{-1}, pH=5.5, Power=200W].

5.1.5.5 *Effect of catalyst recovery*

One of the principle aims of heterogeneous catalytic processes is to recover the catalyst for further reuse. Hence in photocatalytic processes, catalyst recovery and reuse has received considerable attention (Araña et al. 2002, Fernández-Ibáñez et al. 2003,

Pekakis et al. 2006, Reutergådh and Iangphasuk 1997, Rhoads and Davis 2004). From the economical point of view, the main advantage of using titanium dioxide as catalyst is that it can be recovered and used again as a catalyst in the degradation process. Experiments to investigate the performance of reusing the catalyst were carried out. It was observed from Figure 5.20 that the recovered catalyst could be reused. For example, under the same conditions [20 mg/L (3.24×10^{-2} mM) RO16 and 1 g/L TiO_2], fresh catalyst was able to degrade 65.71 and 90.49 % of the RO16 after 10 and 30 minutes respectively. On the other hand the recovered catalyst degraded 58.0 and 89.32 % of the dye at 10 and 30 minutes respectively. From the above observation it was found that the efficiency of recovered catalyst was just slightly lower than that of fresh catalyst. It may be due to a loss of the active sites on the catalyst as a result of the chemical reaction and UV radiation (Sojic et al., 2009). But still the catalyst can be reused since its deactivation was not highly significant.

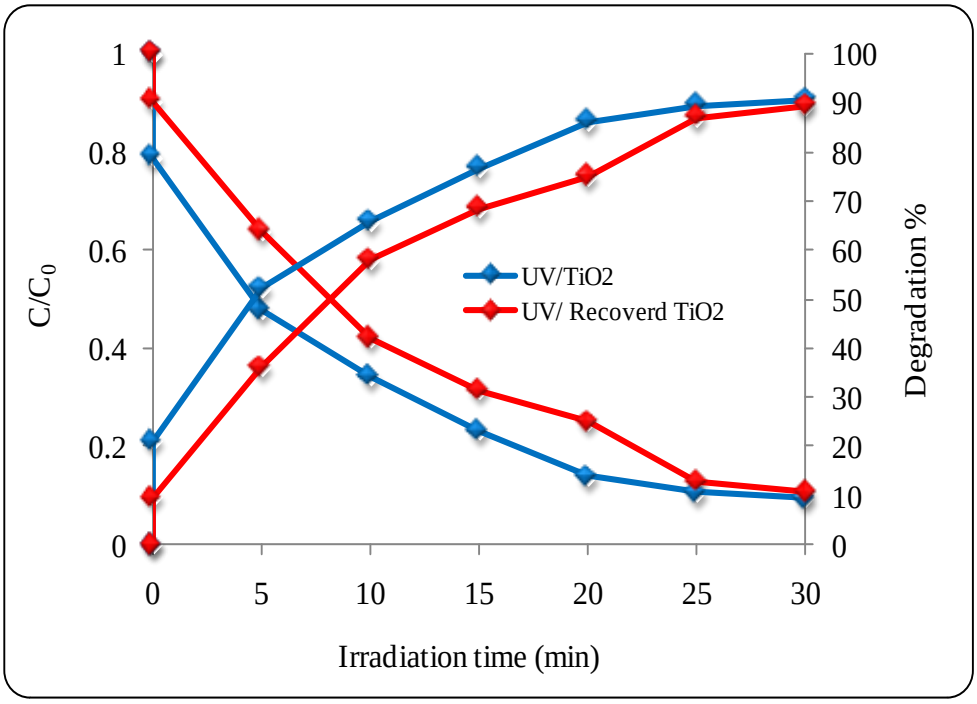

Figure 5.20: Effect of catalyst recovery on the degradation of RO16 [C_0=20 mg L^{-1}, Ccat=1gL^{-1}, pH=5.5, Power=200W].

5.1.5.6 *Effect of light intensity on photodegradation*

Light intensity is a major factor in photocatalytic degradation because electron-hole pair is produced by light energy. The effect of UV lamp power on the rate of photocatalytic degradation of RO16 was investigated by experiments using 100, 120, 150 and 200 W. Figure 5.21 shows that for an initial RO16 concentration of 20 mg/L and after 10 minutes, the overall degradation was 57.97, 65.71, 84.03 and 90.03% for the 100, 120, 150 and 200 W respectively. This indicates that the increase in the intensity of light increased the degradation rate. When irradiated for 20 minutes, the percentage degradation of RO16 was 100% at the highest lamp power (200W). Whereas the percentages were 97.37%, 86.18% and 76.23% at 150, 120 and 100 W respectively. This is because the high lamp power produced the high photon energy which can be strong to excite the active sites of the catalyst. Figure 5.21 inset shows a linear relationship between the rate constant and power. This result is in agreement with the fact that the rate of reaction is proportional to UV light intensity (Ollis et al., 1991; Terzian et al., 1995; Herrmann 1999 and Beltran 2004).

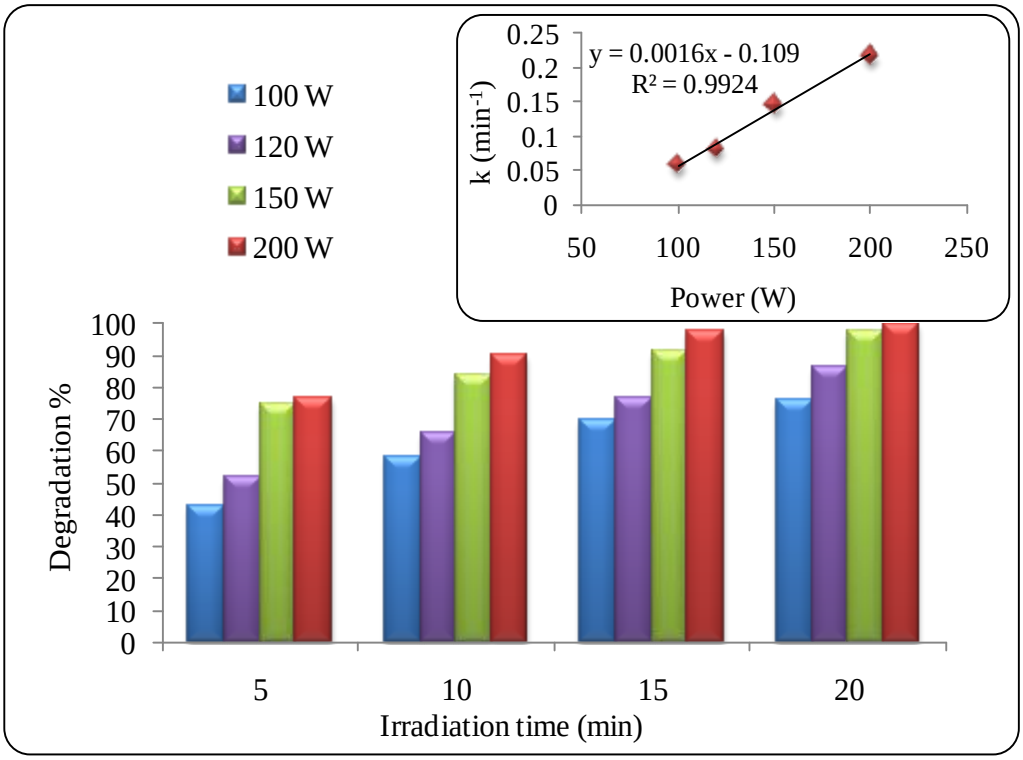

Figure 5.21: Influence of radiation intensity on photodegradation of RO16

5.1.5.7 *Effect of the glass type of the reactor window*

The effect of the glass type used to pass the light through to the solution was studied using in one experiment a reactor with quartz windows and in another experiment the same reactor but with pyrex windows. It was found from Figure 5.22 that the reactor fitted with quartz windows gave faster degradation rates as compared to the pyrex reactor. This clearly was due to the fact that quartz has low attenuation of the UV light in comparison to pyrex (Figure 5.22 inset). Although quartz gave better results than pyrex, it is still possible to use pyrex for these experiments if quartz is not available. This is true since the difference in degradation rates between the two glass types is not highly significant (Figure 5.22).

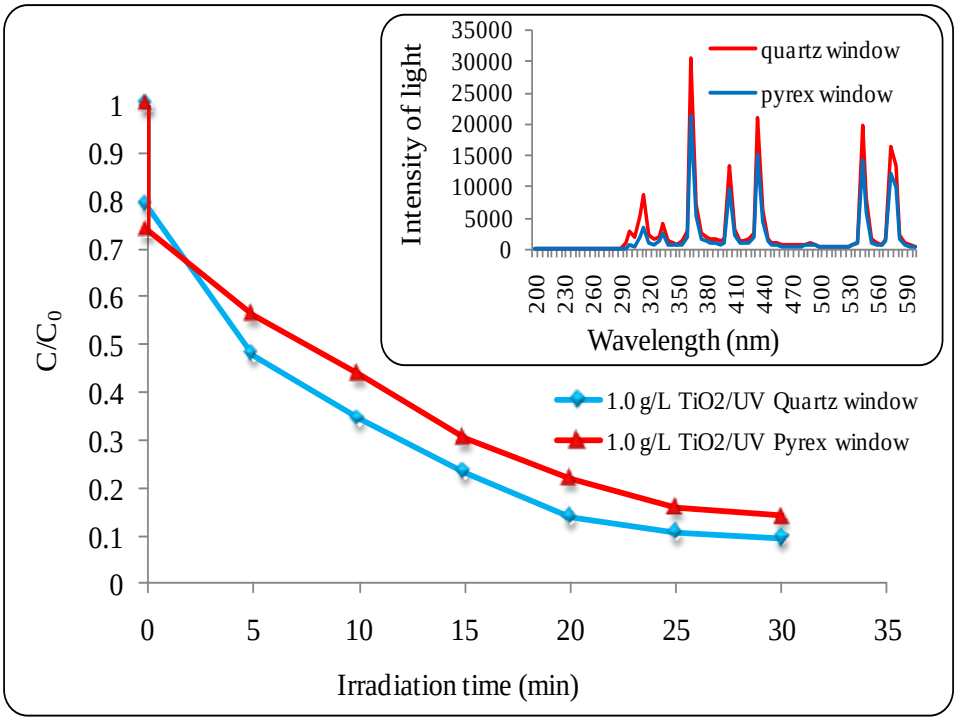

Figure 5.22: Effect of the glass type of the reactor window on degradation of RO16 [C_0=20 mg L^{-1}, Ccat=1gL^{-1}, pH=5.5, Power=200W].

5.1.5.8 *Effect of Hydrogen peroxide on photodegradation*

The rate of RO16 degradation with UV can be significantly increased by the addition of hydrogen peroxide. To investigate the influence of H_2O_2 on the rate of degradation, experiments were conducted using various concentrations of RO16 at 20, 40 and 60 mg/L **(**3.24×10^{-2}, $6.48\times10^{-2}$and 9.72×10^{-2} mM), and were irradiated with UV light (200 W) in the presence of 1.0 g/L H_2O_2 (no TiO_2 was present in solution). The results are shown in Figure 5.23. Clearly the figure shows that UV combined with hydrogen peroxide was also effective in degradation of RO16.

This effect of H_2O_2 can be explained by radical reaction mechanism (Poulios el at., 1999). According to Buxton et al. (1988) ultraviolet radiation cleaves the O-O bond in hydrogen peroxide and generates the hydroxyl radical (Equation 5.6).

$$H_2O_2 + h\nu \rightarrow 2HO^{\bullet} \quad (5.6)$$

$$H_2O_2 + HO^{\bullet} \rightarrow HO_2^{\bullet} + H_2O \quad (5.7)$$

The higher the concentration of hydrogen peroxide, the greater the UV-catalysed generation of hydroxyl radicals up to an optimal H_2O_2concentration. After this optimal concentration the excess hydrogen peroxide engages in an additional reaction which tends to scavenge hydroxyl radicals initially generated (Equation 5.7).

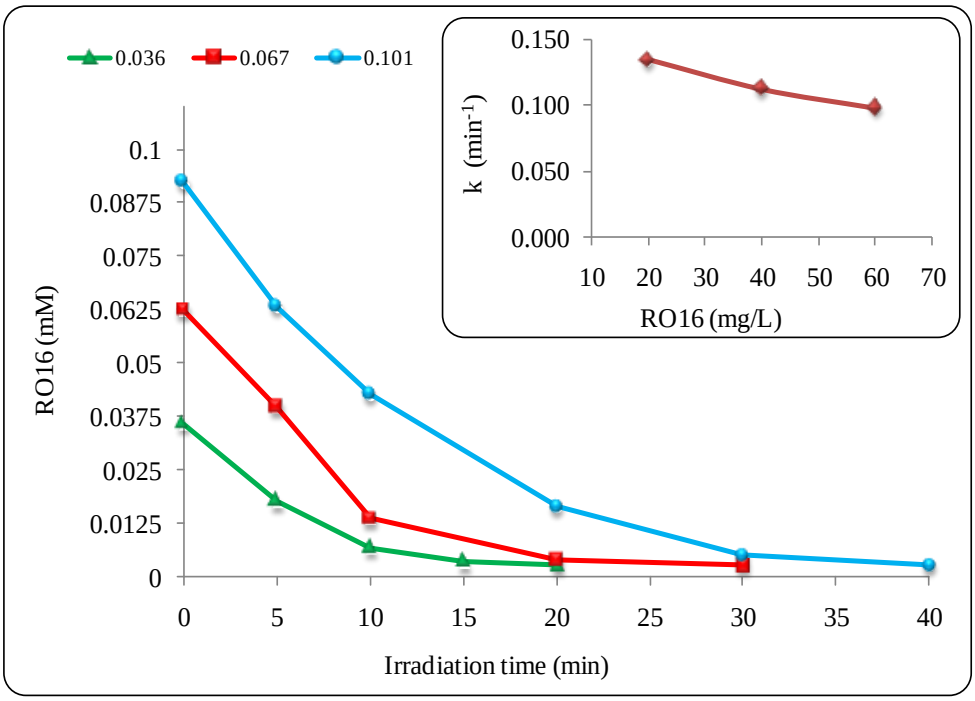

Figure 5.23: Effect of Hydrogen peroxide and UV on degradation of RO16 [(C_{RO16} =3.24×10^{-2}, 6.48×10^{-2} and 9.72×10^{-2} mM), C_{H2O2}=1gL^{-1} (0. 029 M), pH=5.5, Power=200W].

Figure 5.24 shows the experimental results obtained at initial concentration 20 mg/L (3.24$\times 10^{-2}$ mM) RO16 using (1g/L TiO_2, 1g/L H_2O_2, pH = 5.5 and power = 200 W). It is clear from the graph that the high efficiency degradation of RO16 was obtained with

UV/TiO_2 system which gave almost 100% degradation after 20 minutes reaction. On the other hand when H_2O_2 or TiO_2/H_2O_2 was irradiated with UV light, the degradations were 92.28% and 97.64% respectively. When only H_2O_2 was used, the degradation of RO16 was insignificant (only 1.41%). It should be noted that H_2O_2 can capture one electron of the conduction band and produce a hydroxyl radical hence hindering the process of electron-hole recombination and increasing the rate of the photocatalytic process (Anheden el at., 1996). However H_2O_2 can also act as a radical scavenger hence reducing the rate of dye degradation. It is therefore difficult to clearly elucidate the role of H_2O_2.

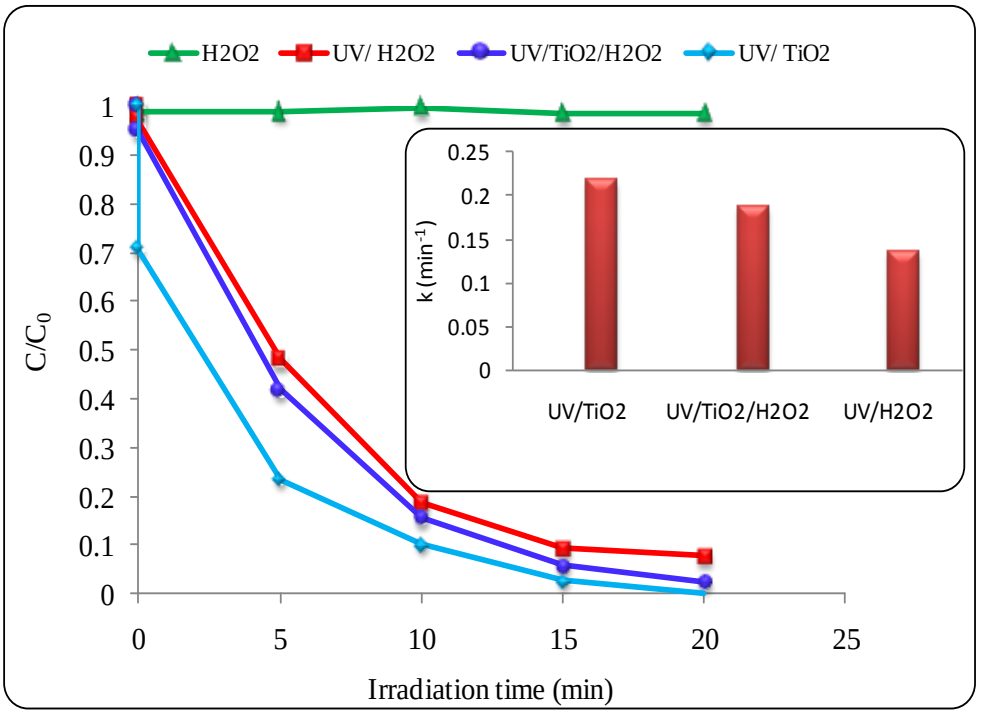

Figure 5.24: Effect of hydrogen peroxide on degradation of RO16 [C_0=20 mg L^{-1}, CH_2O_2=1gL^{-1},$CTiO_2$= 1 gL^{-1}, pH=5.5, Power=200W].

5.2 Photocatalytic degradation of TCC

The photocatalytic degradation of Triclocarban (TCC) was studied in the presence of TiO_2 /UV light. The results of the investigation are presented in this section.

5.2.1 Effect of the operating parameters

This section discusses the effect of the different variables of interest on the photocatalytic degradation of TCC solution.

5.2.1.1 *Effect of catalyst concentration on TCC degradation*

The effect of catalyst concentration on TCC degradation was studied. Figure 5.25 shows the results for the photodegradation of 15 mg/L (4.75×10^{-2} mM) TCC at varying catalyst concentrations of 0, 0.3, 0.5 and 1g/L. Figure 5.25 shows that the addition of the catalyst hindered the oxidation of TCC while UV alone was effective to degrade TCC. It was expected that the addition of the catalyst would achieve higher degradation as compared to UV alone, but this was not the case. Moreover, it was observed that as the catalyst concentration increased, the degradation efficiency decreased (Figure 5.25). It is worth mentioning that this finding was not observed by previous research works. The implication of this finding is that UV light alone is more efficient in the degradation of TCC than UV light in the presence of the catalyst. In other words the catalyst appears to be antagonising the process rather than accelerating it. Consequently the process of degradation of TCC in water is photolytic rather than photocatalytic. Although the reason for this phenomenon is not fully clear it is still suspected that this happens

because the presence of acetonitrile in large quantity in solution may scavenge the radicals formed as a result of the photocatalytic process and may also act as the main electron donor in the photocatalytic reaction. The other explanation is that acetonitrile may also compete TCC adsorption. Hence the photocatalytic degradation rates of TCC are hindered by the presence of acetonitrile.

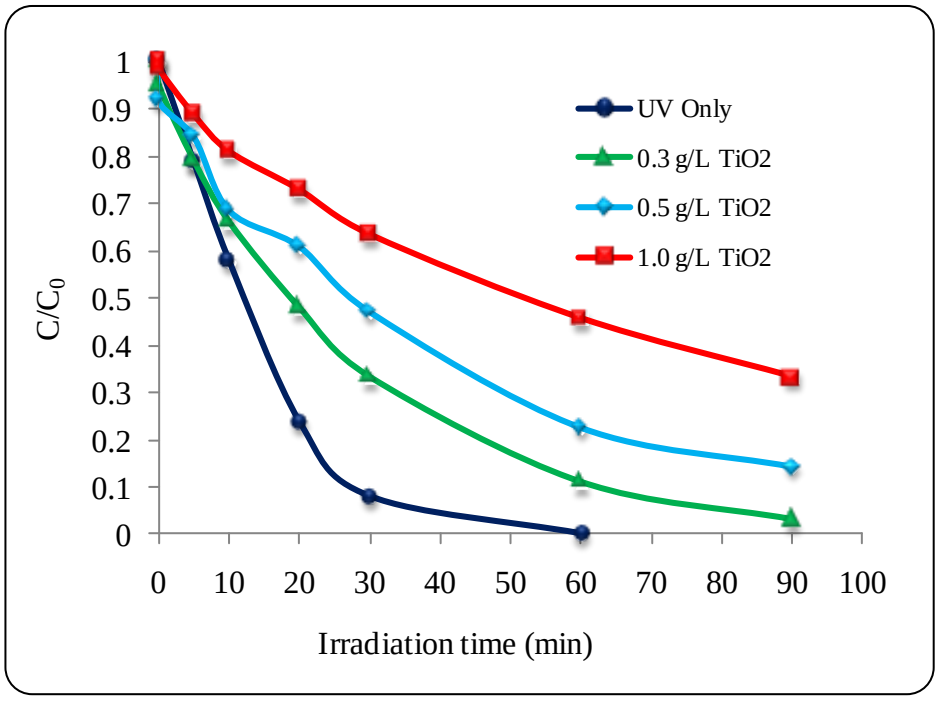

Figure 5.25: Effect of catalyst concentration on degradation of TCC [C_0=15mgL^{-1} (4.75×10^{-2} mM), pH=6.5 and Power=200 W].

Additional experiments at TCC concentrations of 20 and 50 mg/L (6.34×10^{-2} and 1.58×10^{-1} mM) were also carried out. The results of these experiments are shown in Figures 5.26 and 5.27. These figures clearly show that the same behaviour has also been observed at higher TCC concentrations.

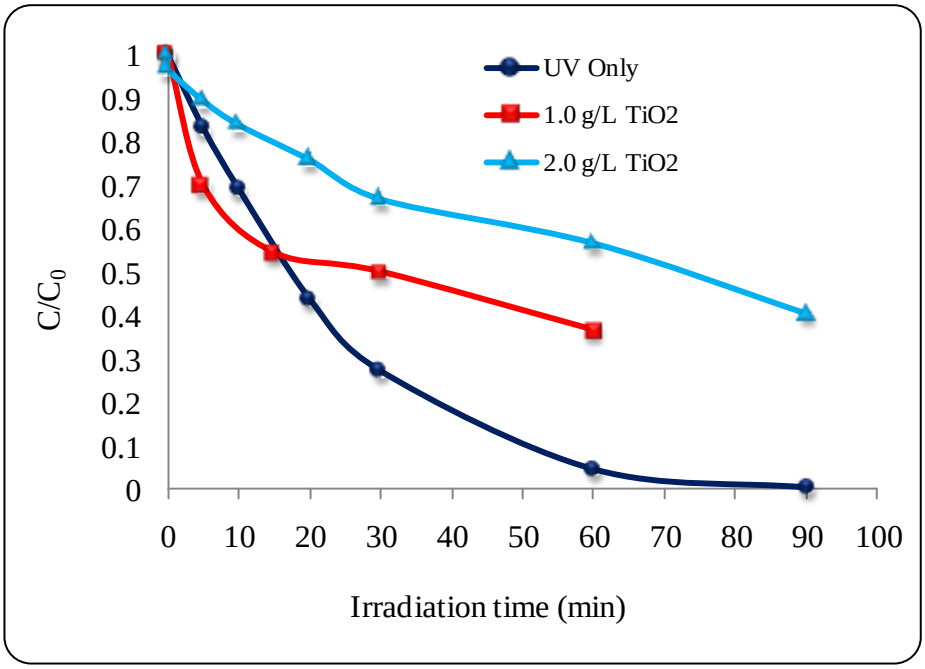

Figure 5.26: Effect of catalyst concentration on degradation of TCC [C_0=20 mgL^{-1} (6.34×10^{-2} mM), pH=6.5 and Power=200 W].

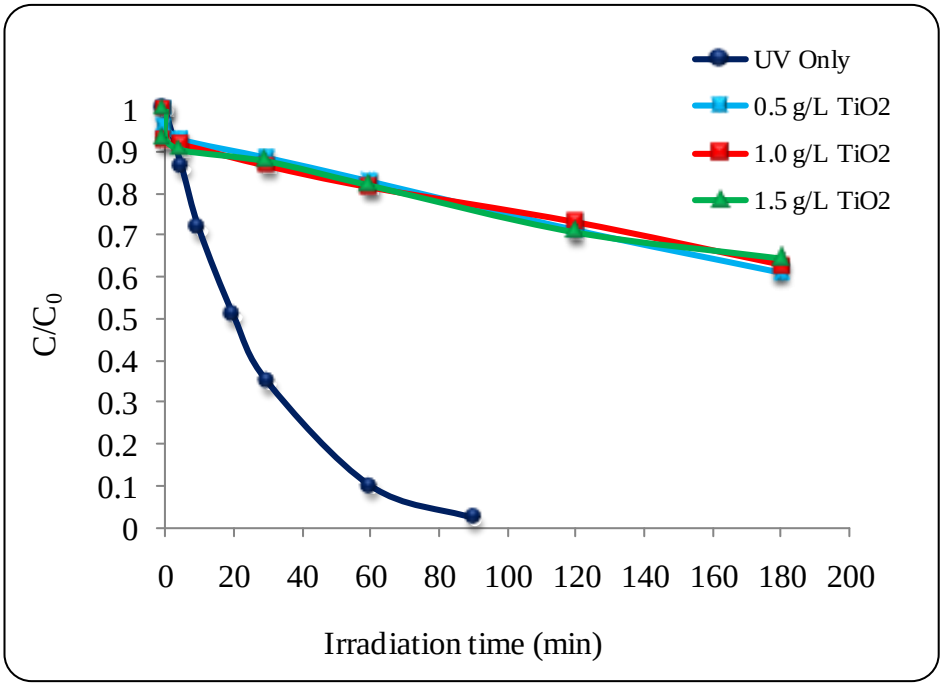

Figure 5.27: Effect of catalyst concentration on degradation of TCC [C_0=50 mgL^{-1} (1.58×10^{-1} mM), pH=6.5 and Power=200 W].

Since the photocatalytic degradation of TCC was not effective, further experiments involving UV only and UV/H_2O_2 systems were carried out. The results obtained are discussed in the following paragraphs.

5.2.1.2 *Effect of TCC concentration on UV alone degradation*

The effect of initial concentration of TCC on the photolytic degradation process was investigated. Three different concentrations of TCC 15, 20 and 50 mg/L (4.75×10^{-2}, 6.34×10^{-2} and 1.58×10^{-1} mM) were tested and the results are shown in Figure 5.28. These results indicate that increasing TCC initial concentration led to a decrease in degradation rates. For 4.75×10^{-2} mM, TCC degradation was 92.10% after 30 minutes irradiation. Whereas at the same time, the degradations were 72.72% and 65.17% for 6.34×10^{-2} and 1.58×10^{-1} mM TCC solutions respectively. Beside that the degradation of TCC reached 100% after 1 hr irradiation at 15 mg/L TCC and reached 95.33 and 89.92% at 6.34×10^{-2} and 1.58×10^{-1} mM TCC respectively.

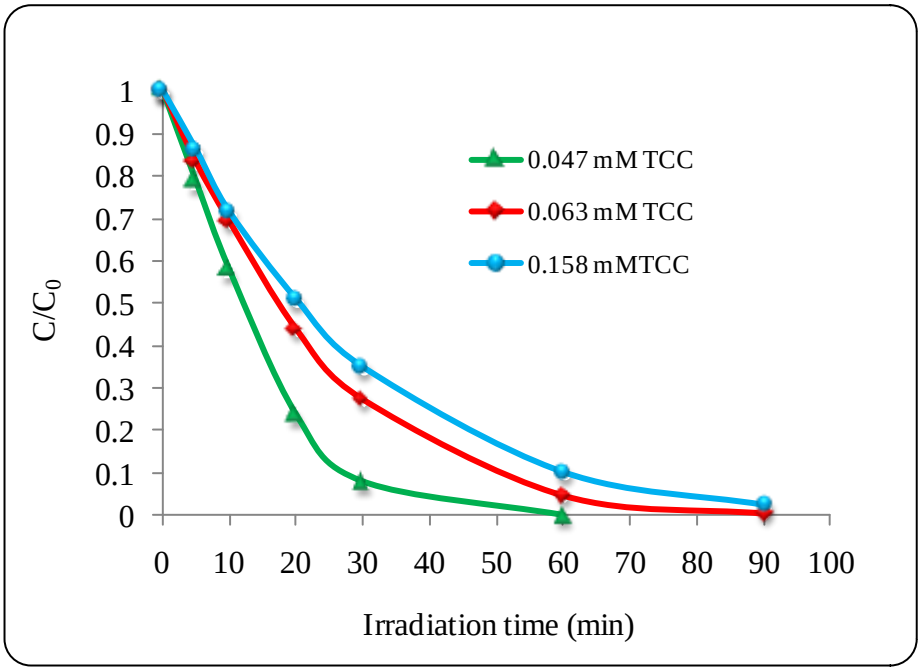

Figure 5.28: Effect of initial concentration on TCC degradation[Ccat= 0 gL^{-1}, pH=6.5 and Power=200 W].

5.2.1.3 *Effect of H_2O_2 on TCC degradation*

To further monitor the degradation behaviour of TCC in the presence of UV light, hydrogen peroxide (H_2O_2) was added to the solution instead of TiO_2. The experiment was carried out with two different concentrations of H_2O_2, 1 and 2 g/L (0.029 and 0.059 M) respectively under the same conditions as in subsection 5.2.1.2. Unlike TiO_2, H_2O_2 was found to be neutral in the degradation process. In other words rather than increasing the efficiency of the process or even retarding the process like TiO_2, H_2O_2 did not cause any significant influence on the degradation of TCC (Figure 5.29).

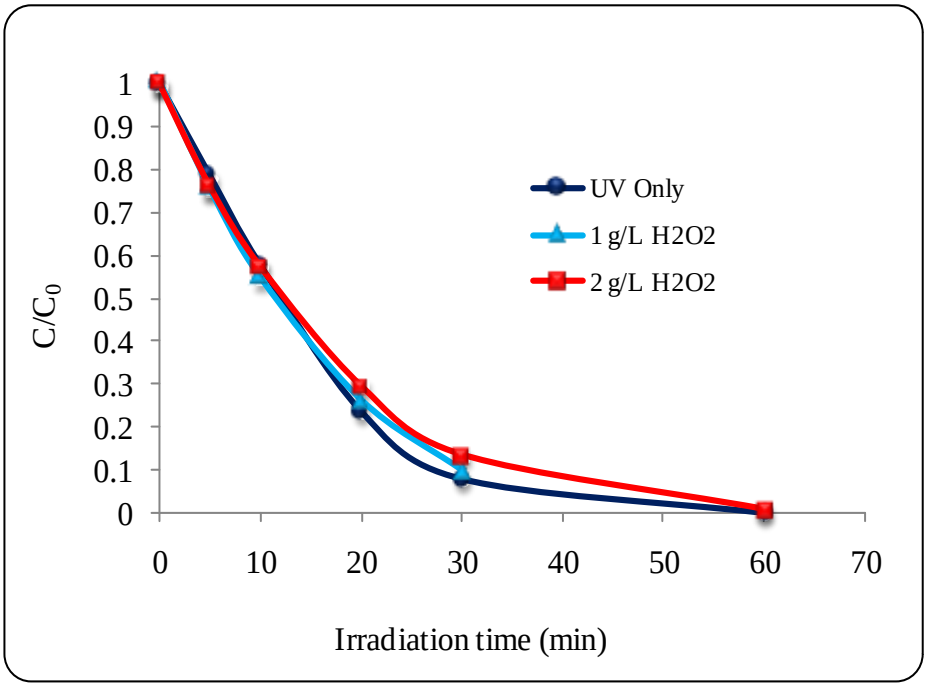

Figure 5.29: Effect of H_2O_2 on degradation of TCC [C_0=15 mgL^{-1} (4.75×10^{-2} mM), pH=6.5 and Power=200 W].

5.3 Photocatalytic degradation of clopyralid (3, 6-DCP)

5.3.1 Photodegradation of 3, 6-DCP with UV/TiO_2

5.3.1.1 *Selection of the photocatalyst*

The determination of optimum operating conditions for photocatalytic processes is essential for their effectiveness. Operating conditions such as pH, adsorption, initial contaminant concentration, catalyst type and concentration, and irradiation intensity all have a profound influence on the kinetics and the extent to which pollutants are degraded by UV/TiO_2. Three types of TiO_2 photocatalysts were used, namely the well-known Degussa P25, its homologue VP Aeroperl, and Hombifine N. The degradation performance of these photocatalysts is shown in Figure 5.31. Hombifine N showed the least performance as compared to Degussa P25 and VP Aeroperl catalysts. Degussa P25

showed almost a linear decrease of clopyralid concentration with time but VP Aeroperl gave almost exponential decrease of the concentration. The figure shows that VP Aeroperl seems to give similar performance to Degussa P25 and outperformed Hombifine N. Higher degradations above 88% were most suitably obtained with Degussa P25 since for example a degradation of 95% is achieved within 82 min for Degussa P25 as compared to 92 min for VP Aeroperl. Similar degradation efficiencies between Degussa P25 and VP Aeroperl were also observed by (Malato et al. 2003). However, the authors did not recommend VP Aeroperl because it forms agglomerates that settles easily, which reduces the photocatalytic degradation.

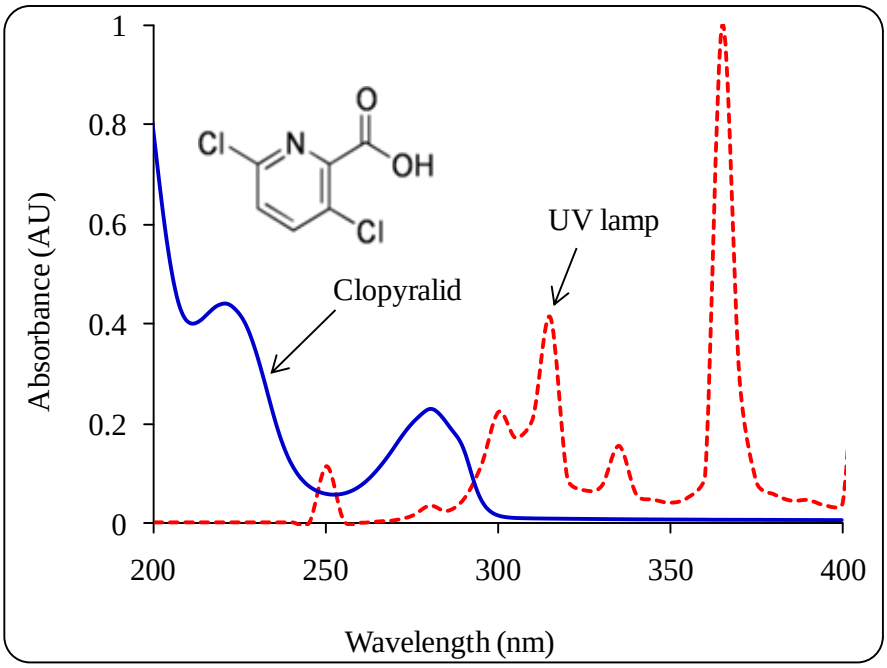

Figure 5.30: Chemical structure of clopyralid, its UV/Vis spectrum, and the relative spectral irradiance of the lamp used in this study.

Light attenuation measured as the percentage of irradiance leaving the reactor containing a suspension of the photocatalyst at 1g/L relative to the irradiance measured

without photocatalyst at a wavelength of 365 nm (the wavelength at which the lamp emits the highest intensity of light - Figure 5.30) is shown in Figure 5.31 inset. Irradiance measurements were made by a spectroradiometer (Bentham Instruments, Reading, UK). If light scattering is assumed negligible and the difference in irradiance is assumed only due to light absorption by the photocatalyst, clearly Figure 5.31 inset shows that Degussa P25 presented the highest light absorption while Hombifine N presented the lowest light absorption. This is possibly the main reason explaining the differences in degradation rates between the photocatalysts as observed in Figure 5.31. Although Hombifine N presents the largest surface area, its poor light absorption capability seems more significant in terms of photocatalytic degradation of clopyralid. This is clearly in agreement with the fact that even though Degussa P25 has low surface area, it showed high degradation rates due to its high capability to absorb UV light. Therefore it can be concluded that photocatalytic degradation of clopyralid is more prone to the photocatalyst efficiency of absorbing light than its surface area. In this respect, it is also important to point out that the crystallinity of the photocatalyst plays equally an important role. Figure 5.31 (inset) also shows that VP Aeroperl was more efficient in absorbing light as compared to Hombifine N, which also explains the better degradation rate obtained by VP Aeroperl. Since Degussa P25 showed better degradation of clopyralid as well as better light absorption, it was selected for carrying out the remaining experiments.

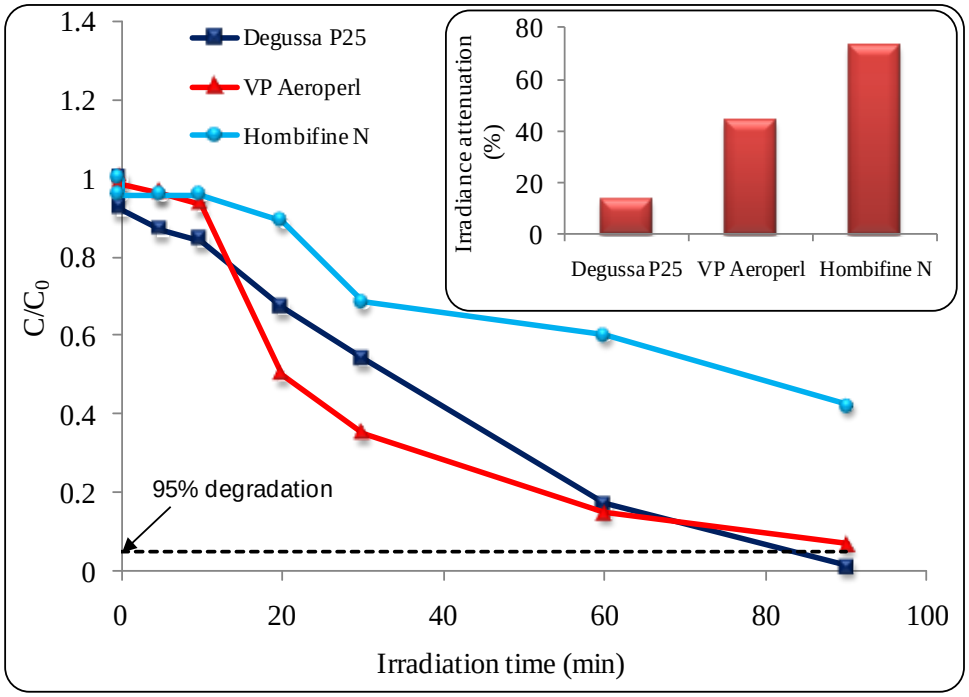

Figure 5.31: Effect of photocatalyst type on the degradation of clopyralid [C_0=0.078 mM, Ccat=1gL^{-1}, pH=7, Power=200W].

5.3.2 Effect of the operating parameters

5.3.2.1 *Effect of catalyst concentration*

Due to the inherent nature of heterogeneous photocatalytic systems, there is always an optimum catalyst concentration at which the degradation rate is at its maximum. In this study, this optimum was determined by changing the concentration of Degussa P25 over the range 0 to 2 g/L. Figure 5.32 shows that irradiation without photocatalyst (i.e. C_{cat}=0 g/L) was ineffective to degrade clopyralid. This was expected since a herbicide should withstand, amongst other processes, photolytic degradation so it can remain active for longer periods of time. Moreover, Figure 5.30 shows that the UV spectral irradiance of the lamp gives low intensities in the region of wavelengths at which clopyralid absorbs UV light, which also explains the inefficient photolytic degradation of clopyralid by UV

only. The addition of Degussa P25 to the solution at a concentration of 0.5 g/L resulted in a rapid degradation rate, which is further improved when the catalyst concentration was increased to 1 g/L. A further increase of catalyst concentration to 2 g/L resulted in a reduction of the degradation rate. The trends of change of clopyralid concentration with time shown in Figure 5.32 for decompositions less than approximately 90% can be described by a pseudo-zero-order reaction kinetics, which is in agreement with the Langmuir-Hinshelwood kinetic model (Alekabi and Serpone 1988). The rate constants were calculated at the different catalyst concentrations and the results are shown in Figure 5.32 inset. The range of rate constants obtained in this study agrees with that reported by Abramovic et al. (2007). Figure 5.32 inset shows clearly that a catalyst concentration of 1 g/L is optimum hence it was selected to carry out the further experiments. Optimum catalyst concentration is a complex function of many parameters including catalyst agglomeration, the suspension opacity, light scattering, mixing, reactor type, and the pollutant type (Mendez-Arriaga et al. 2008, Toor et al. 2006), hence it is not constant for all photocatalytic systems. Indeed, optimum catalyst concentrations have been reported to vary between as low as 0.1 g/L to as high as around 10 g/L (Alhakimi et al. 2003, Chu et al. 2009, Mendez-Arriaga et al. 2008). Notwithstanding, an optimum catalyst concentration of around 1g/L was generally reported by many studies (Chen and Ray 1998, Lu et al. 1999, Mendez-Arriaga et al. 2008, Rajeswari and Kanmani 2009). The drop in concentration observed in Figure 5.32 at time zero is due to clopyralid adsorption on the catalyst (Serrano and deLasa 1997). The extent of such drop increases with increasing the catalyst concentration as shown in Figure 5.32 for points at time zero.

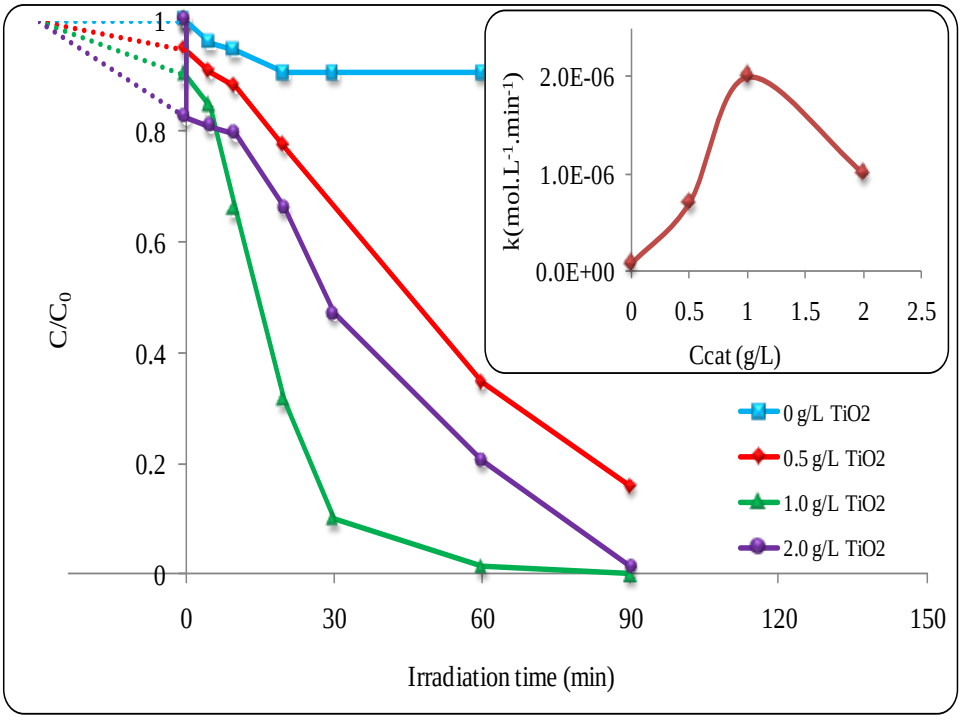

Figure 5.32: Effect of photocatalyst concentration on the degradation of clopyralid [C_0=0.078 mM, Power=200 W, pH=5].

5.3.2.2 *Effect of pH*

The effect of pH is very important in heterogeneous photocatalytic degradation of organic molecules since it influences both the surface charge of TiO_2 and the ionic form of the reactant, hence influencing the electrostatic interactions between the reactant and the catalyst surface. It was reported that TiO_2 has a zero point charge (zpc) of approximately 6.35 (Figure 5.33). Hence the surface of TiO_2 is positively charged ($TiOH^+$) in acidic solutions (pH<6.35), which is favorable for attracting anions, and TiO_2 deprotonates in alkaline solutions (pH>6.35) hence its surface becomes negatively charged (TiO^-), which is favorable for repelling anions (Halmann 1996). Moreover, pH influences the sizes of TiO_2 aggregates, interaction of the solvent molecules with the catalyst and the type of radicals or intermediates formed during the photocatalytic reaction. All of these factors have a significant influence on the adsorption of solutes on

TiO_2 surfaces and as a result the observed degradation rates. In this study the pH of the solution was changed between 3 and 11 to investigate its influence on clopyralid degradation. Figure 5.33 shows that as the pH increased from 3 to 5, the pseudo-zero-order rate constant, k, also increased but a further increase of pH up to 11 resulted in a decline of the rate constant. Clopyralid is a weak acid having pKa values of 1.4 and 4.4 (Corredor et al. 2006), hence its ionisation proceeds as shown by Equations 5.8 and 5.9.

$$AH_2 \xleftrightarrow{pKa=1.4} AH^- + H^+ \quad (5.8)$$

$$AH^- \xleftrightarrow{pKa=4.4} A^{2-} + H^+ \quad (5.9)$$

where: AH_2= 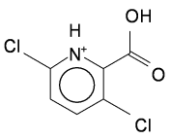 ; AH^-= 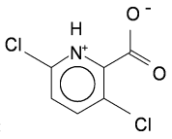 ; A^{2-}= 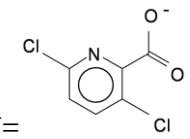

The concentrations of each of the three forms of clopyralid as function of pH are calculated and are presented in Figure 5.33. In addition, the total ionic charge resulted from AH^- and AH^{2-} is also shown in Figure 5.33. On the other hand, depending on the pH, TiO_2 also ionises to positively and negatively charged species and the profile of the ionic forms of TiO_2 as function of pH is also presented in Figure 5.33; data was adopted from (Preocanin and Kallay 2006). Figure 5.33 shows that at low pH, less than the point of zero charge of TiO_2 (pzc≈6.35), clopyralid ionises significantly to anions and the surface charges of TiO_2 is predominantly positive. This creates a favourable condition for adsorption of clopyralid on the surface of TiO_2, hence high degradation rates.

Notwithstanding, at pH 3 the rate of degradation is lower than that at pH 5. This can be explained by the fact that at pH 5 (dominant ionic form is di-anion A^{2-}), the resulting total negative charge of clopyralid is much stronger than at pH 3 (dominant ionic form is mono-anion AH^-) (Figure 5.33), therefore the adsorption of clopyralid on TiO_2 surfaces is stronger at pH 5 than at pH 3, which explains the higher rate constant obtained at pH 5. A further increase of pH above 5, in particular beyond TiO_2 pzc (6.35), results in accumulation of negative charges on the surface of TiO_2 which causes repulsion of clopyralid (found mainly in the form di-anion A^{2-}) (Figure 5.33). Thus under high pH conditions, the level of surface adsorption is reduced due to the strong repulsion forces, which causes a decline of the degradation rates. Several studies have also observed this effect of pH on the photocatalytic degradation of ionisable species (Chen and Ray 1998, Chu et al. 2009, O'Shea and Cardona 1995). Although our results are generally in agreement with those obtained by Sojic et al. (2009) for clopyralid photocatalytic degradation, it is nevertheless noteworthy to mention that in their study they found that at pH 11 the degradation rate increased, which is in contradiction with this study. The authors explained this increase by increased hydroxyl radical production due to high concentrations of OH^- at high pH. Although this sounds a plausible explanation, we believe that due to the strong repulsive forces between clopyralid (i.e. in A^{2-} form at high pH) and TiO_2 (i.e. TiO^-), clopyralid mass transfer becomes very difficult and as a result the short living $^{\bullet}OH$ species will not be able to fully react with clopyralid. Hence a reduction of the degradation rate of clopyralid is most probable when the pH increases beyond circa TiO_2 pzc as has been observed in this study.

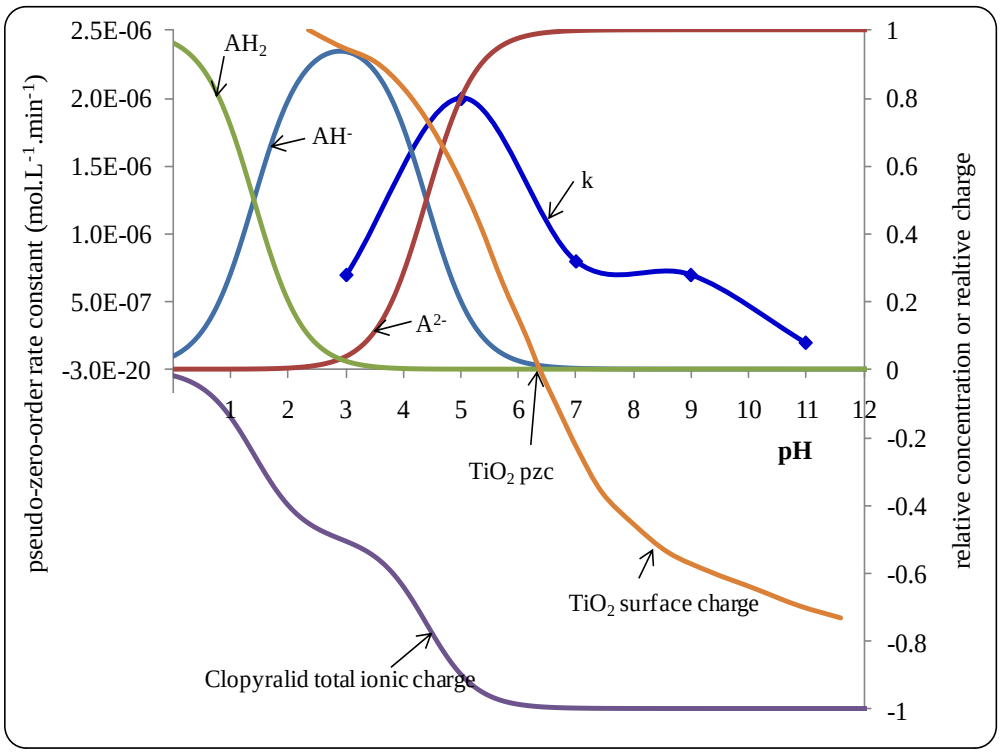

Figure 5.33: Effect of pH on the pseudo-zero-order rate constant of photocatalytic degradation of clopyralid (Cclopyralid = 15 mgL^{-1}; Ccat = 1 gL^{-1}). Data for TiO_2 surface charge was adapted from (Preocanin and Kallay 2006).

5.3.2.3 *Effect of initial clopyralid concentration*

Many studies have shown that the initial pollutant concentration has significant effect on the photocatalytic degradation rates. Too high concentrations cause UV-screening effect and possibly deactivation of the catalyst, which necessitate in certain cases dilution of the highly concentrated waters to achieve successful degradation (Robert and Malato 2002). On the other hand too low concentrations may not be sufficient to achieve a high adsorption rate, which leads to low degradation rates. Hence, the effect of the initial concentration of clopyralid was investigated in this study in the range 0.078-0.521 mM and the results are shown in Figure 5.34. The figure shows that the times required to achieve a given degradation percentage increase substantially with increasing the initial concentration of clopyralid. For example the irradiation times to

achieve 90% degradation (inset Figure 5.34) for initial clopyralid concentrations of 0.078, 0.260, 0.391 and 0.521 mM were 30, 144, 163, and 180 min respectively. A possible explanation is that when the concentration of clopyralid increases, the number of active sites responsible for generating the oxidative species (i.e. holes, $^{\bullet}OH$) has also to follow suit and increase. However, because both the amount of catalyst and the light irradiation intensity are kept constant, the number of active sites is also kept constant. As a result the irradiation time has to increase to compensate for the increase in the ratio of the number of clopyralid molecules relative to the number of active sites so the required degradation percentage (i.e. 90%) can be achieved. Figure 5.34 also shows that the change of clopyralid concentrations as function of time within the first degradation phase gave straight almost parallel lines indicating that zero-order kinetics was applicable and the rate constant did not change significantly with the initial concentration of clopyralid. A value of the zero-order rate constant of $2.09\times10^{-6} \pm 4.32\times10^{-7}$ $M.s^{-1}$ was calculated. Similar results were also obtained in the literature (Ochuma et al. 2007, Robert and Malato 2002). Sojic et al. (2009) used higher initial concentrations of clopyralid up to 3 mM and they found that the degradation rate increased with the initial concentration followed by a decrease. They based their findings on only a small number of points, which makes it difficult to ascertain the trend they obtained.

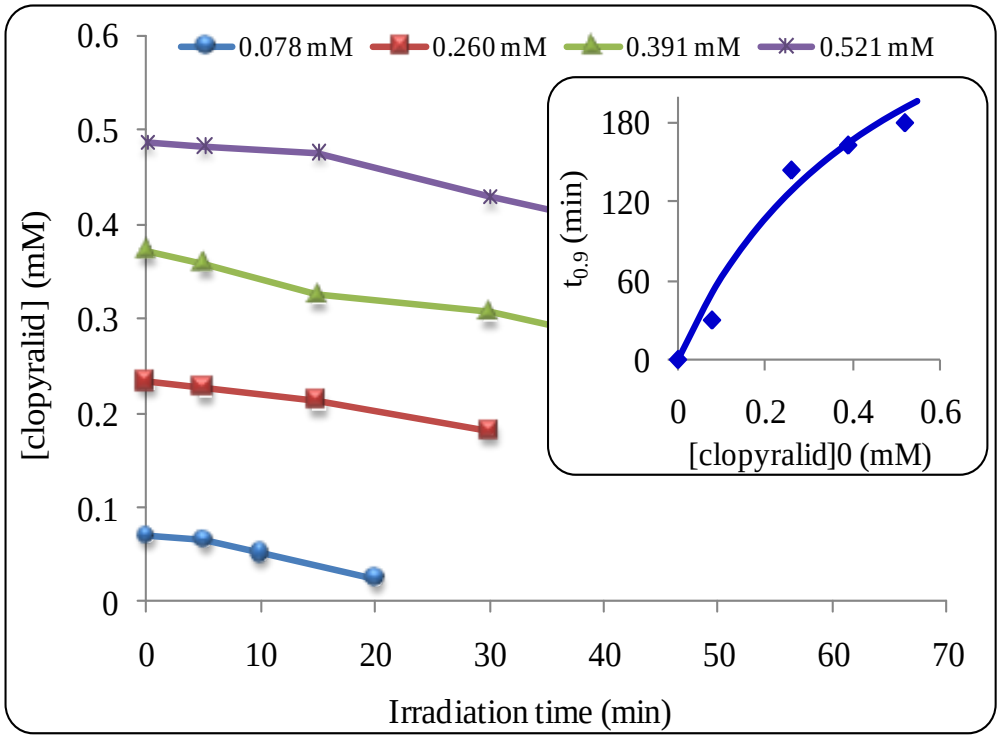

Figure 5.34: Clopyralid degradation at different initial concentrations [Power=200W, pH=5.6, Ccat=1gL-1].

5.3.2.4 *Effect of electron acceptors*

One of the problems associated with photocatalytic processes is the charge-carrier recombination. In order to reduce the likelihood of this from occurring, electron acceptors have to be available in enough quantities in the solution. Dissolved molecular oxygen is the most common electron acceptor used in photocatalysis. TiO_2 electrons react with oxygen to produce superoxide anions ($O_2^{\bullet-}$) (Equation 5.10), which readily protonate and disproportionate to produce hydrogen peroxide and oxygen (Equations 5.11,5.12) (Hoffmann et al. 1995). In addition to oxygen, the formed hydrogen peroxide can also act as an electron acceptor producing hydroxyl radicals (Equation 5.13).

$$TiO_2(e^-) + O_2 \rightarrow O_2^{\bullet-} \quad (5.10)$$

$$O_2^{\bullet-} + H^+ \rightarrow HO_2^{\bullet} \quad (5.11)$$

$$2HO_2^{\bullet} \rightarrow H_2O_2 + O_2 \quad (5.12)$$

$$TiO_2(e^-) + H_2O_2 \rightarrow OH^- + {}^{\bullet}OH \quad (5.13)$$

In this study, pure oxygen and synthetic air were bubbled continuously in the solution so different concentrations of dissolved oxygen are obtained and maintained in the solution; the results are shown in Figure 5.35. Unexpectedly, Figure 5.35 shows that the degradation rate of clopyralid slightly reduced when pure oxygen was used as compared to air. The bubbling of pure oxygen in the solution leads to higher dissolved oxygen concentrations in the solution as compared to air and as a result the concentration of hydrogen peroxide is expected to also increase (Equations 5.10 - 5.12). Although hydrogen peroxide enhances the efficiency of the photocatalytic process (Equation 5.13), it can also react with the holes (Hoffman et al. 1994) (Equation 5.14) and can act as a hydroxyl radical scavenger forming much weaker oxidant hydroperoxyl radical (Equation 5.15). Therefore, the overall performance of the photocatalytic process may reduce as a result.

$$H_2O_2 + 2\ TiO_2(h^+) \rightarrow O_2 + 2H^+ \quad (5.14)$$

$$H_2O_2 + {}^{\bullet}OH \rightarrow H_2O + HO_2^{\bullet} \quad (5.15)$$

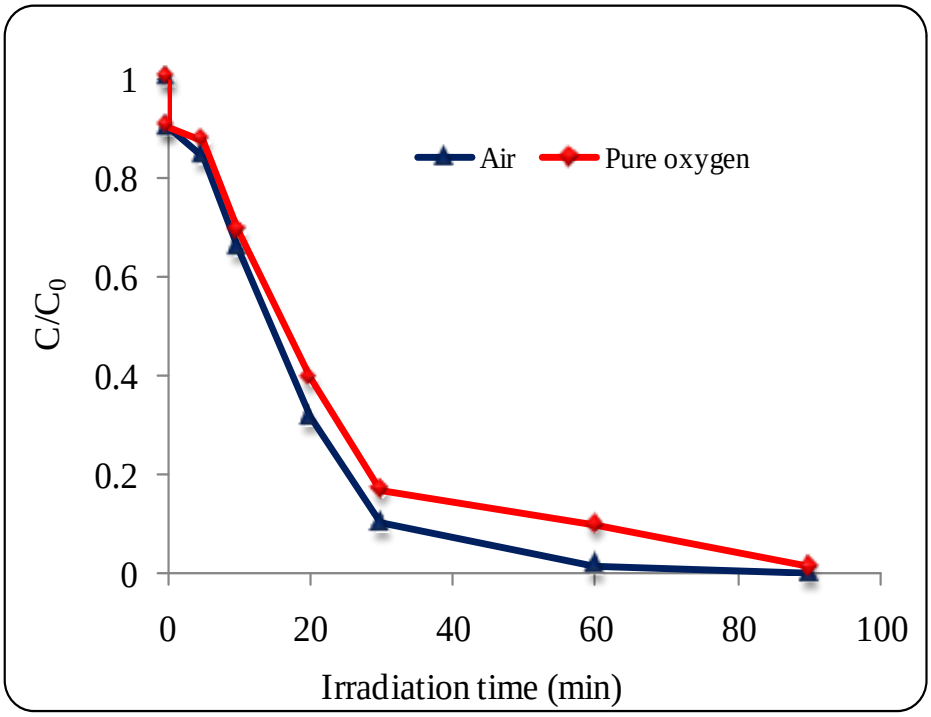

Figure 5.35: Effect of electron acceptor on clopyralid degradation [C_0=0.078 mM, Ccat=1 gL^{-1}, Power =200 W, pH=5.6].

5.3.2.5 *Effect of catalyst reuse*

One of the principle aims of heterogeneous catalytic processes is to recover the catalyst for further reuse. Hence in photocatalytic processes, catalyst recovery and reuse has received considerable attention (Araña et al. 2002, Fernández-Ibáñez et al. 2003, Pekakis et al. 2006, Reutergådh and Iangphasuk 1997, Rhoads and Davis 2004). Several studies have shown that the reuse of the catalyst did not affect significantly its performance (Alsayyed et al. 1991, Barbeni et al. 1987, Mills et al. 1993). In the contrary, other studies have shown that the presence of chloride, for example, reduces the catalyst performance by scavenging oxidising radicals (Equation 5.16) or blocking the active sites on the catalyst surface (Abdullah et al. 1990, Fernández-Ibáñez et al. 2003). Dominguez et al. (1998) have concluded that exposure of the catalyst (initially

75% anatase, 25% rutile) to UV light reduced the active anatase form to its counterpart rutile form to 70%, which may also reduce the catalyst activity.

$$^{\bullet}Ox + Cl^{-} \rightarrow Cl^{\bullet} \qquad (5.16)$$

In this study, the effect of reusing the catalyst was studied and the results are shown on Figure 5.36. The figure shows that the performance of the reused catalyst was reduced during the first degradation phase (i.e. t<60 min) as compared to fresh catalyst. After 60 min, reused catalyst was not as effective as the fresh catalyst to completely degrade clopyralid while a complete degradation was achieved with fresh catalyst after 90 min. This clearly indicates deactivation of the catalyst possibly as a result of the presence of chloride originating from the degradation of the parent molecule (Sojic et al. 2009). Moreover, the extent of initial drop in concentration due to adsorption was less apparent with reused catalyst as compared to fresh catalyst, which also supports possible deactivation of the active sites on the catalyst.

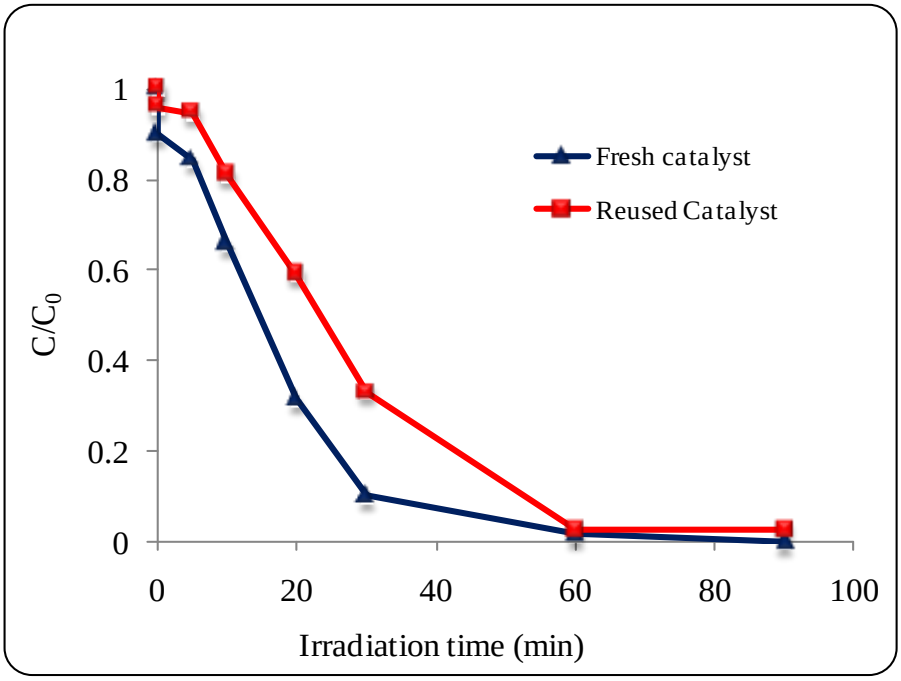

Figure 5.36: Effect of catalyst reuse on clopyralid degradation [C_0=0.078 mM, Ccat=1 gL^{-1}, Power=200 W, pH=5.6].

5.3.3 Photodegradation of 3, 6-DCP with UV/H_2O_2

UV/H_2O_2 is a relatively more practical process than UV/TiO_2 hence it is widely studied and applied in water and wastewater purification. Exposure of hydrogen peroxide to UV light results in its photolysis leading to the formation of hydroxyl radicals (Baxendale and Wilson 1957):

$$H_2O_2 \xrightarrow{UV} 2^{\bullet}OH \qquad (5.17)$$

In the present work, the degradation of clopyralid with UV/H_2O_2 was studied and the results are shown in Figure 5.37. Clearly UV/H_2O_2 was effective in degradation of clopyralid within the first 30 min by reducing the initial concentration by about 83%. For times higher than 30 min, the degradation of clopyralid became more difficult and reached only 92% degradation after a further 60 min irradiation. On one hand, knowing that hydrogen peroxide was added to the reaction system a concentrations much higher than clopyralid, its concentration can be assumed not changed significantly during the reaction time (Zang and Farnood 2005). On the other hand, at the end of the reaction time (i.e. the time at which the concentration of clopyralid was reduced to less than approximately 20% ≈ 30 min) the scavenging reactions of hydroxyl radicals with hydrogen peroxide became significant and competed with the main degradation reaction. This hence leads to very low degradation rates as observed in Figure 5.37, which makes the process less effective. Similar concentration trends were obtained for both H_2O_2 concentrations used in this study. The degradation of clopyralid with UV/H_2O_2 may be represented by a pseudo-first-order reaction kinetics (Beltran 2004). A rate constant around 1.7×10^{-3} s^{-1} was found in this study. Similar rate constant values were also reported in the literature for the degradation of benzene, toluene, phenol, 2,4-dichlorophenol, 2,4,6-trichlorophenol and pesticides with UV/H_2O_2 (Parsons 2004).

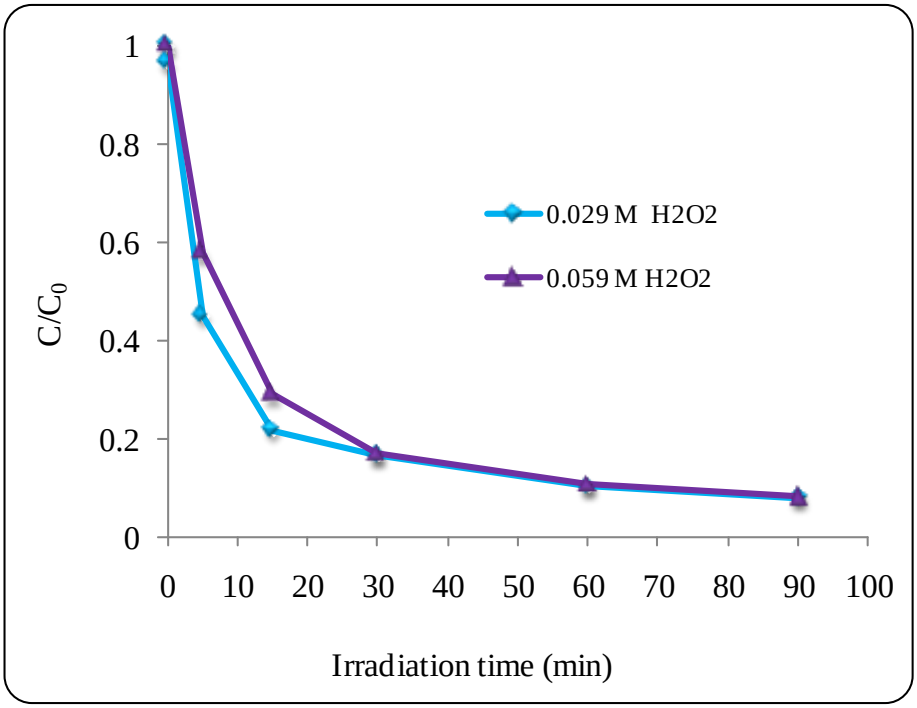

Figure 5.37: Clopyralid degradation with UV/H_2O_2 [C_0=0.078 mM, Power=200 W, pH=5.6].

5.3.4 Photodegradation of 3, 6-DCP with Ozone

Ozone degradation of clopyralid at different initial concentrations was studied and the results are shown in Figure 5.38. The degradation of clopyralid with ozone is relatively fast within the first 10 min approximately and subsequently becomes slow. The figure shows that as the initial concentration of clopyralid increased, the degradation reaction became slower. Clearly complete degradation of clopyralid was not achieved for all initial concentrations used even after longer ozonation times of 3hr. This indicates that clopyralid is resistant to ozone attack possibly due to the electron-withdrawing property of the nitrogen atom, which makes the molecule stable since the N atom resists the removal of electrons (Morrison and Boyd 1966). Moreover, the two chloride atoms add more stability to the molecule also due to their electron-withdrawing property (Yao and

Haag 1991). Indeed, the electron-withdrawing chlorine groups decrease the electron density on the ring and deactivate it. This may result in a rather nucleophilic attack with ozone, which proceeds generally at slow rates. Sojic et al. (2009) postulated that the oxidation of clopyralid with hydroxyl radicals resulted in the formation of intermediates having hydroxyl groups substituted the hydrogen in the pyridine cycle to result 3,6-dichloro-4-hydroxypyridine-2-carboxylic acid and 3,6-dichloro-5-hydroxypyridine-2-carboxylic acid, and substituted the carboxylic group to result 3,6-dichloropyridin-2-ol. They also reported that complete mineralisation of clopyralid was achieved after a long time of about 12 h. It is expected that similar intermediates may also form during the ozonation of clopyralid as a result of similar reactions with $^{\bullet}OH$. The presence of the hydroxyl group increases the reactivity of the intermediate with ozone due to its activating effect on the C-H bond. As a result ozone reactions with the intermediates compete strongly with those of the parent molecule and this provides a plausible explanation of the low degradation rates of clopyralid observed after approximately 10 min of reaction (Figure 5.38).

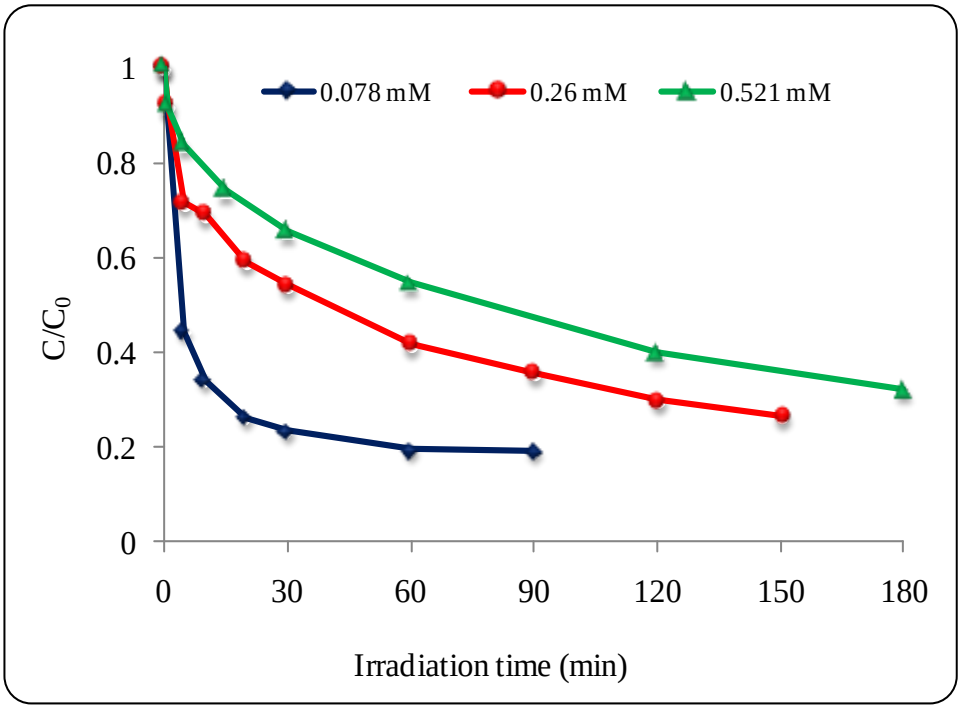

Figure 5.38: Ozone degradation of clopyralid [gas flow rate = 200 mLmin^{-1}, ozone gas concentration = 60 g/m^3 NTP, pH=5.6].

5.3.5 Comparison with UV/H_2O_2, UV/TiO_2 and O_3 oxidation

Figure 5.39 shows the degradation of clopyralid using the three systems (i.e. UV/TiO_2, UV/H_2O_2, and O_3). UV/H_2O_2 and O_3 gave similar relatively fast degradation rates of clopyralid within the first 10 min followed by a clear slow down of the rates. Both systems gave similar trends for the variation of concentration with time. After reaction times of 90 min, both systems were not capable of completely degrading clopyralid due to possible competitive reactions of intermediates and H_2O_2. On the other hand the UV/TiO_2 system gave relatively slower degradation rate of clopyralid within the initial phase of the reaction (i.e. approx. the first 10 min) but led to complete disappearance of clopyralid after 60 min, hence it outperformed the other two systems. Although the three systems may involve hydroxyl radicals to achieve the degradation of clopyralid, UV/TiO_2 system is different from the other two since it involves in addition to oxidation

reactions adsorption mechanisms. In fact clopyralid has to adsorb on the surface of TiO_2 in order for the reaction to occur and it is most probable that the reaction products desorb faster to the solution, which reduces the effect of competition reactions. Moreover, the physical adsorption of clopyralid on the catalyst surface contributes to its disappearance from the solution. Therefore the combined effect of oxidation and adsorption is the main reason for complete removal of clopyralid in the UV/TiO_2 system. Since the degradation of clopyralid is fastest within the first phase of the reaction with either UV/H_2O_2 or O_3 and fastest within a second phase of the reaction with UV/TiO_2, a hybrid system involving UV/H_2O_2 or O_3 followed by UV/TiO_2 may provide a rapid method for the complete degradation of clopyralid.

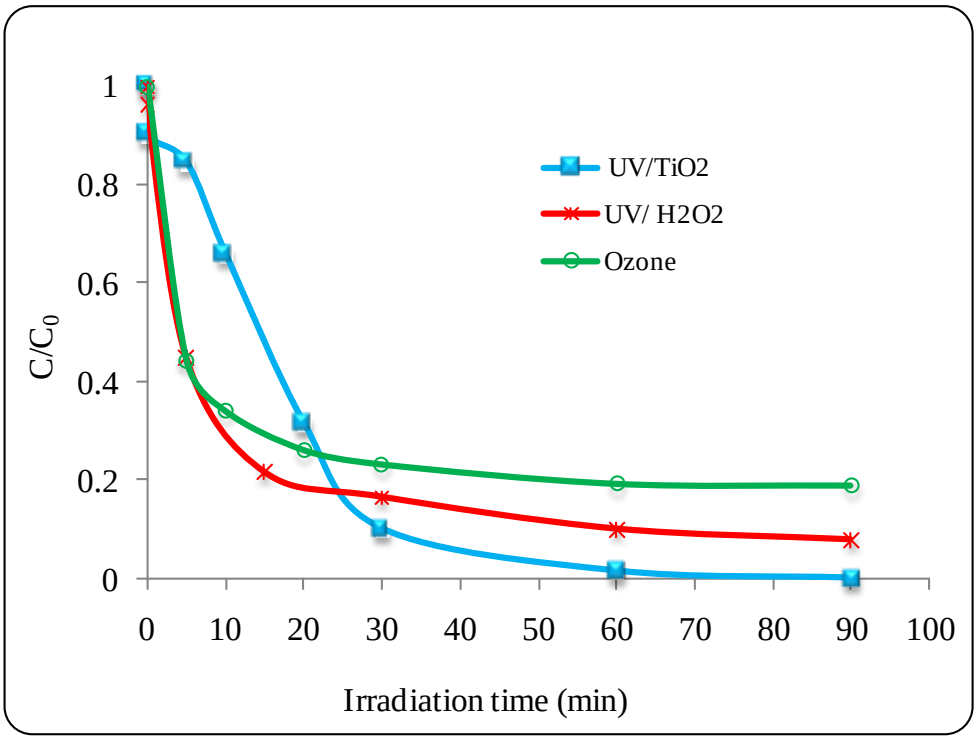

Figure 5.39: Comparison on the degradation of clopyralid with UV/TiO_2, UV/H_2O_2 and O_3 systems (initial clopyralid conc. = 0.078 mM, pH=5.6; catalyst conc.=1gL^{-1}, power=200 W; initial H_2O_2 conc.= 1g/L, power=200W; gas flow rate=200 mLmin^{-1}, ozone gas concentration=60 g/m^3 NTP).

5.4 Photodegradation of EDCs

5.4.1 Photodegradation of EDCs with UV only

The photodegradation of the three EDCs was carried out using single component and mixtures of the three components. The results are discussed in this section.

5.4.1.1 *Photodegradation of E1, E2 and EE2*

Experiments to investigate the effectiveness of UV light on the degradation of a single EDC (i.e. photolysis) were carried out at 5 mg/L (E1=1.85×10^{-2}, E2=1.84×10^{-2} and EE2=1.69×10^{-2} mM) initial concentration (power of 200 W and pH=5.8). As can be seen from Figure 5.40, the degradation of E1 after the first five minutes irradiation was about twice higher than the degradation of E2 and EE2. Figure 4.9 shows that E1 absorbs more light at 365 nm (a wavelength at which the UV lamp emits the highest light intensity) as compared to E2 and EE2, which explains the rapid degradation of E1 obtained in this study. After 1 hour irradiation, the degradation of E2, EE2 and E1 was almost similar (86.26%, 85.24% and 92.06% for E2, EE2 and E1 respectively). It is also important to note that after 5 minutes, the rate of degradation of E1 became slower relative to the other EDCs possibly due to the rapid reduction of E1 concentration.

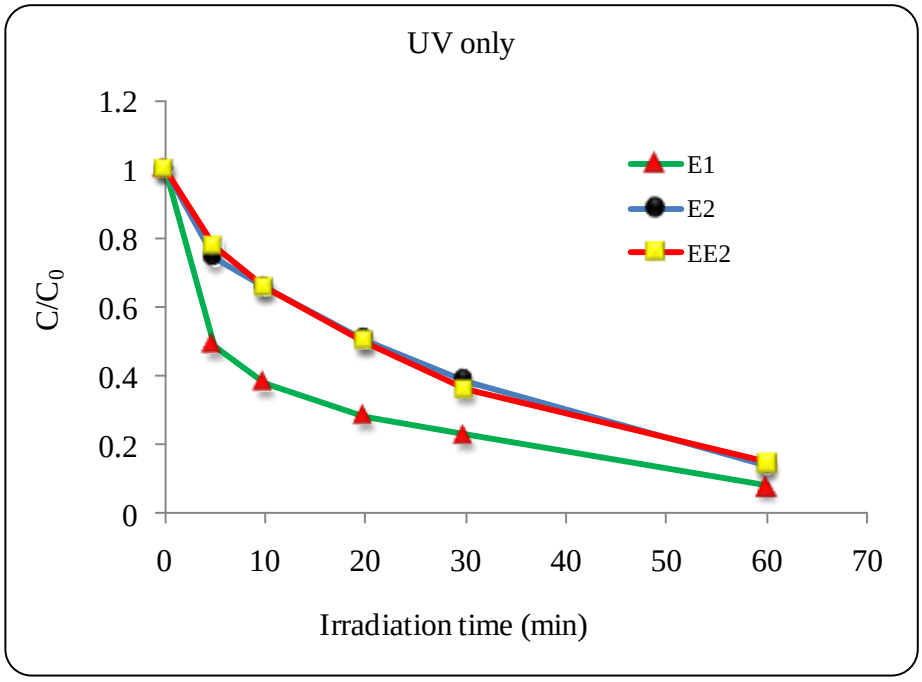

Figure 5.40: Effect of UV light on the degradation of single EDC

The photodegradation of mixtures of the three EDCs was also studied and the results are shown in Figure 5.41. Generally the pattern of degradation of the EDCs is more or less similar for single components or in mixtures. In both cases E1 was degraded faster than E2 and EE2. For the mixture of EDCs, a very rapid degradation of E1 within the first 5 minutes was observed, followed by almost nil degradation afterwards. Although this behaviour is difficult to explain, it is clear that E1 degrades rapidly either as a single component or in mixtures. The trend of degradation of E2 and EE2 is very similar, possibly due to the high similarity between their chemical structures and the fact that they represent similar light absorption properties as shown in Figure 4.9. If the interest is the extent of degradation at the end of the assigned time then it can be argued that the degradation efficiency was slightly better for the EDCs treated individually than for the mixed EDCs. This agrees with the fact that the amount of UV light irradiation was the same for both situations though the concentration of compounds susceptible for light absorption increased when the EDCs are mixed. As a result of the greater concentration

in mixtures, two possible points should be considered. Firstly for the mixed EDCs, there is greater competition for exposure to UV light than for the less concentrated individually treated EDC. Secondly a masking effect results as a result of the greater concentration. Looking at Figure 5.41, the degradation of E1 was initially steeper in the mixture than for single component. This may be explained by additional reactions taking place between E1 and formed radicals as a result of the photolysis of the other EDCs.

To date the photochemical behaviour and specifically the contribution of direct photolysis to the degradation of these compounds have not been deeply studied (Patrick et al., 2008). Zhang and Zhou (2008) studied the effect of UV light on the degradation of E1 and E2 and found the E1 and E2 were prone to UV photodegradation.

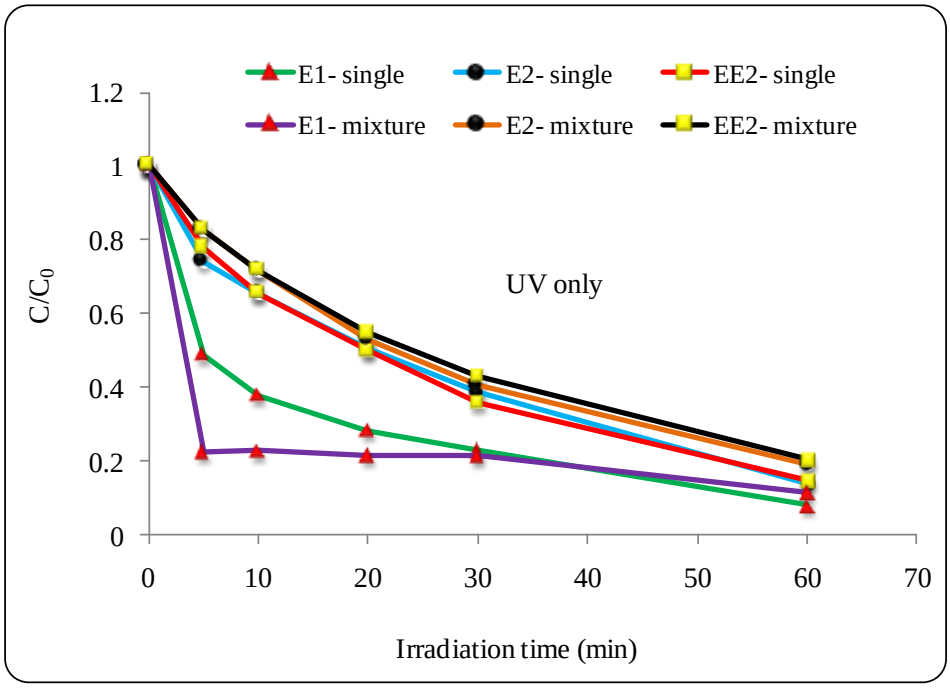

Figure 5. 41: Effect of UV on the degradation of EDCs single and mixture [C_0=5 mgL^{-1} (E1= 1.85×10^{-2}, E2= 1.84×10^{-2} and EE2= 1.69×10^{-2} mM), pH=5.8 and Power =200 W].

The degradation rates of the three EDCs may be described by a pseudo-first-order kinetic model, which is represented on Figure 5.42. The degradation rate constant (k) was found to be 3.2×10^{-2}, 3.1×10^{-2} and 3.0×10^{-2} min^{-1} for E1, E2 and EE2 respectively for the EDCs treated singly. Whereas it was 1.3×10^{-2}, 2.6×10^{-2} and 2.5×10^{-2} min^{-1} for E1, E2 and EE2 respectively as mixture. Nakashima et al. (2003) studied the degradation of E1 and E2 in discharge water, and found that 98% of initial E1 was degraded under UV light, resulting in a first-order rate constant of 1.2×10^{-1} for E1 and 1.5×10^{-1} for E2. Tanizaki et al. (2002) found the rate constants for E1, E2 and EE2 to be 5.8×10^{-2}, 1.5×10^{-2} and 5.0×10^{-2} min^{-1} respectively. These rate constants obtained in the literature are within the same range to those obtained in this study.

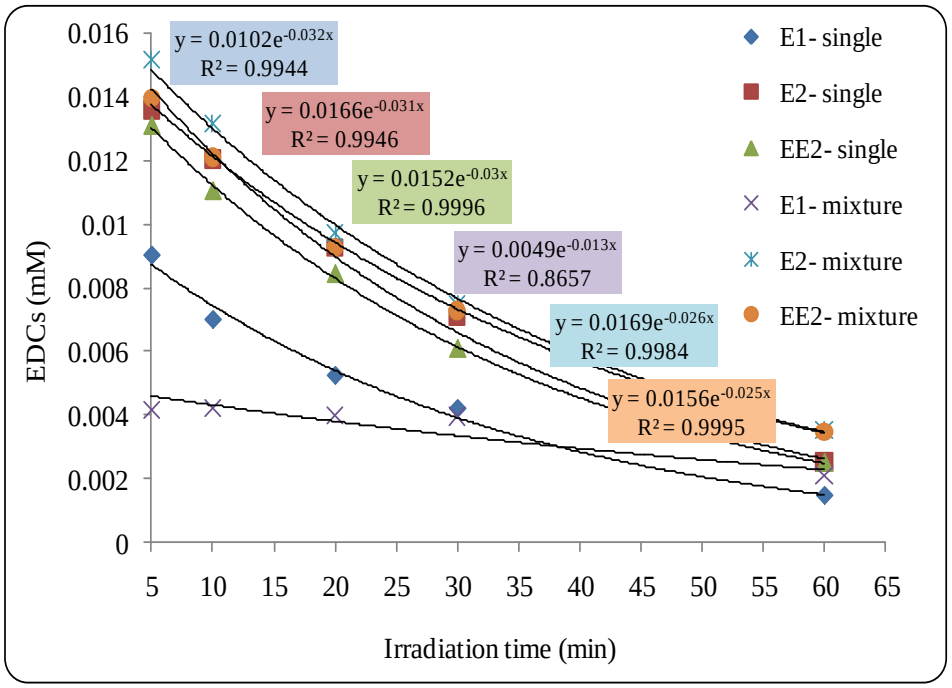

Figure 5.42: Kinetic of reaction using UV light for the degradation of the EDCs.

5.4.2 Photodegradation of EDCs with UV/TiO_2

This section discusses the photocatalytic degradation of the three EDCs using Degussa P25 TiO_2 photocatalysts.

5.4.3 Effect of the operating parameters

5.4.3.1 *Effect of catalyst concentration*

Degussa P25 was used as a photocatalyst and the effect of its concentration on the degradation of EDCs was investigated (Figure 5.43). Two concentrations of TiO_2 (1 and 2 g/L) were used with fixed initial EDCs mixture concentration of 0.5 mg/L (E1= 1.85×10^{-3}, E2= 1.84×10^{-3} and EE2= 1.69×10^{-3} mM). It was observed that when the TiO_2 concentration increased from 1 to 2 g/L, the degradation of E1, E2 and EE2 decreased. (So et al., 2002), explained this phenomenon in terms of availability of active sites on TiO_2 surface and the penetration of photoactivating light into the suspension. According to these authors the availability of active sites increases with the suspension of catalyst loading, but the light penetration, and hence, the photoactivated volume of the suspension shrinks. The authors further suggested that the decrease in the percentage of degradation at higher catalyst loading may be due to the deactivation of activated molecules by collision with ground state molecules. Agglomeration and sedimentation of TiO_2 particles were observed elsewhere when 2g/L of TiO_2 was added to a dye solution (So et al., 2002). In the following study, a catalyst concentration of 1g/L was selected.

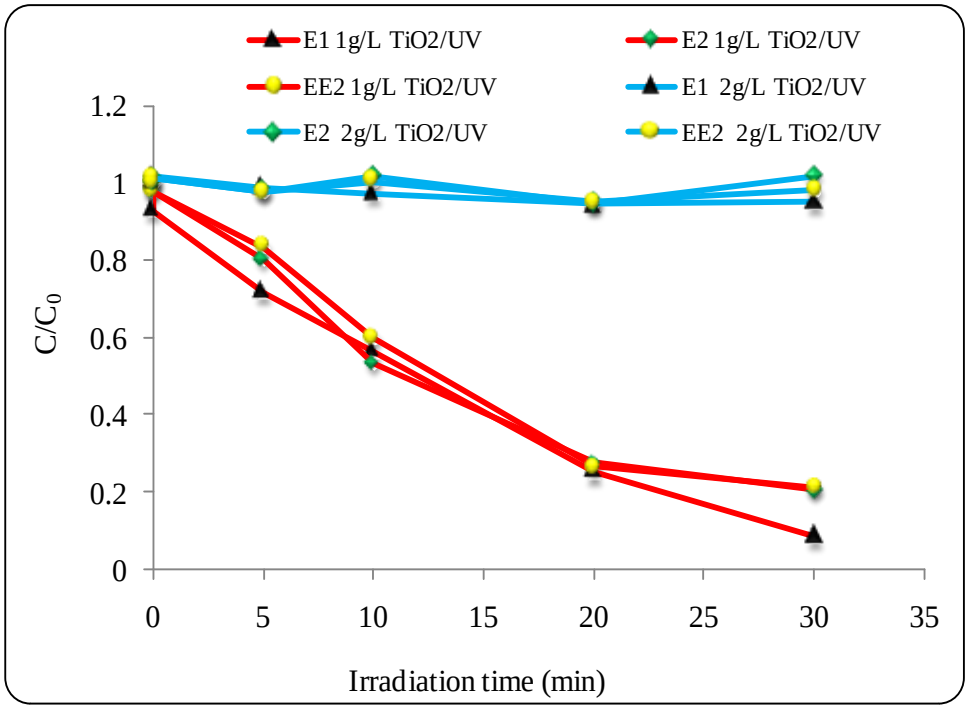

Figure 5.43: Effect of catalyst concentration on the degradation of EDCs (mixture) [Catalyst is Degussa P25, C_0=0.5 mgL^{-1} (E1= 1.85×10^{-3}, E2= 1.84×10^{-3} and EE2= 1.69×10^{-3} mM), pH=5.8, Power=200 W].

5.4.3.2 *Effect of initial concentrations of EDCs*

Different initial concentrations of EDCs (mixture) with fixed catalyst concentration at 1 g/L were used to investigate the effect of initial concentrations on the degradation rates of the EDCs. From Figure 5.44 it can clearly be seen that low concentration of EDCs 0.5 mg/L (E1=1.85×10^{-3}, E2=1.84×10^{-3} and EE2=1.69×10^{-3}mM) resulted in higher degradation as compared to higher concentrations 1 and 5 mg/L (E1= 3.70×10^{-3}, E2= 3.67×10^{-3} and EE2=3.37×10^{-3}mM) and (E1=1.85×10^{-2}, E2=1.84×10^{-2} and EE2= 1.69×10^{-2} mM). For example at 0.5 mg/L the degradations of E2, EE2 and E1 after 10 minutes were 46.85%, 40.31% and 43.83% respectively, whereas after 60 minutes of irradiation the degradations were 100% for both EE2 and E1 and 87.27% for E2. When the initial concentration was increased to 1 mg/L EDCs, the extent of degradation

reduced significantly as compared to 0.5 mg/L EDCs. For instance the degradations of E2, EE2 and E1 after 10 minutes were only 5.34%, 4.19% and 7.28% respectively, whereas after 60 minutes of irradiation the degradations increased to 36.49%, 36.13% and 46.11% respectively. The degradation rates decreased even further with increasing initial EDCs concentrations to 5 mg/L EDCs. At 5 mg/L EDCs and after 10 minutes of irradiation, the degradations of E2, EE2 and E1 were 4.05%, 3.26% and 4.66% respectively. The degradation increased slightly to 9.54%, 10.75% and 13.12% for E2, EE2 and E1 respectively after 60 minutes. These results clearly indicate that the initial concentration of EDCs has a significant effect on the extent of degradation of these compounds. For a fixed concentration of catalyst, the higher the concentration of EDCs, the lower the degradation efficiency. Knowing that in real wastewaters, the concentrations of these compounds are very low (~ng/L), hence a photocatalytic system seems suitable for their removal.

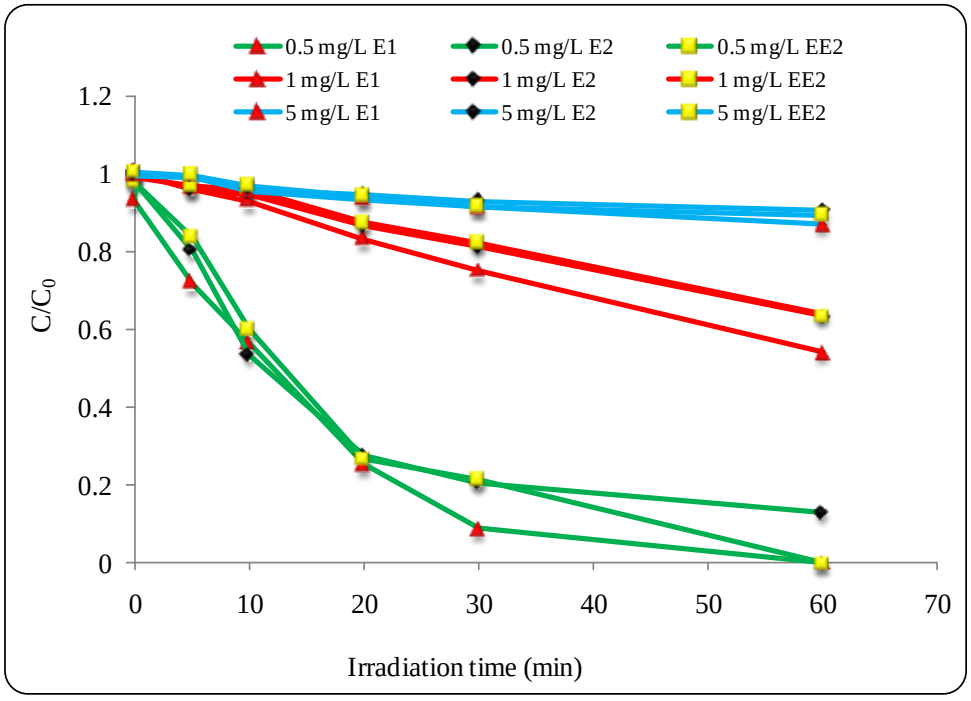

Figure 5.44: Effect of initial concentrations of EDCs (mixture) on the degradation rate [$C_{\text{Degussa P25}}$=1 gL^{-1}, pH=5.8 and Power=200 W].

The rate constant was determined with first-order kinetic reaction Table 5.4. It was observed that the photodegradation rate constant *k* decreases with increase of the initial concentrations of EDCs. The same observation was reported for EE2 in an earlier research (Liu et al., 2003).

Table 5.4: Kinetic data for photocatalysis of different initial concentrations of EDCs.

Concentration (mg/L)	EDCs	Rate of constant k (min^{-1})
0.5	E1	7.9×10^{-2}
	E2	5.5×10^{-2}
	EE2	5.5×10^{-2}
1.0	E1	1.0×10^{-2}
	E2	7.0×10^{-3}
	EE2	6.0×10^{-3}
5.0	E1	3.0×10^{-3}
	E2	2.0×10^{-3}
	EE2	3.0×10^{-3}

5.4.3.3 *Effect of catalyst type*

The degradation of EDCs 1 mg/L (E1= 3.70×10^{-3}, E2= 3.67×10^{-3} and EE2=3.37×10^{-3} mM) as single, using 2 different catalysts (Degussa P25 and Hombifine N) and UV light was investigated Figure 5.45. The degradation of EDCs using Degussa P25 with UV was explained in sections (5.4.3.1, 5.4.3.2). Under similar conditions the efficiency of Hombifine N in degrading E2 and EE2 was found to be lower than that of Degussa P25. On the other hand Hombifine N was found to be more efficient than Degussa P25 in the degradation of E1. The reason behind the greater efficiency of Hombifine N in the degradation of E1 may due to its large surface area as compared to Degussa P25.

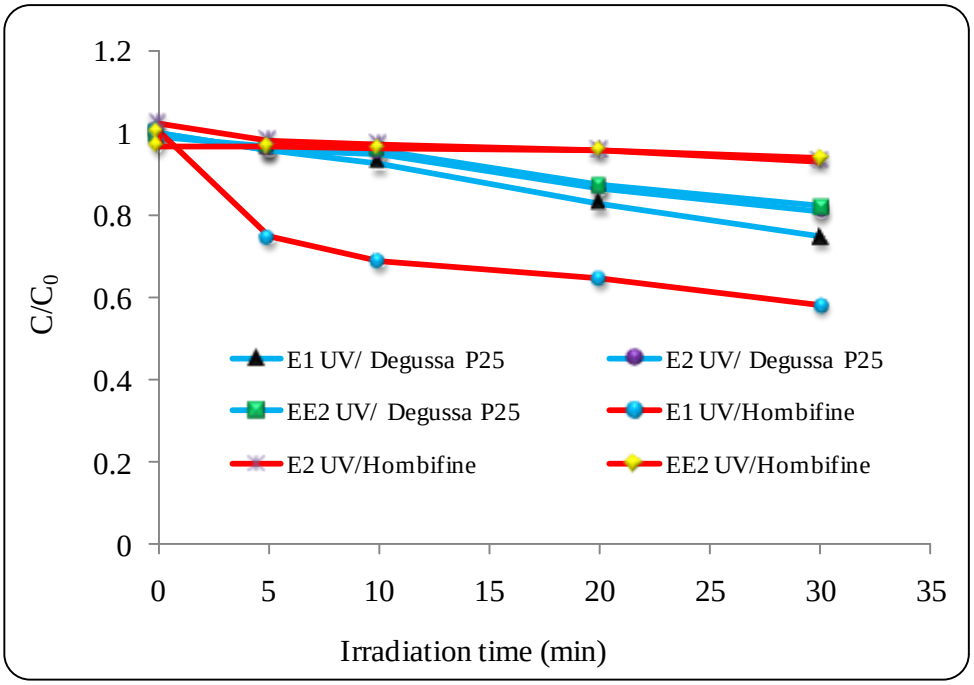

Figure 5.45: Effect of catalyst type on the degradation of single EDC [Ccat=1 gL^{-1}, C_0=1 mgL^{-1}(E1= 3.70×10^{-3}, E2= 3.67×10^{-3} and EE2=3.37×10^{-3} mM), pH=5.8 and Power=200 W].

5.4.4 Photodegradation of EDCs with UV/ H_2O_2

The degradation of E1, E2 and EE2 as single components and in mixtures was studied using the UV/H_2O_2 system. The initial concentration of each EDC was 20 mg/L (E1= 7.40×10^{-2}, E2=7.34×10^{-2} and EE2=6.75×10^{-2} mM) and that of H_2O_2 was 1g/L (2.94×10^{-2} M). The power of the UV light was 200 W.

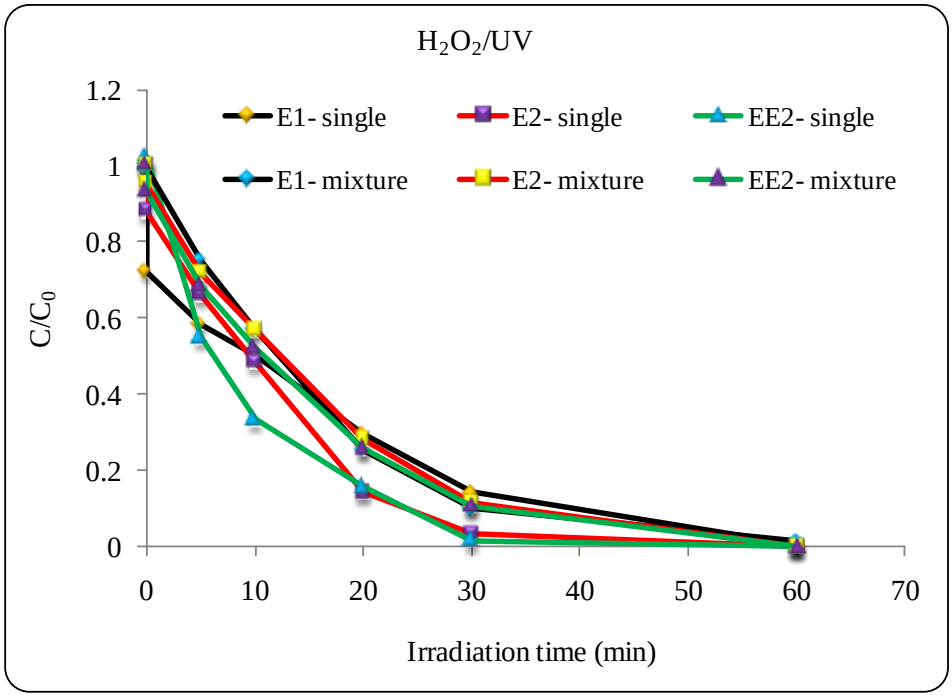

Figure 5.46: Effect of H_2O_2/UV on the degradation of EDCs single and mixture EDCs [CH_2O_2=1 gL^{-1} (2.94×10^{-2} M), C_0=20 mgL^{-1} (E1= 7.40×10^{-2}, E2=7.34×10^{-2} and EE2=6.75×10^{-2} mM), pH=5.8 and Power=200 W].

Figures 5.46 shows the effect of H_2O_2/UV on photocatalytic degradation of EDCs treated separately and as a mixture. For individual treatment, E2 degraded about 34.02% after the first five minutes of irradiation. At the same time EE2 and E1 were reduced to about half the initial concentration (45.27 and 41.01% respectively). For the mixed solutions, the degradation was lower than for individual compounds in the first five minutes of irradiation. The degradations for the three mixed EDCs after five minutes were 28.29, 31.93 and 25.15% for E2, EE2 and E1 respectively. Complete degradation of single E2 and EE2 was achieved after 30 min, but it required 60 min when a mixture was used. On the other hand, the degradation of single E1 was more difficult and required 60 min to be almost complete. For individual treatment E2, EE2 and E1 were degraded by 100, 100 and 99.73% respectively after 60 min and for mixed treatment E2, EE2 and E1 were degraded by 100, 100 and 98.65% respectively. Table 5.5 shows the values of rate constant of single and mixed EDCs

Table 5.5: Kinetic data for photocatalysis of EDCs using UV/H_2O_2.

Concentration (20 mg/L)	EDCs	Rate constant k (min^{-1})
Single	E1	5.4×10^{-2}
	E2	1.1×10^{-1}
	EE2	1.32×10^{-1}
Mixture	E1	7.7×10^{-2}
	E2	7.0×10^{-2}
	EE2	7.2×10^{-2}

5.4.5 Effect of the operating parameters

5.4.5.1 *Effect of UV light on the degradation of the EDCs*

The effect of UV light in the presence of hydrogen peroxide was studied in experiments with and without UV light. Before UV/H_2O_2 degradation experiments, the compounds E2, EE2 and E1 were scanned in UV spectrophotometry and the results show that the 3 EDCs generally have enhanced UV absorbance at low wavelength (Chapter 4, Figure 4.9). Their spectra indicate that E2, EE2 and E1 are prone to UV photodegradation. In the absence of UV light, a clear instantaneous drop in the concentrations of the EDCs by about 40% occurred as a result of oxidation with hydrogen peroxide (Figure 5.47). The concentration then remains constant throughout the remaining time. The most likely explanation for this inference is the high concentration of H_2O_2 used (~ 0.03M). Bledzka et al. (2010) found insignificant result of photodegradation of EDCs with only H_2O_2 (0.01M). Xianghua et al. (2005) studied the degradation of E2 with only H_2O_2. These authors found the increase of H_2O_2 concentration resulted in the increase in the degradation of E2. This could be explained by Equation 5.18. H_2O_2 can also become a scavenger of $^{\bullet}OH$, when present at high concentration (Daneshvar et al., 2003).

$$H_2O_2 + {}^{\bullet}OH + h\nu \rightarrow H_2O + {}^{\bullet}HO_2 \quad (5.18)$$

The degradation of the EDCs using UV light only (Figure 5.41) resulted in better efficiency than using 1g/L H_2O_2 (2.94×10^{-2} M). On the other hand coupling H_2O_2 with UV light (Figure 5.47) resulted in better degradation efficiency than using only H_2O_2 or only UV light. For instance E2 degraded 100% after 10 minutes irradiation, while EE2 and E1 were degraded 89.95 and 93.24% after 10 minutes respectively when UV/H_2O_2 system was used as compared to 28.36, 28.23 and 77.27% after 10 min when only UV was used. The effectiveness of the UV/H_2O_2 is due to the production of hydroxyl radicals at significant amounts following the photolysis of hydrogen peroxide (Equation 5.19).

$$H_2O_2 + h\nu \rightarrow 2HO^{\bullet} \quad (5.19)$$

The kinetic reaction followed pseudo-first-order, (Equation 5.20).

$$\ln(C/C_0) = -kt \quad (5.20)$$

The rate constants obtained with UV/H_2O_2 were 2.49×10^{-1}, 2.02×10^{-1} and 2.03×10^{-1} min^{-1} for E1, E2 and EE2 respectively.

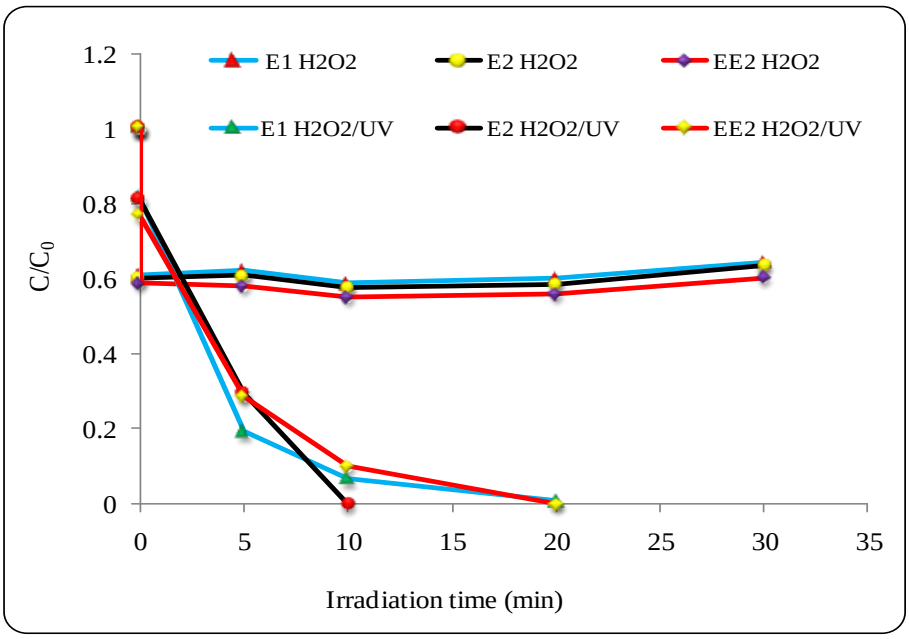

Figure 5.47: Effect of H_2O_2 on the degradation of mixed EDCs without UV and with UV [CH_2O_2=1 gL^{-1} (2.94×10^{-2} M), C_0=5 mgL^{-1} (E1= 1.85×10^{-2}, E2= 1.84×10^{-2} and EE2= 1.69×10^{-2} mM), pH=5.8 and Power=200 W].

5.4.5.2 *Effect of initial concentration on photodegradation of EDCs*

Experiments were carried out to investigate the effect of initial concentrations of mixed EDCs 5 and 20 mg/L (E1=1.85×10^{-2}, E2=1.84×10^{-2} and EE2=1.69×10^{-2} mM) and (E1=7.40×10^{-2}, E2=7.34×10^{-2} and EE2=6.75×10^{-2} mM) at fixed concentration of H_2O_2 1g/L (2.94×10^{-2} M) in the presence of UV light. It was found from the result in Figure 5.48 that the degradation was higher at 5 mg/L than 20 mg/L EDCs. The result indicated that the initial concentration of EDCs plays an important role in the degradation of these compounds. After 10 minutes irradiation, E2 at 5 mg/L was completely degraded but 60 minutes were required to achieve its complete degradation when its initial concentration was 20 mg/L. Tables 5.6 and 5.7 show the degradation percentages of the EDCs after the times 10, 30 and 60 minutes. Clearly these tables show that the degradation of the

EDCs was slower when the initial concentration was high. A first-order model was used to calculate the rate constants of E1, E2 and EE2. Figure 5.49.

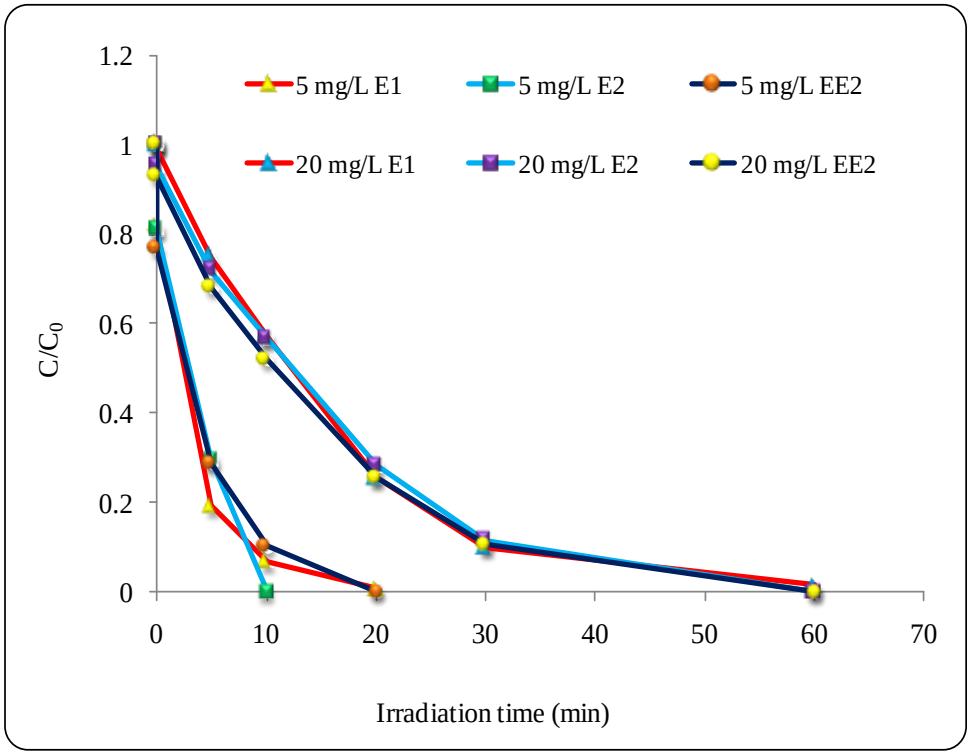

Figure 5.48: Effect of initial concentration of mixed EDCs [C_{H2O2}=1 gL^{-1} (2.94×10^{-2} M), pH=5.8 and Power=200 W].

Table 5.6: Data of 5 mgL^{-1} EDCs with 1 gL^{-1} (2.94×10^{-2} M) H_2O_2

Irradiation time (min)	10	30
Photodegradation efficiency	%	%
E2	100	-
EE2	89.95	100
E1	93.24	100

Table 5.7: Data of 20 mgL^{-1} EDCs with 1 gL^{-1} (2.94×10^{-2} M) H_2O_2.

Irradiation time (min)	10	30	60
Photodegradation efficiency	%	%	%
E2	43.43	88.47	100
EE2	48.03	89.44	100
E1	43.08	90.16	98.65

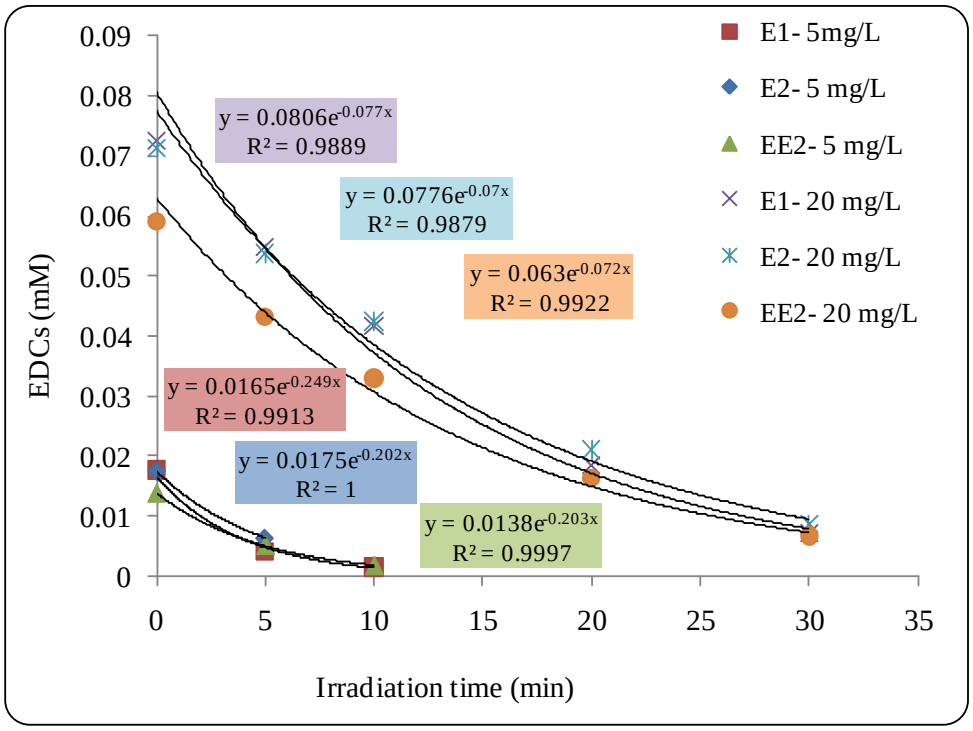

Figure 5.49: Kinetic of reaction using different concentrations of EDCs.

5.4.5.3 *Effect of H_2O_2 concentration*

To investigate the effect of H_2O_2 concentration on the degradation of mixed EDCs in the presence of UV light two different concentrations of H_2O_2 were used 0.5 and 1 g/L (1.47×10^{-2} and 2.94×10^{-2} M) and the EDCs concentrations were 20 mg/L (E1=7.40×10^{-2}, E2=7.34×10^{-2} and EE2=6.75×10^{-2} mM) each. The results in Figure 5.50 and Table 5.8

revealed that increasing the concentration of H_2O_2 from 0.5 to 1g/L did not significantly affect the degradation rates of the EDCs. This is expected since hydrogen peroxide was added in excess.

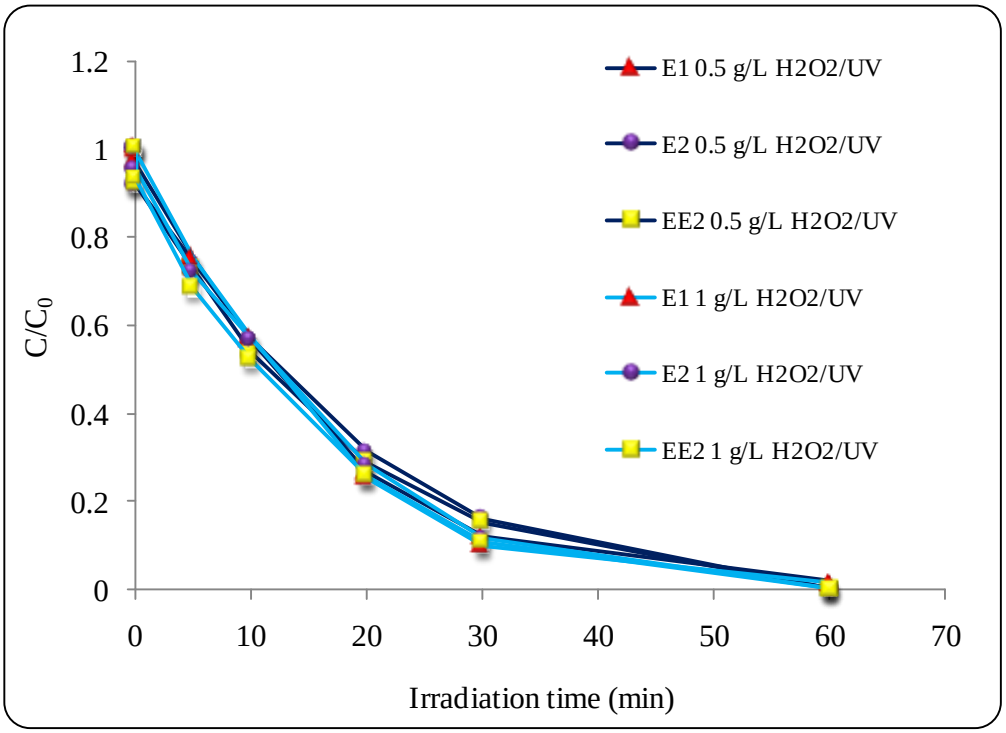

Figure 5.50: Effect of H_2O_2 concentration on the degradation of mixed EDCs [C_0=20 mgL^{-1} (E1=7.40×10^{-2}, E2=7.34×10^{-2} and EE2=6.75×10^{-2} mM), pH=5.8 and Power=200 W].

Table 5.8: Data of degradation percentages of 20 mgL^{-1} (E1=7.40×10^{-2}, E2=7.34×10^{-2} and EE2=6.75×10^{-2} mM) EDCs using 0.5 and 1gL^{-1} (1.47×10^{-2} and 2.94×10^{-2} M) H_2O_2.

H_2O_2 (g/L)	Irradiation time (min)	10	30	60
	Photodegradation efficiency	%		
0.5	E1	43.85	87.98	98.12
	E2	43.31	83.83	100
	EE2	46.34	84.82	100
1	E1	43.08	90.16	98.65
	E2	43.43	88.47	100
	EE2	48.03	89.44	100

5.4.5.4 *Effect of electron acceptors*

Experiments were conducted to investigate the extent to which oxygen as electron acceptor influences the degradation of EDCs (mixed). Streams of pure oxygen, synthetic air, and nitrogen were bubbled into solution to achieve different concentrations of oxygen. These experiments revealed that no significant effect (Figure 5.51).

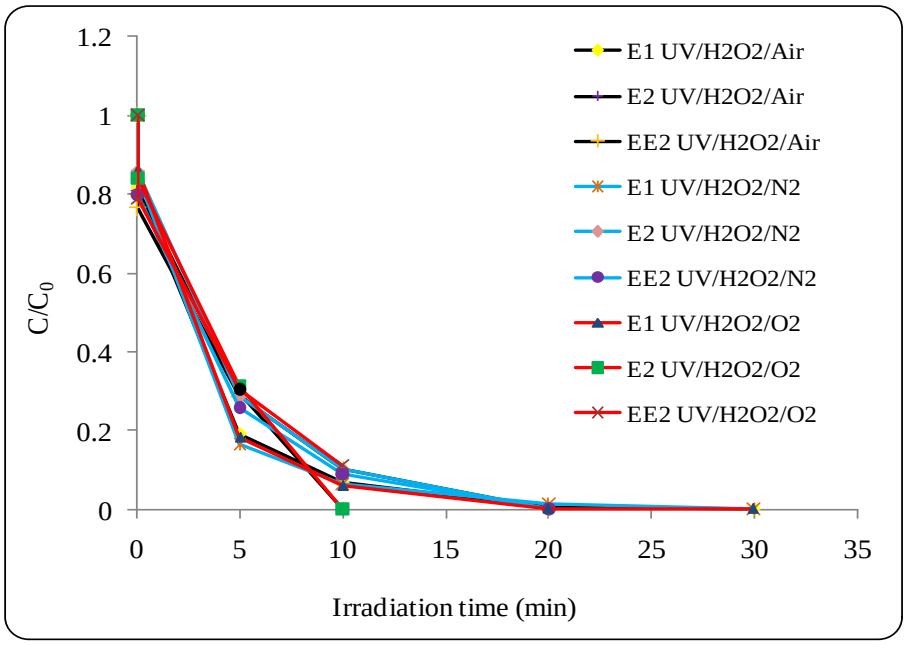

Figure 5.51: Effect of oxygen as electron acceptor on the degradation of mixed EDCs [C_{H2O2}=1 gL^{-1} (2.94×10^{-2} M), C_0=5 mgL^{-1} (E1=1.85×10^{-2}, E2=1.84×10^{-2} and EE2=1.69×10^{-2} mM), pH=5.8 and Power=200 W].

5.4.5.5 *Effect of light intensity on photodegradation of EDCs*

The effect of UV lamp power on the rate of photocatalytic degradation was investigated. An initial concentration of 20 mg/L (E1=7.40×10^{-2}, E2=7.34×10^{-2} and EE2=6.75×10^{-2} mM) of mixed EDCs with 1 g/L (2.94×10^{-2} M) H_2O_2 (pH 5.8) was used. The investigated lamp powers were 120 and 200 W. From the results in Figure 5.52 an

increase in lamp power (by about 67%) did not result in significant increase on the EDCs degradation. This indicates that lower lamp powers may be used.

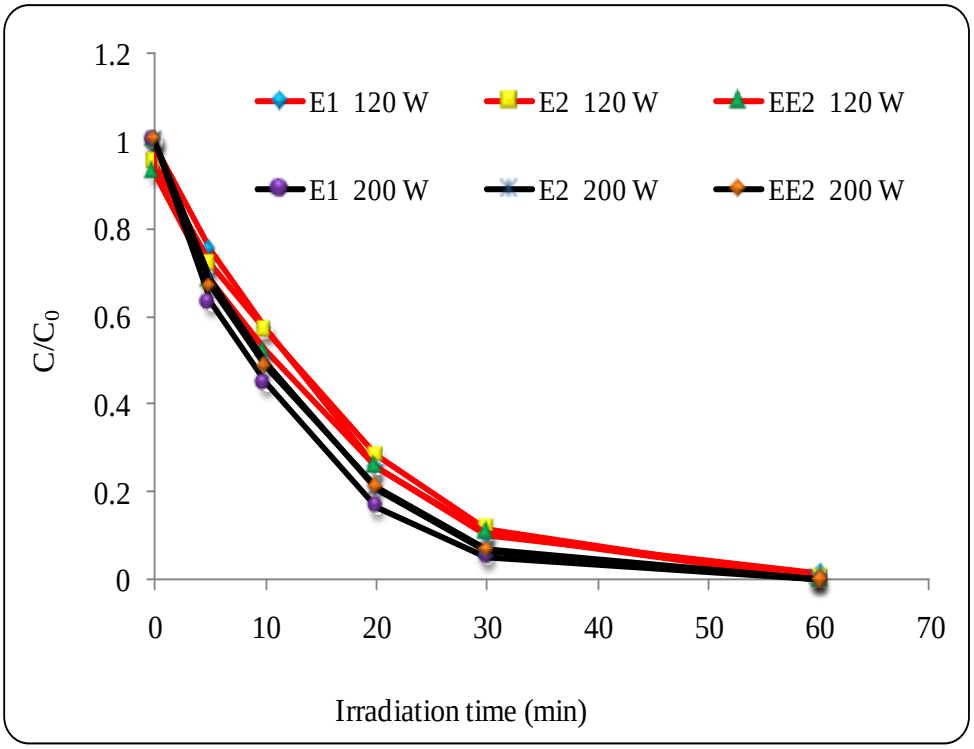

Figure 5.52: Effect of light intensity on the degradation of mixed EDCs [C_{H2O2}=1 gL^{-1} (2.94×10^{-2} M), C_0=20 mgL^{-1} (E1=7.40×10^{-2}, E2=7.34×10^{-2} and EE2=6.75×10^{-2} mM), pH=5.8].

This result indicates that within this lamp power range the rate of degradation is not proportional to lamp power. The range of degradation should be directly proportional to UV light intensity up to a certain value of intensity (Ollis et al., 1991; Terzian et al., 1995 and Herrmann 1999). In this case the direct proportionality relationship did not show most likely because the lamp intensity value at which the direct proportionality applies has been exceeded. Figure 5.53 indicates that the change of UV light power fitted first-order kinetics and the rate constant did not change significantly with the different UV light powers. It was also observed for three EDCs the rate constant was almost similar.

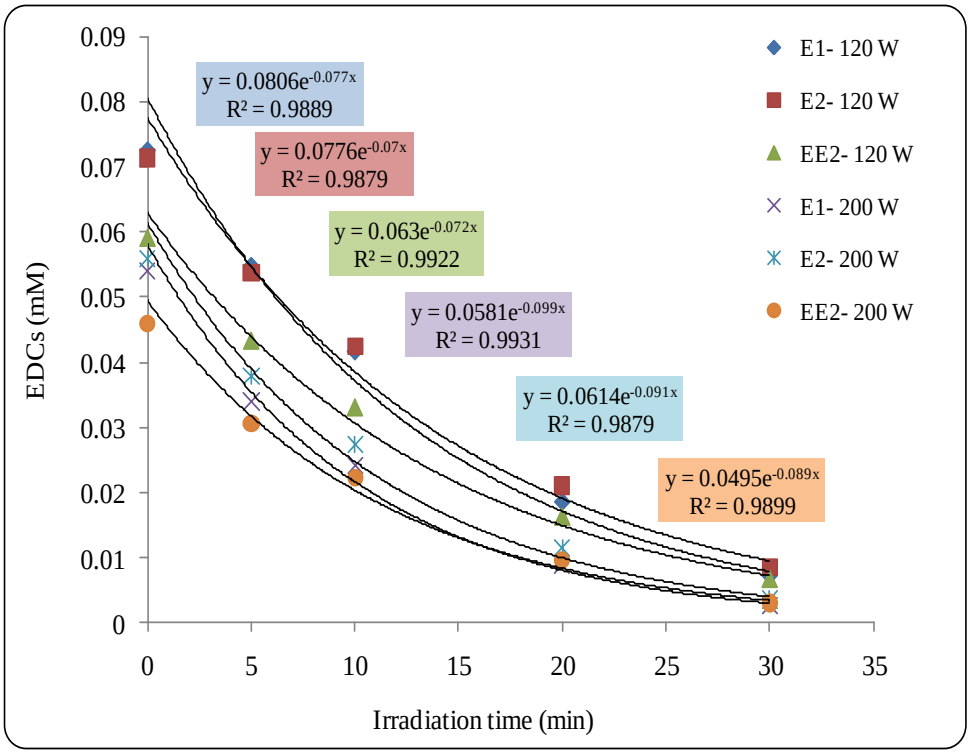

Figure 5.53: Kinetic of reaction using different light power.

5.4.5.6 *Effect of pH on the degradation of EDCs with UV/H_2O_2*

An important parameter in the UV/H_2O_2 reaction is the pH of the dispersion. Depending on the nature of the organic pollutant, an increase in pH will have a positive or negative effect on its degradation rate and consequently the mineralisation rate of the solution (Liu et al., 2003a). The effect of pH on the degradation of the three EDCs with UV/H_2O_2 was investigated at pH values of 3, 5, 7, 9, and 11. Figure 5.54 and Table 5.9 show the results of the photodegradation of 20 mg/L (E1=7.40×10^{-2}, E2=7.34×10^{-2} and EE2=6.75×10^{-2} mM) EDCs as mixture using 1 g/L (2.94×10^{-2} M) H_2O_2 in the presence of UV light at the five pH values.

The degradation efficiency of EE2 and E1 increased with increasing the pH of the solution up to 7 and 9 respectively and then remained constant. As stated by Coleman et al., (2000) as pH increases to 11, the hydroxide ion concentration increases, thereby the

generation of hydroxyl radicals will increase which increases the rate of degradation. Actually Liu et al., (2003) reported observing an increase in oxidation of EE2 with increased pH. It has been reported that photocatalytic reaction is faster in alkaline media than in acid media Doong et al., (2000). However the authors only studied EE2. In this work E1 was also found to behave in the same way. On the other hand E2 behaved differently in that its degradation, within the studied pH range, was not affected by the change of pH. The different behaviour of E2 in comparison to the other EDCs with changing the pH is almost certainly due to differences in the effect of pH on their structures. Table 5.10 shows the values of the rate constants for E1, E2 and EE2.

Table 5.9: Data of pH effect on degradation of the EDCs with UV/H_2O_2

pH value	Irradiation time (min)	10	20	30	60
	Photodegradation percentages	%			
3.0	E1	42.96	73.58	89.29	97.68
	E2	42.31	67.44	83.81	100.00
	EE2	46.08	70.47	85.03	99.10
5.0	E1	39.68	72.96	90.66	97.89
	E2	47.90	74.56	89.49	100.00
	EE2	42.93	71.71	88.20	99.56
7.0	E1	43.08	74.67	90.16	98.65
	E2	43.43	71.92	88.47	100.00
	EE2	48.03	74.40	89.44	100.00
9.0	E1	66.45	84.29	97.89	99.93
	E2	64.52	81.69	100.00	100.00
	EE2	67.81	82.49	98.59	100.00
11	E1	72.54	96.95	100.00	100.00
	E2	71.16	96.74	100.00	100.00
	EE2	69.79	95.70	100.00	100.00

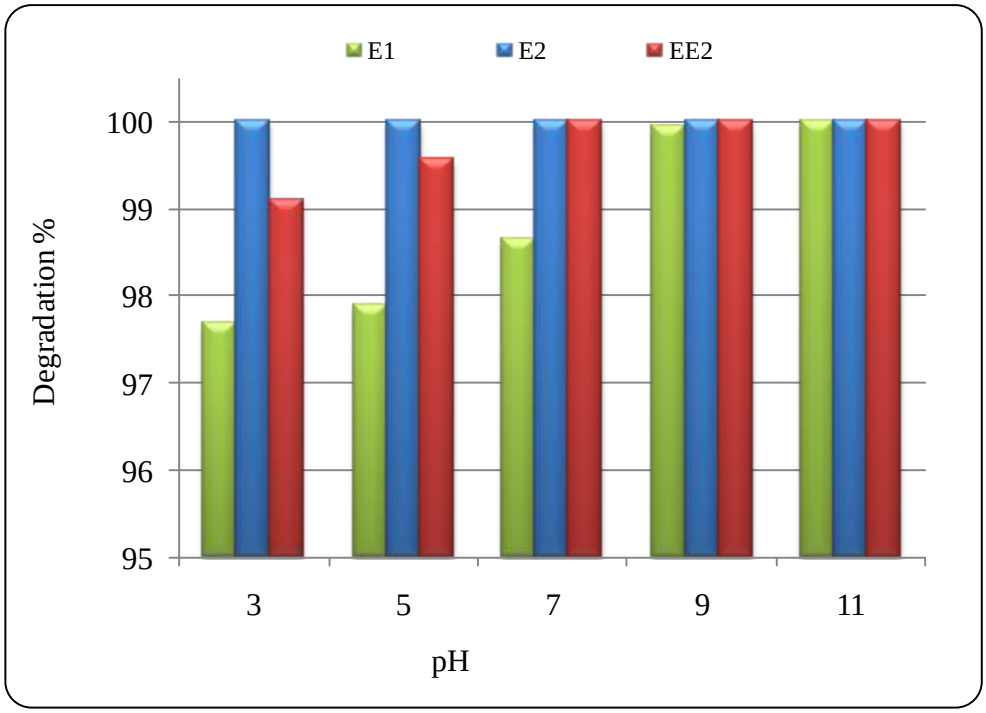

Figure 5.54: Effect of pH on the degradation of mixed EDCs with UV/H_2O_2 [C_{H2O2}=1 gL^{-1} (2.94×10^{-2} M), C_0=20 mgL^{-1} (E1=7.40×10^{-2}, E2=7.34×10^{-2} and EE2=6.75×10^{-2} mM), Irradiation time=1h and Power=200 W].

Table 5.10: First-order rate constant of EDCs degradation with UV/H_2O_2 at different pH values.

pH	EDCs	Rate of constant k (min^{-1})
3	E1	7.4×10^{-2}
	E2	5.7×10^{-2}
	EE2	5.9×10^{-2}
5	E1	6.7×10^{-2}
	E2	6.9×10^{-2}
	EE2	6.8×10^{-2}
7	E1	7.7×10^{-2}
	E2	7.0×10^{-2}
	EE2	7.2×10^{-2}
9	E1	1.18×10^{-1}
	E2	6.0×10^{-2}
	EE2	1.16×10^{-1}
11	E1	1.67×10^{-1}
	E2	1.66×10^{-1}
	EE2	1.66×10^{-1}

5.5 Photodegradation of EDCs with Ozone

Even though ozonation was not the main theme of this research experiments were carried out to investigate the effect of ozone on the degradation the three EDCs mixed in solution for the purpose of comparison with other photocatalytic degradation systems. The experimental setup was described in section 3.7.3. Several investigators have studied the ozonation of water containing EDCs (Hai-yan et al., 2006; Bila et al., 2007; Auriol et al., 2006; and Irmak et al., 2005). The degradation of EDCs increased with the increase in pH (Chu and Lau, 2007). Likewise Deborde et al. (2005) found that they could effectively remove more than 95% of 4-n-nonylphenol, bisphenol A, 17α-ethinylestadiol, 17β-estradiol, estrone and estriol by exposure to ozone (~2×10^{-3} mg min L^{-1}). Figure 5.55 shows that the degradation of the three EDCs with ozone was much faster than the other systems used in this study. After 1 minute, the degradation percentages were 77.02, 83.35 and 84.66% for E1, E2 and EE2 respectively and complete degradation of the three EDCs was achieved after about 2 minutes of ozonation.

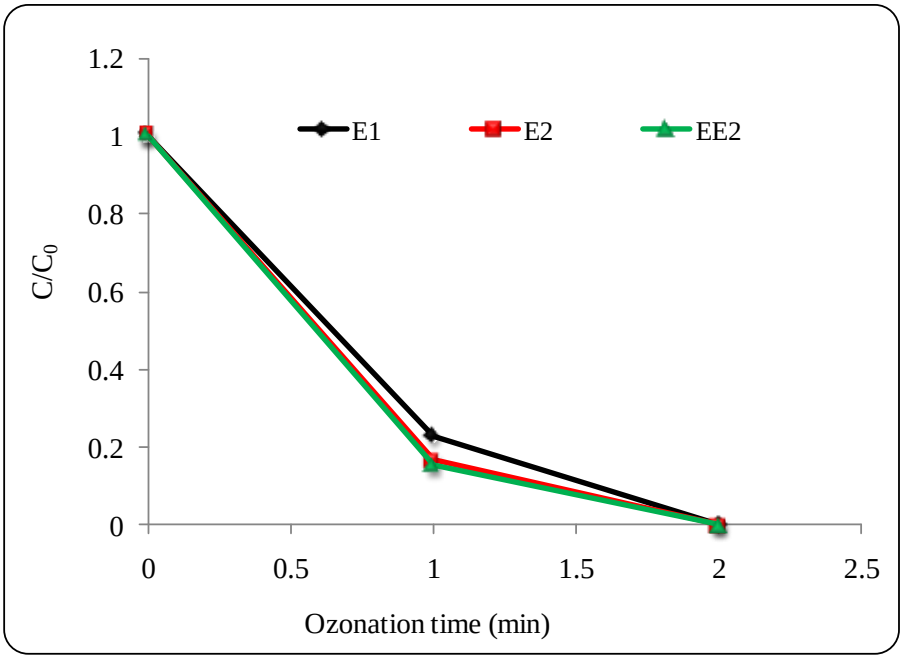

Figure 5.55: Degradation of EDCs mixture with ozone [Cozone= 10 gm^{-3} NTP, C_0=20 mgL^{-1} (E1=7.40×10^{-2}, E2=7.34×10^{-2} and EE2=6.75×10^{-2} mM), pH=5.8].

5.6 Comparison with UV/TiO_2, UV/H_2O_2 and Ozone oxidation

A comparison between the performance of the three systems used (i.e. UV/TiO_2, UV/H_2O_2 and O_3) to degrade the three EDCs was made. The initial concentrations of the EDCs were 20 mg/L (E1=7.40×10^{-2}, E2=7.34×10^{-2} and EE2= 6.75×10^{-2} mM) and the results are shown in Figure 5.56. Ozonation was the most effective, since it resulted in total degradation of the EDCs within the shortest time duration. The degradation of E2 was fastest reaching about 100% removal in almost 2 minutes. However about 99.92% and 99.72% degradation of EE2 and E1 were achieved respectively after the same 2 minutes. Deborde et al. (2005) studied the degradation of E1, E2 and EE2 with ozone and found that the oxidation reactions proceed at high rates. The rate constants with molecular ozone measured by Deborde et al. (2005) were 2.21×10^5, 1.83×10^5 and 1.53×10^5 ($mol.L^{-1}.s^{-1}$) for E2, EE2 and E1 respectively. The UV/H_2O_2 system was also effective in degrading the three EDCs but at much lower rates than ozone. It was

surprising to observe that the UV/TiO_2 photocatalytic system was ineffective for degrading the EDCs (Figure 5.56). This is most likely due to the high concentration of EDCs used. Indeed it was shown that UV/TiO_2 significantly degraded the EDCs when lower initial concentrations of 0.5 mg/L (E1=1.85×10^{-3}, E2=1.84×10^{-3} and EE2=1.69×10^{-3} mM) were used (section 5.4.3.2). Coleman et al., (2004) using UV/TiO_2 reported 50 and 100% removal of E1, E2 and EE2 (single component) at 10 μg/L within 10 and 60 minutes of photocatalytic process respectively. Additionally these authors determined the rate constants of E1, E2 and EE2 as 8.6×10^{-2}, 10.6×10^{-2} and 8.6×10^{-2} correspondingly. From these results, it can be inferred that ozone displayed highest efficiency in the degradation of the EDCs followed by UV/H_2O_2 and UV/TiO_2, with UV/TiO_2 being the least efficient. The low effect of the UV/TiO_2 process on the degradation of the EDCs may due to rapid recombination of the produced holes and conduction band electrons (Equations 5.21 and 5.22) before they undergo any chemical reactions as reported by Stasinakis (2008).

$$TiO_2 + h\nu \rightarrow e_{cb} + h^+ \quad (5.21)$$

$$TiO_2 \rightarrow TiO_2\left(e_{cb}^-, h_{vb}^+\right) \rightarrow recombination \quad (5.22)$$

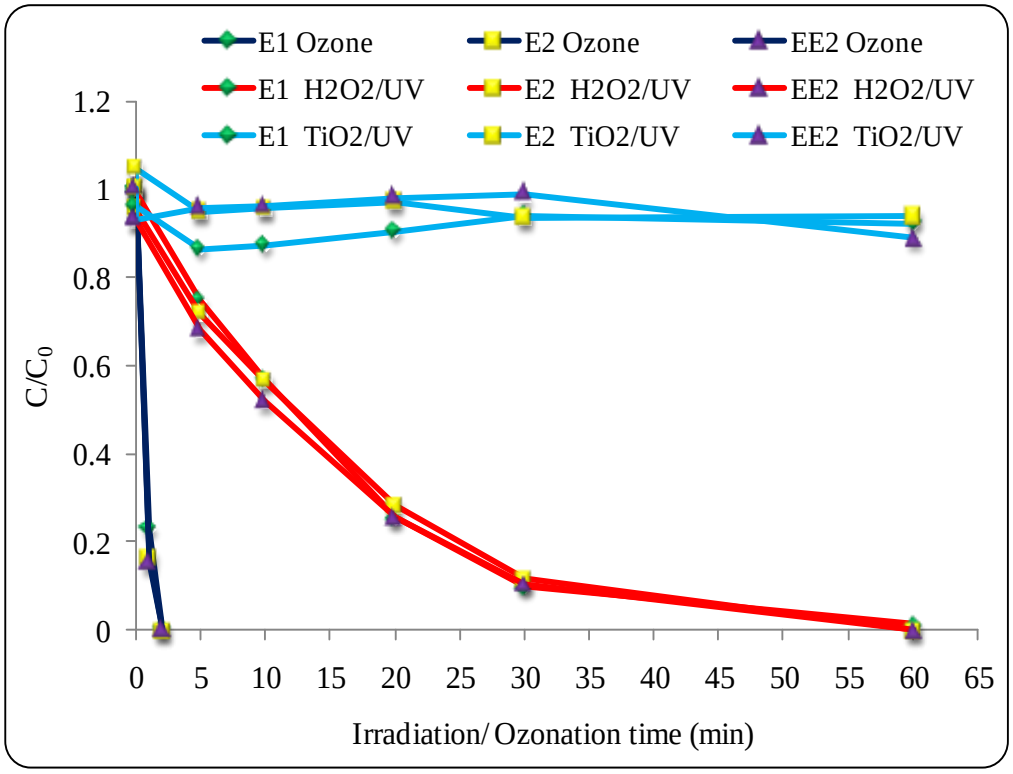

Figure 5.56: Effect of different oxidation processes on the degradation of mixed EDCs [Cozone= 10 gm^{-3} NTP, C_0=20mgL^{-1} (E1=7.40×10^{-2}, E2=7.34×10^{-2} and EE2=6.75×10^{-2} mM), C_{H2O2}=1 gL^{-1} (2.94×10^{-2} M), C_{TiO2}= 1gL^{-1}, pH=5.8, and Power=200 W].

5.7 Cost estimation

Cost estimation was carried out to compare the costs of using H_2O_2/UV and ozone processes for the degradation of the EDCs in water. It was found that the removal of 20 mg/L EDCs by ozonation will cost 0.001528 pence/mg, whereas the cost at same concentration using H_2O_2/UV will be 0.8 pence/mg. The assumptions used and the costs calculated are summarised in Tables 5.11 and 5.12.

Table 5.11: Calculation data of cost estimation for ozonation of EDCs.

Ozonation cost	Values	Unit
ρ oxygen	1.428	kg/m^3
O_3 concentration	10	g/m^3
Energy demand for O_3 production	10	kwh/kg
Unit Cost of electricity	10	pence/kwh
Unit cost of oxygen	10	pence/kg
Unit cost of oxygen	14.28	$pence/m^3$
Cost O_3 production - electricity	100	pence/kg O_3
Cost O_3 production - oxygen	1428.2	pence/kg O_3
Total cost O_3 production	1528.2	pence/kg O_3
flow rate of oxygen	200	mL/min
time of ozonation	2	min
volume of water sample	200	mL
EDCs concentration	20	mg/L
weight of EDCs	4	mg
weight of Ozone	0.000004	kg
cost of ozone production	0.00611	pence
cost of EDCs removal	0.00152	pence/mg
cost of EDCs removal	30.6	$pence/m^3$

Table 5.12: Calculation data of cost estimation for photocatalysis of EDCs.

Photocatalysis cost	Values	Unit
EDCs concentration	20	mg/L
volume of H_2O_2 (30%)	0.6	mL
volume of water	200	mL
concentration of H_2O_2	1	g/L
cost of H_2O_2	0.27	£/L
cost of H_2O_2	26.80	pence/L
cost of H_2O_2	0.02	pence
Unit Cost of electricity	10	pence/kwh
Power	200	W
time	60	min
Energy	0.2	kWh
cost of UV light	2	pence
total cost	2.02	pence
weight of EDCs	0.2	mg
cost of EDCs removal	10.08	pence/mg
cost of EDCs removal	10080	pence/m^3

5.8 Summary

The results of the degradation of RO16, TCC, clopyralid and EDCs using three oxidation systems UV/TiO_2, UV/H_2O_2 and O_3 were presented in this chapter. The degradation rate of RO16 was found to increase with decreasing the initial dye concentration. No degradation of RO16 was found when only UV was used. UV/TiO_2 gave more efficient degradation of RO16 than UV/H_2O_2. Triclocarban can be degraded with photolysis processes (UV light). The photocatalytic degradation of TCC was efficient with UV/H_2O_2 but not with UV/TiO_2. It was found that increasing H_2O_2 concentration had no significant effect on TCC degradation. Complete degradation of clopyralid was achieved with UV/TiO_2 in about 90 min at an optimum catalyst concentration of 1g/L. UV/H_2O_2 and O_3 gave rapid degradation of clopyralid within the first 10 min but were not effective to achieve its complete degradation even after longer times. E1 was found to be degraded more as compared to E2 and EE2 in photolysis. The efficiency of degradation of EDCs with ozone was higher as compared to UV/H_2O_2 and UV/TiO_2.

Chapter Six

Conclusions and recommendations for future work

6.1 Conclusions

Heterogeneous photocatalytic oxidation has been found to be effective in degrading a large number of persistent organics in water. In this work the major factors affecting the photocatalytic process are the initial concentration of the target compounds, the amount of catalyst, the light intensity, type of catalyst, electron acceptor though to a lesser extent, the irradiation time and the pH.

Reactive orange 16 (RO16) was degraded by photocatalytic (UV/TiO_2 and UV/H_2O_2) processes. TiO_2 can efficiently catalyse the decomposition of dye RO16 in the presence of light and oxygen. Degussa P25 showed superior photocatalytic activity compared to other catalysts such as TiO_2 (Hombifine N), ZnO, SnO_2 and FeO_3 powders. The dye RO16 was resistant to direct photolysis and there was no degradation for RO16 in the dark and in the presence of TiO_2. The current work found no degradation of RO16 with hydrogen peroxide (H_2O_2) alone. Besides it was found UV/TiO_2 gave more efficient degradation of RO16 compared to UV/H_2O_2. Increasing the initial dye concentration from 3.24×10^{-2} mM (20 mg/L) to 60 mg/L (9.72×10^{-2} mM) led to a decrease in the degradation rate. The optimum conditions for fastest RO16 degradation at initial concentrations of 3.24×10^{-2} and 6.48×10^{-2} mM RO16 were pH 5.5 and a catalyst concentration of 0.5 g/L. On the other hand for 9.72×10^{-2} mM at the same pH the optimum catalyst concentration was 1 g/L. For the photocatalytic oxidation, it was found that the disappearance of RO16 satisfactorily followed pseudo first-order kinetics

according to Langmuir-Hinshelwood (L-H) model. On the other hand it was observed that the recovered catalyst could be reused.

The results from the present laboratory experimental work suggests that triclocarban can be degraded with photolysis processes (UV light). On the other hand photocatalytic degradation of TCC was efficient with UV/H_2O_2 but not with UV/TiO_2. An increase in the initial concentration of TCC led to a decrease of the degradation rates of TCC with UV. It was found that increasing the H_2O_2 concentration from 2.94×10^{-2} to 5.88×10^{-2} M gave similar results for TCC degradation.

The results of this study indicate that the photocatalytic system using TiO_2 Degussa P25 as photocatalyst was effective in degrading the herbicide clopyralid completely in the presence of UV light. The results indicated that the different operating parameters including catalyst type, pH, catalyst concentration, clopyralid initial concentration, electron acceptors influenced the rate and the extent of the degradation of clopyralid. pH 5 and a catalyst concentration of 1g/L gave optimum conditions for fastest degradation rates. In the range of concentrations used, zero-order kinetics was most suitable to describe the change of clopyralid concentration with time in the initial photocatalytic degradation phase. A comparison of the results showed that the degradation of clopyralid with ozone or UV/H_2O_2 was not as effective as with UV/TiO_2 though both oxidation systems were faster than UV/TiO_2 only within the first 10 minutes.

The current research showed that the three EDCs [estrone (E1), 17β-estradiol (E2) and 17α-ethinylestradiol (EE2)] used in this study can be degraded with both photolysis and photocatalysis. E1 was found to degrade rapidly as compared to E2 and EE2 in photolysis. In photocatalysis, increasing catalyst concentration resulted in decreasing degradation of the EDCs. In addition increasing the initial concentration resulted in decreasing degradation rates of the EDCs. Near complete degradation of the EDCs (E1=

7.40×10^{-2}, E2=7.34×10^{-2} and EE2=6.75×10^{-2} mM) either as single component or in mixtures was achieved in 1 hour irradiation using UV/H_2O_2. Increasing the initial concentration of the EDCs resulted in decreased degradation rates. On the other hand the increase of H_2O_2 concentration from 2.94×10^{-2} to 5.88×10^{-2} M did not result in significant changes in the degradation rates of the EDCs. Moreover, an increase in UV power from 120 to 200 W did not affect significantly the degradation rates. The current work found no degradation of EDCs with hydrogen peroxide (H_2O_2) alone.

Ozonation was more effective in degrading the EDCs. Almost complete degradation was achieved in 2 minutes ozonation. It was found that mixtures of EDCs were degraded by ozone to the same extent as single components. The efficiency of degrading the EDCs with ozone was higher as compared to UV/H_2O_2 and UV/TiO_2.

6.2 Recommendations

This thesis described the decomposition of various chemicals including Reactive Orange dye RO16, triclocarban, clopyralid and endocrine disrupting chemicals in synthetic solutions using photocatalytic processes. Future works may explore the removal of these chemicals from real waste streams using the same procedures.

The chemistry of the decomposition reactions involving the by-products formed could be studied further using HPLC, GC/MS, Ion Chromatography and LC/MS/MS.

The TiO_2 semiconductor has a large band gap (Eg>3.2 eV, excited only by UV light) limiting the use of sunlight or visible light as an irradiation source in photocatalytic reactions. In addition, photogenerated electron-hole pairs can recombine easily on pure TiO_2 surface. Therefore the photocatalytic efficiency of pure TiO_2 semiconductor is very low. In order to overcome these drawbacks of TiO_2 semiconductor as a photocatalyst, there is a need for modification of the TiO_2 semiconductor surface for

enhancing electron-hole separation and extending the light absorption range of TiO_2 into the visible range. In fact initial work has already started during this research and involved modifying the surface of TiO_2 with gold and silver nanoparticles. The work is at its very early stages and for clarity purposes the data have neither been presented nor discussed in this thesis and the results presented in appendix.

References

Abdullah, M., low, G.K.C. and matthews, R.W. (1990). Effects of common inorganic anions on rates of photocatalytic oxidation of organic-carbon over illuminated titanium-dioxide. journal of physical chemistry 94(17), pp 6820-6825.

Abramovic, B. F.; Anderluh, V. B.; Sojic, D. V.; Gaal, F. F., (2007). Photocatalytic removal of the herbicide clopyralid from water. J. Serb. Chem. Soc., 71, pp 1477–1486.and pharmaceuticals and personal care products (PPCPs) in reclaimed water in Australia. ISBN 0 643 09180 7, pp 1-35.

Ahmed, S.A. (2000). The immune system as a potential target for the environmental estrogens endocrine disruptors: a new emerging field. Toxicol., 150, pp 191-206.

Alekabi, H. and Serpone, N. (1988). Kinetic-studies in heterogeneous photocatalysis .1. photocatalytic degradation of chlorinated phenols in aerated aqueous-solutions over TiO_2 supported on a glass matrix. journal of physical chemistry 92(20), pp 5726-5731.

Alhakimi, G., Studnicki, L.h. and Al-ghazali, M. (2003). Photocatalytic destruction of potassium hydrogen phthalate using TiO_2 and sunlight: application for the treatment of industrial wastewater. journal of photochemistry and photobiology a-chemistry 154(2-3), pp 219-228.

Alsayyed, G., Doliveira, J.C. and Pichat, P. (1991). Semiconductor-sensitized photodegradation of 4-chlorophenol in water. journal of photochemistry and photobiology a-chemistry 58(1), pp 99-114.

Andreozzi R, Caprio V. Marotta R, and Radovnikovic A. (2003b). Ozonation and H_2O_2/UV treatment of clofibric acid in water: a kinetic investigation. Journal of Hazardous Materials 103: pp 233-246.

Andreozzi, R., Caprio, V., Insola, A. and Marotta, R. (1999). Advanced oxidation processes (AOP) for water purification and recovery. catalysis today 53(1), pp 51-59.

Anheden, M. Goswami, D.Y. Svedberg, G. (1996). J. Solar Energy Eng. 118, 2.

Araña, J., Herrera Melián, J.A., Doña Rodríguez, J.M., González díaz, O., Viera, A., Pérez Peña, J., Marrero Sosa, P.M. and Espino Jiménez, V. (2002). TiO_2-photocatalysis as a tertiary treatment of naturally treated wastewater. catalysis today 76(2-4), pp 279-289.

Auriol, M., Y. Filali-Meknassi, C. Adams and R. Tyagi, (2006). Natural and synthetic hormone removal using the horseradish peroxidise enzyme: Temperature and pH effects. Water Research 40 (15): pp 2847-2856.

Bahnemann, D. Bockelmann D. and Goslich., R. (1991). Mechanistic studies of water detoxification in illuminated TiO_2 suspensions, Solar Energy Materials, 24, pp 564-583.

Bahnemann, D. in: P. Boule (Ed.), (1999). The Handbook of Environmental Chemistry, vol. 2, Part L, Springer-Verlag, Berlin, Heidelberg, p. 285.

Bahnemann, D., Cunningham, J., Fox, M.A., Pelizzetti, E., Pichat, P., Serpone, N., (1994). Photocatalytic Treatment of Waters. Aquatic and Surface Photochemistry. G.R., Helz, R.G., Zepp, D.G., Crosby, Eds., Lewis Publishiers, Boca Raton, pp 261-316.

Balcioglu, A. Arslan, L. and M. Scan, (2001). Homogenous and heterogeneous advanced oxidation of two commercial reactive dyes, Environ. Technol., vol. 22, pp 813-821.

Barbeni, M., Morello, M., Pramauro, E., Pelizzetti, E., Vincenti, M., Borgarello, E. and Serpone, N. (1987). Sunlight photodegradation of 2,4,5-trichlorophenoxy-acetic acid and 2,4,5,trichlorophenol on TiO_2 - identification of intermediates and degradation pathway. chemosphere 16(6), pp 1165-1179.

Baxendale, J.H. and Wilson, J.A. (1957). The photolysis of hydrogen peroxide at high light intensities. transactions of the faraday society 53(3), pp 344-356.

Bekbolet, M. Ozkosemen, G. (1996). Water Sci. Technol. 3, pp 189-194.

Bekbolet, M., (2001). Separation of titanium dioxide photocatalyst by physicochemical treatment methods. The Sixth International Conference on TiO_2 Photocatalytic Purification and Treatment of Water and Air. Ontario, Canada. 25-29 June 2001. p 157.

Beltran, F. (2004). Ozone reaction kinetics for water and wastewater systems, lewis publishers, boca raton florida.

Benitez, F.J., Beltranheredia, J. and Gonzalez, T. (1994). Degradation by ozone and uv-radiation of the herbicide cyanazine. ozone-science & engineering 16(3), pp 213-234.

Bhatkhande, D.S. Pangarkar V.G. and Beenackers., A.A. (2002). Photocatalytic degradation for environmental applications: a review. J. Chem. Technol. Biotechnol., 77: pp 102-116.

Bickley R.I, Slater M.J. and Wang W-J., (2005). Engineering Development of a Photocatalytic Reactor for Waste Water Treatment, Process Safety and Environment Protection, 83(B3): pp 205-216.

Bila, D., Montalvao A.F., Azevedo D., Dezotti M., (2007). Estrogenic activity removal of 17 beta-estradiol by ozonation and identification of by-products. Chemosphere 69: pp 736-746.

Blake, D. M., (2001). Bibliography of work on photocatalytic removal of hazardous compounds from water and air. Golden: National renewable energy laboratory.

Bledzka, D., Gmurek, M., Gryglik, M., Olak, M., Miller, J., Ledakowicz, S. (2010). Photodegradation and advanced oxidation of endocrine disruptors in aqueous Solutions. J. Catalyst today 151: pp 125-130.

Bolton, J. R., (1999). Ultraviolet applications handbook, Bolton Photosciences.

Broseus, R., Vincent, S., Aboulfadl, K., Daneshvar, A., Sauve, S., Barbeau, B. and Prevost, M. (2009). Ozone oxidation of pharmaceuticals, endocrine disruptors and pesticides during drinking water treatment. water research 43(18), pp 4707-4717.

Buxton G.V., Greenstock W., Helman P. and Ross A.B., (1988). Critical review of rate constants for reactions of hydrated electrons, hydrogen atoms and hydroxyl radicals in aqueous solution, J. Phys. Chem. Ref. Data, 17, pp 513-886.

Carey J. (1992). An Introduction To Advanced Oxidation Processes (AOP) For Destruction of organics in Wastewater. Wat. Pollut. Res. J. Canada, 27: pp 1-21.

Carp, O. Huisman C.L. and A. Reller, (2004). Photoinduced reactivity of titanium dioxide.

Carp, O., Huisman, C. L., Reller, A. (2004). Photoinduced reactivity of titanium dioxide, Progress in Solid State Chemistry, 32: pp 33-177.

Chang JS, Lin YC. Bitechnol Prog, (2000). Fed-Batch Bioreactor Strategies for Microbial Decolourizations of Azo Dye Using a Pseudomonas luteola Strain16: (9) pp 79-85.

Chen, D. W. and Ray, A. K., (1998). Photodegradation kinetics of 4-nitrophenol in TiO_2 suspension. Water Research, Vol. 32, No. 11, pp 3223-3234.

Chignell, C.F. Kalymmm, B. and. Ilhson, R.P (1980). Pliotochem. Pliorobioi., 32, 563.

Chu, W. and T. K. Lau, (2007). Ozonation of endocrine disrupting chemical BHA under the suppression effect by salt additive-With and without H_2O_2. Journal of Hazardous Materials 144 (1-2): pp 249-254.

Chu, W., Rao, Y. and Hui, W.Y. (2009). Removal of simazine in a UV/TiO_2-heterogeneous system. journal of agricultural and food chemistry 57(15), pp 6944-6949.

Cohen, Z.Z., Eiden C., Lober, M.N., In: W.Y. Gerner, ED., (1986). Evaluation of Pesticide in Ground Water, ACS Symp. Ser. 315, American Chemical Society, Washington, DC, pp 170-196.

Coleman HM, Eggins BR, Byrne JA, Palmer FL, King E. (2000). Photocatalytic degradation of 17β-oestradiol on immobilised TiO_2. Appl Catal B: Environ; 24: pp 1-5.

Coleman, H.M., Routledge, E.J., Sumpter, J.P., Eggins, B.R., Byrne, J.A. (2004). Rapid loss of estrogenicity of steroid estrogens by UVA photolysis and photocatalysis over an immobilised titanium dioxide catalyst. Water research 38: pp 3233-3240.

Corredor, M.C., Mellado, J.M.R. and Montoya, A.R. (2006). Process in the reduction of the herbicide clopyralid on mercury electrodes. electrochimica acta 51(20), pp 4302-4308.

Da Silva, C.G. Faria, L., (2003). Photochemical and photocatalytic degradation of an azodye in aqueous solution by UV irradiation. J. Photochem Photobiol A Chem; 155: pp 133-143.

Dahlstrom, D. A., Bennett, R.C., Emmett, R.C., Harriott, P., Laros, T., Leung, W., (1997). Liquid-solid operations and equipment. In: Perry, R. H. and Green, D. W. Perry's Chemical Engineer's Handbook. 7th ed. USA: The McGraw-Hill, pp 18-59.

Dalrymple, O. Yeh D. and Trotz., M. (2007). Removing pharmaceuticals and endocrine disrupting compounds from wastewater by photocatalysis. J. Chem. Technol. Biotechnol., 82, pp 121-134.

Damiani, E. L. Greci, R. Parson, and J. Knowland., (1999). Free Rudical Biologv & Medicine, 26, 809.

Daneshvar, N., Salari, D., Khataee, A.R., (2003). Photocatalytic degradation of azo dye acid red 14 in water: investigation of the effect of operational parameters. J. Photochem. Photobiol.A Chem. 157: pp 111–116.

Daniela V. ˇSoji ´c, Vesna B. Anderluh, Dejan Z. Orˇcci ´c, Biljana F. Abramovi ´c., (2009). Photodegradation of clopyralid in TiO_2 suspensions: Identification of intermediates and reaction pathways.

Deborde, M., S. Rabouan, J.P. Duguet, and B. Legube, (2005). Kinetics of Aqueous Ozone-Induced Oxidation of Some Endocrine Disruptors,'Environ. Sci. Technol., 39(16): pp 6086-6092.

Desbrow, C. Routledge, E. J. Brighty, G. C. Sumpter, J. P. and Waldock, M. (1998). Identification of estrogenic chemicals in STW effluent. 1. Chemical fractionation and in vitro biological screening, Environmental Science and Technology, vol. 32, no. 11, pp 1549-1558.

Dictionary of Science and Technology, (1992). Academic press, ed. by Morris, C., p 2432.

Diebold, U., (2003). The Surface Science of TiO_2. Surface Science Reports, 48: pp 53-229.

Diffey B.L. and Robson, J. (1 989). J.Soc.Cosmer. Cltem., 40, 127.

Dominguez, C., Garcia, J., Pedraz, M.A., Torres, A. and Galan, M.A. (1998). Photocatalytic oxidation of organic pollutants in water. catalysis today 40(1), pp 85-101.

Donald, D.B. Cessna, A.J. Sverko, E. Glozier, N.E. (2007). Pesticides in surface drinking-water supplies of the northern Great Plains, Environ. Health Perspect. 115: pp 1183–1191.

Doong, R. A., Maithreepala, R. A. and Chang, S-M., (2000). Heterogeneous and homogeneous photocatalytic degradation of 2-chlorophenols in aqueous titanium dioxide and ferrous ion. Wat. Sci. Tech., vol. 42. No. 7-8, pp 253-260.

Dowd, R.M. Anderson M.P. and M.L. Johnson, (1988). In: Proe. Second National Outdoor Action Conference on Aquifer Restoration, Ground Water Monitoring Geophysical Methods, National Water Well Association, Dublin, OH, pp 1365-1379.

Feng, X.H., S.M. Ding, J. Tu, F. Wu and N. Deng, (2005). Degradation of estrone in aqueous solution by photo-fenton system. Science of Total Environment 345 (1-3): pp. 229-237.

Ferguson, S.A. (2002). Effects on brain and behaviour caused by developmental exposure to endocrine disrupters with estrogenic effects. Neurotoxicol. Teratol., 24, pp 1-3.

Fernández-ibáñez, P., Blanco, J., Malato, S. and Nieves, F.J.D.L. (2003). Application of the colloidal stability of TiO_2 particles for recovery and reuse in solar photocatalysis. water research 37(13), 3180-3188.

Fujishima, A. Rao, T. N.Tryk, D. A. (2000). Titanium dioxide photocatalysis. Journal of Photochemistry and Photobiology C: Photochemistry Reviews, 1, pp 1-21.

Ganesh, G. Boardman, D. Michelssen, D. (1994). Water Res. 28, pp 1367-1376.

Garcia, J.C. Takashima, K. (2003). J. Photochem. Photobiol. A: Chem. 155, pp 215-222.

Gottschalk., C., J. A. Libra, and Saupe, (2000). Ozonation of water and waste water, Wiley-Vch.

Gulston M. and Knowland J., (1999). Mutat. Res. Gen. Tox. En, 444, 49.

Hai-yan L., Jiu-hui Q., Hui-juan L., (2006). Removal of a type of endocrine disruptors di-n-butyl phthalate from water by ozonation. Journal of Environmental Sciences (China) 18(5): pp 845-851.

Halden, R. U., Paull, D. H., (2005). Co-occurrence of triclocarban and triclosan in US water resources. Environmental Science and Technology, 39: pp 1420-1426.

Halmann, M.M. (1996). Photodegradation of water pollutants, crc press, boca raton.

Handbook of Chemistry and Physics. (1976). 57th edn., ed. by Weast, R., C., pp 749-750.

Hanley, TL., Luca, V., Pickering, I. And Howe, R.F., (2002). Structure of Titania Sol-Gel Films: A Study by X-Ray Absorption Spectroscopy. Journal of Physical Chemistry B, 106 (6): pp 1153-1160.

Hassan, S.A., Bigler, F., Bogenschutz, H., Boller, E., Brun, J., Calis, J.N.M., Coremanspelseneer, J., Duso, C., Grove, A., Heimbach, U., Helyer, N., Hokkanen, H., Lewis, G.B., Mansour, F., Moreth, L., Polgar, L., Samsoepetersen, L., Sauphanor, B., Staubli, A., Sterk, G., Vainio, A., Vandeveire, M., Viggiani, G. and Vogt, H. (1994). Results of the 6th joint pesticide testing program of the iobc/wprs working group pesticides and beneficial organisms. entomophaga 39(1), pp 107-119.

Heintz, Robert. D., Weber, J.V., (2000). Comparison of the degradation of benzamide and acetic acid on different TiO_2 photocatalysts. J. Photochem. Photobiol. A Chem., 135, pp 77-80.

Herrmann, J. M. (1999). Heterogeneous Photocatalysis: Fundamentals And Applications To The Removal of Various Types of Aqueous Pollutants. Catalysis Today, 53, pp 115-129.

Hess, R.A. Bunick, D. Lee, K.H. Bahr, J. Taylor, J.A. Korach K.S. and Lubahn, D.B. (1997). A role for oestrogens in the male reproductive system. Nature, 390, pp 509-512.

Hoffman, A.J., Carraway, E.R. And Hoffmann, M.R. (1994). Photocatalytic Production of H_2O_2 And Organic Peroxides on Quantum-Sized Semiconductor Colloids. Environmental Science & Technology 28(5), pp776-785.

Hoffmann, M. Martin, S. Choi W. And Bahnemann D. (1995). Environmental Applications of Semiconductor Photocatalysis. Chem. Rev., 95: pp 69-96.

Hoigne, J., (1997). Inter-calibration of OH radical sources and water quality parameters. Water Sci. Technol. 35 (4): pp 1-8.

Hua, W.Y., Bennett, E.R. And Letcher, R.J. (2006). Ozone Treatment And The Depletion of Detectable Pharmaceuticals And Atrazine Herbicide In Drinking Water Sourced From The Upper Detroit River, Ontario, Canada. Water Research 40(12), pp 2259-2266.

Huang, X.J., Pedersen, T., Fischer, M., White, R. And Young, T.M. (2004). Herbicide Runoff Along Highways. 1. Field Observations. Environmental Science & Technology 38(12), pp 3263-3271.

Huber, M.M., T.A. Ternes, and U. von Gunten, (2004). Removal of Estrogenic Activity and Formation of Oxidation Products During Ozonation of 17alpha-Ethinylestradiol, Environ. Sci. Technol., 38(19): pp 5177–5186.

Hughes, D; Jewell, T; Parpworth, N., (1996). Environmental Law, 3rd ed., London, Reed Elsevier Ltd.

Ikehata, K. And El-Din, M.G. (2005a). Aqueous Pesticide Degradation by Ozonation And Ozone-Based Advanced Oxidation Processes: A Review (Part I). Ozone-Science & Engineering 27(2), pp 83-114.

Irmak, S., O. Erbatur, And A. Akgerman, (2005). Degradation of 17 Beta- Estradiol And Bisphenol A In Aqueous Medium by Using Ozone And Ozone/UV Techniques, J. Hazard. Mater., 126 (13): pp 54-62.

Jagger, J., (1967). Ultraviolet photobiology, Prentice-Hall, Inc., Englewood Cliffs, N.J.

Jayanty, R.K.M., Photocatalysis on TiO_2. Ph.D. Thesis. 1972, University of Bradford: Bradford, UK.

Jefferson, B., Bedel, C. and Parsons, S. A., (2001). Photo-catalytic reactors for in-building grey water reuse. The Sixth International Conference on TiO_2 Photocatalytic Purification and Treatment of Water and Air. Ontario, Canada. 25-29 June 2001. p 89.

Jobling, S., Nolan, M., Tyler, C.R., Brighty G., and Sumpter, J.P. (1998).Widespread sexual.

Johnson, A.C. Belfroid A. and Di Corcia, A. (2000). Estimating steroid oestrogen inputs into activated sludge treatment works and observations on their removal from the effluent. Environ. Sci. Technol., 256, pp 163-173.

Kavan, L. Rathousky, J. Gratzel, M. Shklover V. and Zukal A., (2001). Mesoporous thin film TiO_2 electrodes. Micropor.Mesopor.Mater. 44/45, pp 653-659.

Kim, S.E., H. Yamada, and H. Tsuno, (2008). Evaluation of Estrogenicity for 17 beta-Estradiol Decomposition During Ozonation, Ozone Sci Eng., 26: pp 563–572.

Kim, Y.; Lee, K. h.; Sasaki, S.; Hashimoto, K.; Ikebukuro, K.; Karube, I., (2000). Anal. Chem. on web. Photocatalytic Sensor for Chemical Oxygen Demand Determination Based on Oxygen Electrode, 72 (14), pp 3379 -3382.

Knowland, J. E.A. McKenzie, P.J. McHugh, and N.A. Cridland, (1993). FEBS Lett., pp 309- 324.

Kruithof, J.C., Kamp, P.C. And Belosevic, M. (2002). Innovations In Conventional And Advanced Water Treatment Processes. Malzer, H.J., Gimbel, R. And Schippers, J.C. (Eds), pp. 113-122, I W A Publishing, London.

Langlais B., D. Reckhow and D. Brink (1991). "Ozone in water treatment application and engineering" Lewis publishers.

Lee, H. Y. Park, Y. H. Ko, K., (2000). Langmuir, (Correlation between Surface Morphology and Hydrophilic/Hydrophobic Conversion of MOCVD-TiO_2 Films), 16 (18), pp 7289 -7293.

Legrini, O. Oliveros, E. and Braun, A. M., (1993). Photochemical processes for water treatment. Chem. Rev., Vol. 93: pp 671-698.

Levy, B., (1997). Photochemistry of Nanostructured Materials for Energy Applications Journal of Electroceramies1 (3): pp 239-272.

Liakou, S; Pavlou, S; Lyberatos, G., (1997). Ozonation of Azo Dye. Water Science and Technology, vol. 35, No. 4, pp 279-286.

Lindner, M. Bahnemann, D. Hirthe. B. Griebler, W., (1995). Magnetic photocatalyst assessment of activity and stability Solar Engineering vol 1, ASME, pp 399-408.

Linsebigler, A.L. Lu, G. and Yates, J.T. (1995). Chemical Reviovs,95: pp 735.

Litter, M. I.(1999). Review: Heterogeneous photocatalysis transition metal ions in photocatalytic systems. Applies Catalysis B: Environmental, 23: pp 89-114.

Liu B and Liu XL., (2004). Direct photolysis of estrogens in aqueous solutions. Science of the Total Environment 320: pp. 269-274.

Liu, B., Wu, F., Deng, N. (2003). UV-light induced photodegradation of17α-ethynylestradiol in aqueous solutions. J. Hazardous Material B98: pp 311-316.

Liu, B., Wu, F., Deng, N.S., (2003a). UV-light induced photodegradation of 17α-ethynylestradiol in aqueous solutions. J. Hazard. Mater. B 98: pp 311-316.

Lu, M.C., Chen, J.N. And Tu, M.F. (1999) Photocatalytic Oxidation of Propoxur In Aqueous Titanium Dioxide Suspensions. Journal of Environmental Science And Health Part B-Pesticides Food Contaminants And Agricultural Wastes 34(5), pp 859-872.

Malato, S., Blanco, J., Campos, A., Cáceres, J., Guillard, C., Herrmann, J.M. And Fernández-Alba, A.R. (2003). Effect of Operating Parameters on The Testing of New Industrial Titania Catalysts At Solar Pilot Plant Scale. Applied Catalysis B: Environmental 42(4), pp 349-357.

Martin, C. A., Baltanas, M. A. and Cassano, A. E., (1996). Photocatalytic reactors kinetics of the decomposition of chloroform including absorbed radiation effects. Environ. Sci. Technol., vol. 30, pp 2355-2364.

Mccallum JEB, Madison SA, Alkan S, Depinto RL, Rojas Wahl RU., (2000). Analytical Studies on the Oxidative Degradation of the Reactive Textile Dye Uniblue Environ Sci Technol; A, 34 (24), pp 5157-5164.

Mellanby K., (1992). Waste and Pollution. The Problem for Britain. London, Glasgow: HarperCollins. pp 9-14.

Mendes, A. (2002). The endocrine disrupters: A major medical challenge. Food Chem. Toxicol., 40, pp 781-788.

Mendez-Arriaga, F., Esplugas, S. And Gimenez, J. (2008). Photocatalytic Degradation of Non-Steroidal Anti-Inflammatory Drugs With TiO_2 And Simulated Solar Irradiation. Water Research 42(3), pp 585-594.

Mendez-Arriaga, F., Esplugas, S. And Gimenez, J. (2008). Photocatalytic Degradation of Non-Steroidal Anti-Inflammatory Drugs With TiO_2 And Simulated Solar Irradiation. Water Research 42(3), pp 585-594.

Mills, A. Le Hunt, S., (1997). An overview of semiconductor photocatalysis. Journal of Photochemistry and Photobiology A: Chemistry, 108, pp 1-35.

Mills, A., Davies, R.H. And Worsley, D. (1993). Water-Purification by Semiconductor Photocatalysis. Chemical Society Reviews 22(6), pp 417-425.

Morrison, R.T. And Boyd, R.N. (1966). Organic Chemistry, Allyn And Bacon, Boston-USA.

Mumma, A., (1995). Environmental Law: Meeting UK&EC Requirements, Surry, McGraw-Hill International (UK) Limited.

Muneer, M. And Boxall, C. (2008). Photocatalyzed Degradation of A Pesticide Derivative Glyphosate In Aqueous Suspensions of Titanium Dioxide. International Journal of Photoenergy.

Muruganandham, M. Swaminathan, M. (2004). Sol. Energy Mater. Sol. Cells 81, pp 439-457.

Muszkat, L. D. Rancher, M. Magaritz and D. Ronen, In: U. Zoller, ed., (1994).Groundwater Contamination and Control, Marcel Dekker, pp 257-271.

Muthukumar, M., Selvakumar, N., Venkata, J., (2001). Effect of dye structure on decolouration of anionic dyes by using ozone. In: Proceedings of the 15th Ozone World Congress of International ozone Association 2001, London, United Kingdom, pp 410-421.

Nakashima, T., Ohko, Y., Kubota, Y., Fujishima, A., (2003). Photocatalytic decomposition of estrogen in aquatic environment by reciprocating immersion of TiO_2-modified polytetrafluoroethylene mesh sheets. J. Photochem. Photobiol., A 160, pp 115-120.

Nakonechny Maureen, Nigel Graham, Yanping Zhang, Bo Ning and Mohamed Gamal El Din, (2008). Degradation of Endocrine Disrupting Chemicals by Ozone/AOPs. Ozone: Science and Engineering, 29: pp 153-176.

Ning, B., N. Graham, Y. Zhang, M. Nakonechny, and M. El-Din, (2007). Degradation of endocrine disrupting chemicals by ozone/AOPs. Ozone- Science and Engineering 29 (3): pp 153-176.

Ochuma, I.J., Fishwick, R.P., Wood, J. And Winterbottom, J.M. (2007). Photocatalytic Oxidation of 2,4,6-Trichlorophenol In Water Using A Cocurrent Downflow Contactor Reactor (CDCR). Journal of Hazardous Materials 144(3), pp 627-633.

Ollis, D.F., Ekabi, H.A., (1993). Photocatalytic purification and treatment of water and air. Amsterdam.

Ollis, D.F.; PeliPem; E.; Serpone, N. (1991). Environ. Sci. Technol., pp 1523.

O'shea, K.E. And Cardona, C. (1995). The Reactivity of Phenol In Irradiated Aqueous Suspensions of TiO_2. Mechanistic Changes As A Function of Solution Ph. Journal of Photochemistry And Photobiology A: Chemistry 91(1), pp 67.

O'Shea, K.E.; Garcia, I.; Aguilar, M. (1997). Res. Chem. Intermed, 23 (4): pp 325.

Ozcan, A., Oturan, N., Sahin, Y. And Oturan, M.A. (2010). Electro-Fenton Treatment of Aqueous Clopyralid Solutions. International Journal of Environmental Analytical Chemistry 90(3-6), pp 478-486.

Pareek, V. K., Brungs, M. P. and Adesina. A. A., (2001). Continuous process for photodegradation of industrial Bayer liquor. Ind. Eng. Chem. Res., vol. 40. No. 23, pp 5120-5125.

Park, J. H., Choi, E. and Gil, K. L., (2003). Removal of reactive dye using UV/TiO_2 in circular type reactor. J. Environ. Sci. Health A, vol.38, No.7, pp 1389-1399.

Patrick Mazellier, Ladji Méité, Joseph De Laat, (2008). Photodegradation of the steroid hormones 17b-estradiol (E2) and 17a-ethinylestradiol (EE2) in dilute aqueous solution. Journal of Chemosphere 73: pp 1216-1223.

Pekakis, P.A., Xekoukoulotakis, N.P. And Mantzavinos, D. (2006). Treatment Of Textile Dyehouse Wastewater by TiO_2 Photocatalysis. Water Research 40(6), pp1276-1286.

Perkowski, J. Kos, L. and Ledakowicz, S., (2000). Advanced oxidation of textile wastewater, Ozone-Sci. Eng. 22 pp 535-550.

Poulios, I. and Aetopoulou, I., (1999). Photocatalytic degradation of the textile dye Reactive Orange16 in the presence of TiO_2 suspensions. Environmental Technology, vol. 20, No. 5, pp 479-187.
pp 115-120.

Preocanin, T. And Kallay, N. (2006). Point of Zero Charge And Surface Charge Density of TiO_2 In Aqueous Electrolyte Solution As obtained by Potentiometric Mass Titration. Croatica Chemica Acta 79(1), pp 95-106.

Qamar, M. Muneer, M. Bahnemann, D. (2006). Heterogeneous photocatalysed degradation of two selected pesticide derivatives, triclopyr and daminozid in aqueous suspensions of titanium dioxide, J. Environ. Manage. 80, pp 99-106.

Rajeswari, R. And Kanmani, S. (2009). A Study on Degradation of Pesticide Wastewater by TiO_2 Photocatalysis. Journal of Scientific & Industrial Research 68(12), pp 1063-1067.

Rao, N. N., Dubey. A. K., Mohanty, S., Khare, P., Jain. R. and Kaul, S. N., (2003). Photocatalytic degradation of 2-chlorophenol: a study of kinetics. Intermediates and biodegradability. Journal of' Hazardous: Materials, vol. 101, No. 3, pp 301-314.

Reutergådh, L.B. And Iangphasuk, M. (1997). Photocatalytic Decolourization of Reactive Azo Dye: A Comparison Between TiO_2 And Us Photocatalysis. Chemosphere 35(3), pp 585-596.

Rhoads, K.R. And Davis, A.P. (2004) Metal Recovery And Catalyst Reuse From The Photocatalytic Oxidation of Copper-Ethylenediaminetetraacetic Acid. Journal of Environmental Engineering-Asce 130(4), pp 425-431.

Rivas, F. J. Beltran, F. J. Carbajo, M. and Gimeno, O., (2003). Homogeneous catalyzed ozone decomposition in the presence of Co (II), Ozone-Sci. Eng. 25 pp 261-271.

Robert, D. And Malato, S. (2002). Solar Photocatalysis: A Clean Process For Water Detoxification. The Science of The Total Environment 291(1-3), pp 85-97.

Rosenfeldt EJ and Linden KG., (2004). Degradation of endocrine disrupting chemicals bisphenol A, Ethinyl estradiol, and estradiol during UV photolysis and advanced oxidation processes. Environmental Science and Technology 38: pp 5476-5483.

Sagawe, G., Schlichting, K., Lohmann, J. and Bahnemann, D., (2001). The aerated cascade photoreactor (ACP) concept: a noval continuous photocatalytic water treatment process. The Sixth International Conference on TiO_2 Photocatalytic Purification and Treatment of Water and Air. Ontario, Canada. 25-29 June 2001. pp 113-115.

Sakaliene, O., Papiernik, S.K., Koskinen, W.C., Kavoliunaite, I. And Brazenaitei, J. (2009). Using Lysimeters To Evaluate The Relative Mobility And Plant Uptake of Four Herbicides In A Rye Production System. Journal of Agricultural And Food Chemistry 57(5), pp1975-1981.

Sapkota, A., Heldler, J., Halden, R. U., (2007). Detection of triclocarban and two co-contaminating chlorocarbanilides in US aquatic environments using isotope dilution liquid chromatography tandem mass spectrometry. Environmental Research, 103, pp 21-29.

Sastry, K. V. S., Cooper, H., Hogg, R., Jespen, T. L. P., Knoll, F., Parekh, B., et al., (1997). Solid-solid operation and equipment. In: Perry, R. H. and Green, D. W. Perry's Chemical Engineer's Handbook. 7th ed. USA: The McGraw-Hill.

Sawyer, D.T. (1991). Oxygen Chemisny, Oxford University Press, New York, pp 120-160.

Schiavello, M. Sclafani, A., (1989). Photocatalysis: Fundamentals and Applications. N. Serpone. E. Pelizzetti (Eds) John Wiley & Sons. pp 159-173.

Serpone, N. and Emeline, A. V., (2002). Suggested terms and definitions in Photocatalysis and radiocatalysis. International journal of photoenergy, vol. 4, pp 91-131.

Serpone, N., Lawless. D. Pelizzetti. E., (1996). Fine Particles Science and Technology, E. Pelizzetti (Ed), Kluwer Academic Publishers. pp 657-673.

Serpone, P.; Borgarello, E.; Pelizzetti, E. (1988). Photoreduction and photodegradation of inorganic pollutants: II. Selective reduction and recovery of Au, Pt, Pd, Rh, Hg and Pb. In: M. Schiavello (Ed.), Photocatalysis and Environment, Trends and Applications. Kluwer Academic Publishers, Dordretch/ Boston/ London. pp 527-565.

Serrano, B. And Delasa, H. (1997). Photocatalytic Degradation of Water Organic Pollutants. Kinetic Modeling And Energy Efficiency. Industrial & Engineering Chemistry Research 36(11), pp 4705-4711.

Sharma, K.K., Rao BSM, Mohan H, Mittal JP, Oakes J, O'Neill P., (2002). A radiation chemistry study. J. Phys Chem A; 106 (29) pp 15-23.

Sharma, S., Pathak, S., & Sharma, K. P., (2003). Toxicity of the azo dye methyl red to the organisms in microsystems, with special reference to the guppy (Poecillia reticulate Peters). Bulletin of Environmental Contamination and Toxicology, 70, pp 753-760.

Shaw, A.A. Wainschel, L.A. and M.D. (1992). Shetiar, Phorockem.Phorobiol. 55, 657.

Sohrabi, M.R. Ghavami, M. (2010). Comparison of Direct Yellow 12 dye degradation efficiency using UV/semiconductor and UV/H_2O_2/semiconductor systems. Desalination 252, pp 157-162.

Sojic, D.V., Anderluh, V.B., Orcic, D.Z. And Abramovic, B.F. (2009). Photodegradation of Clopyralid In TiO_2 Suspensions: Identification of Intermediates And Reaction Pathways. Journal of Hazardous Materials 168(1), pp 94-101.

So, C.M., Cheng, M.Y., Yu, J.C., Wong, P.K., (2002). Degradation of azo dye Procion Red MX-5B by photocatalytic oxidation. Chemo- sphere 46, pp 905-912.

Stasinakis, A. S. (2008). Use of selected advanced oxidation processes (AOPs) for wastewater treatment -a mini review. J. global nest, vol 10, No 3, pp 376-385.

Stryer, L. (2000). Biochemistry. 4th edn., W.H. Freeman and company, New York, p 1064.

Stylidi, M., Kondarides DI, Verykios XE., (2004). Visible light-induced photocatalytic degradation of Acid Orange 7 in aqueous TiO_2 suspensions. Stylidi, M., Kondarides, D.I., Verykios, X.E., Appl Catal B Environ 47(3): pp 189-201.

Svarovsky, L., (2000a). Introduction to solid-liquid separation. In: Svarovsky, L. Solid-liquid separation. 4th. Oxford: Butterworth-Heinemann, pp 1-28.

Taborda, A. V.; Brusa, M. A.; Grela. M. A., (2001). Photocatalytic degradation of phthalic acid on TiO_2 nanoparticles Applied Catalysis A: General, 208, pp 419-426.

Tanizaki, T., Kadokam, K., Shinohara, R. (2002). Catalytic photodegradation of Endocrine disrupting chemicals using titanium dioxide photosemiconductor thin films. Environ. Contam. Toxicol, 68: pp 732-739.

Terzian, R. and Serpone, N., (1995). Heterogeneous Photocatalyzed oxidation of creosote components: mineralization of xylenols by illuminated TiO_2 in oxygenated aqueous media. J. Photochem. Photobiol. A: Chem., Vol. 89, No.2. pp 1633-1675.

Toor, A.P., Verma, A., Jotshi, C.K., Bajpai, P.K. And Singh, V. (2006). Photocatalytic Degradation of Direct Yellow 12 Dye Using Uv/TiO_2 In A Shallow Pond Slurry Reactor. Dyes And Pigments 68(1), pp 53-60.

Turro, N.J. Modern Molecular Photochemistry, (1978). The Benjamin/Cummings, Menlo.

US.EPA, (1998). Handbook on Advanced Photochemical Oxidation Processes. U.S. Environmental Protection Agency, Cincinnati, Ohio 45268.

Vogna, D MR., Andreozzi, R., Napolitano, A., and d'Ischia, M., (2004b). Advanced oxidation of the pharmaceutical diclofenac with UV/H_2O_2 and ozone. Water Research 38: pp. 414-422.

Vogna, D., Marotta, R., Andreozzi, R., Napolitano, A., and d'Ischia, M., (2004a). Kinetic and chemical assessment of the UV/H_2O_2 treatment of antiepileptic drug carbamazepiine. Chemosphere 54: pp 497-505.

Walker, G. M., Hansen, L., Hanna, J. A., & Allen, S. J., (2003). Kinetics of reactive dye adsorption onto dolomitic sorbents. Water Research, 37, pp 2081–2089.

wall, D.A. (1994). Potato (solanum-tuberosum) response to simulated drift of dicamba, clopyralid and tribenuron. weed science 42(1), pp110-114.

Wayne, R. P., (1988). Principles and applications of photochemistry, Oxford Science Publications.

Wellburn, A. Air Pollution and Acid Rain: The Biological Impact. New York: Wiley, 1988.

Weller, H. Angew, (1993). Chem. Int. Engl. 32, pp 41-53.

Wong, Y.S. Szeto, **W.H. Cheung** and G. McKay, (2003). Equilibrium Studies for Acid Dye Adsorption onto Chitosan, *Langmuir*, vol. 19, pp 7888-7894.

Wu, C.L. and linden, k.g. (2008). degradation and byproduct formation of parathion in aqueous solutions by uv and UV/H_2O_2 treatment. water research 42(19), pp 4780-4790.

Wu, J and Wang, T., (2001a). Ozonation of Aqueous Azo Dye in a Semi-batch Reactor, Water. Res. 35: pp 1093-1099.

Xianghua, F., Jianfeng, Tu., Shimin, D., Feng, Wu., Nansheng, D., (2005). Photodegradation of 17β-estradiol in water by UV-vis/Fe (III)/H_2O_2 system. J. Hazardous Materials B127: pp 129-133.

Xiong, F. And Graham, N.J.D. (1992). Rate Constants for Herbicide Degradation by ozone. Ozone-Science & Engineering 14(4), pp 283-301.

Xu, Y.M., Langford, C.H., (2001). UV- or visible light induced degradation of X3B on TiO_2 nanoparticles: The influence of adsorption, Langmuir 17(3): pp 897-902.

Yao, C.C.D. And Haag, W.R. (1991). Rate Constants For Direct Reactions of Ozone With Several Drinking-Water Contaminants. Water Research 25(7), pp 761-773.

Ying, G.G. Kookana R.S. and Waite, T.D. (2004). Endocrine disrupting chemicals (EDCs)

Yu, J.; Yu, J. C.: Ho, W.: Jiang, Z., (2002). (Effects of calcination temperature on the photocatalytic activity and photo-induced super-hydrophilicity of mesoporous TiO_2 thin films) New J. Chem., 26, 607.

Yue, P. L., (1992). Degradation of Organic Pollutants by Advanced Oxidation Process Safety and Environmental Protection 70 (B3): pp 145-148.

Zang, Y. And Farnood, R. (2005). Effects of Hydrogen Peroxide Concentration And Ultraviolet Light Intensity on Methyl Tert-Butyl Ether Degradation Kinetics. Chemical Engineering Science 60(6), pp 1641-1648.

Zhang, Y., Crittenden, J.C., Hand, D.W., Perram, D.L., (1994). Fixed-Bed Photocatalysts for Solar Decontamination of Water. Environmental Science Technology.28: pp 435-442.

Zhang, Y., Zhou, J. (2008). Occurrence and removal of endocrine disrupting chemicals in wastewater. Chemosphere. 73: pp 848-853.

Appendix

Figure A. 1: System of the Photocatalysis experimental

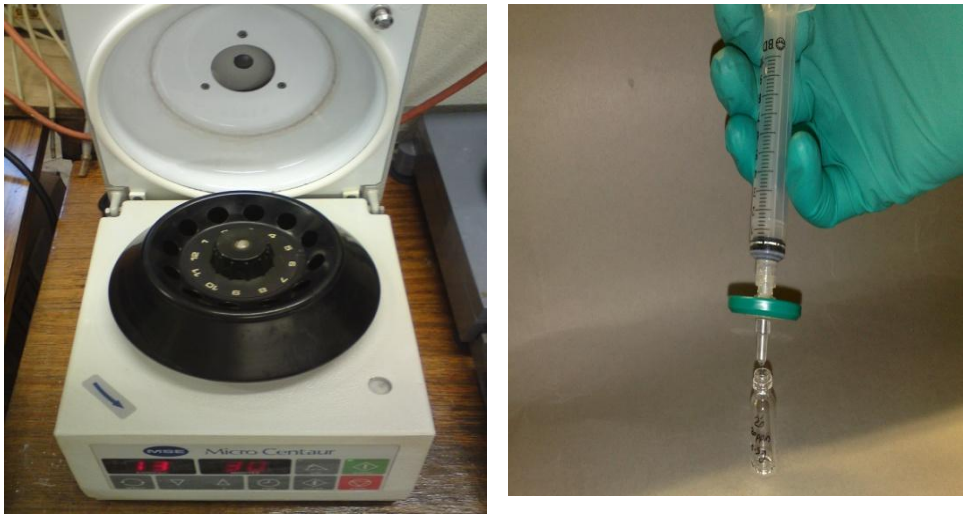

Figure A. 2: Mini Centrifuge and sample filtration using membrane filter Miliex GP 0.22µm

Figure A. 3: Dye (RO16) during the photocatalysis processes

Figure A. 4: HPLC (Waters 2695) and UV Lamp

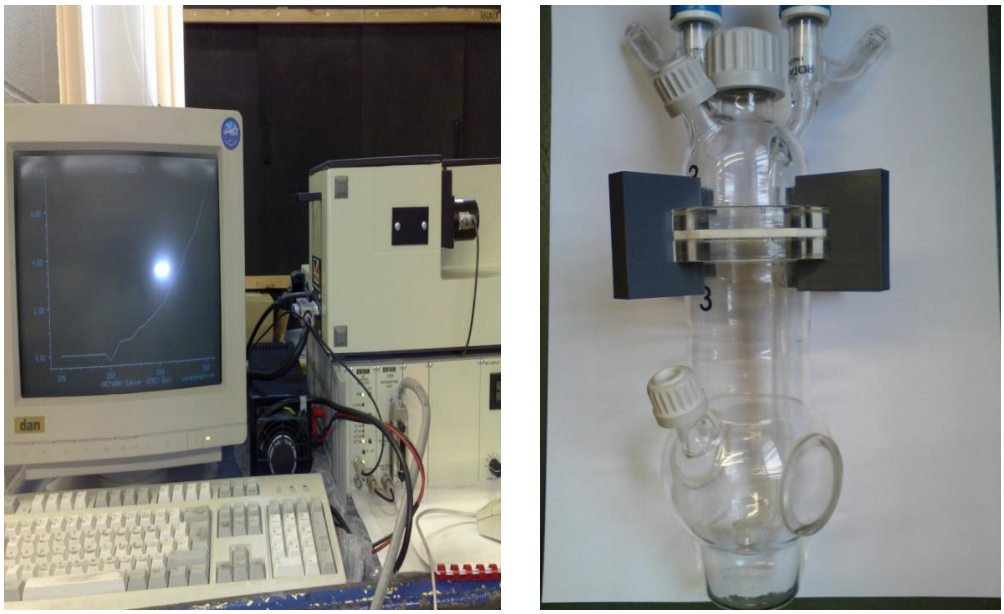

Figure A. 5: Bentham system and photocatalysis reactor

Figure A. 6: Instrument of deionised water and pH meter

Figure A. 7: System of ozonation experimental and Ozone reactor

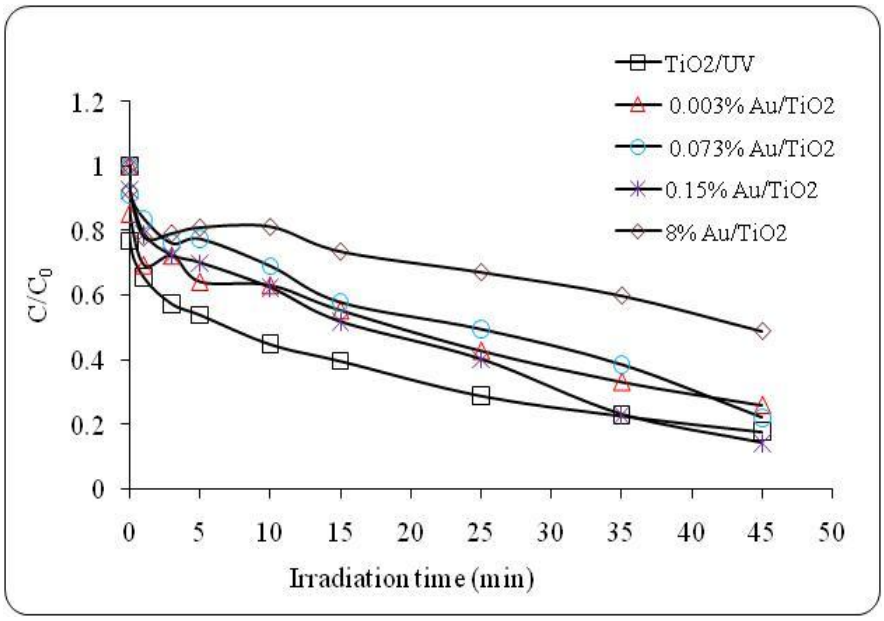

Figure A. 8: Photocatalytic degradation of 20 mg/L RO16 using 1g/L modified catalyst (TiO_2 doped with gold)

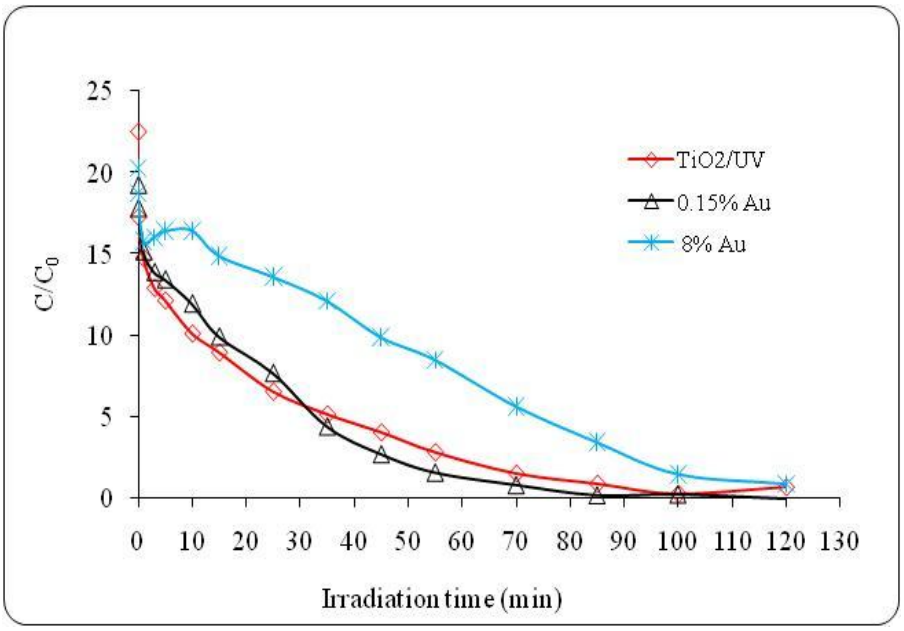

Figure A. 9: Photocatalytic degradation of 20 mg/L RO16 using 1g/L modified catalyst (TiO_2 doped with gold)

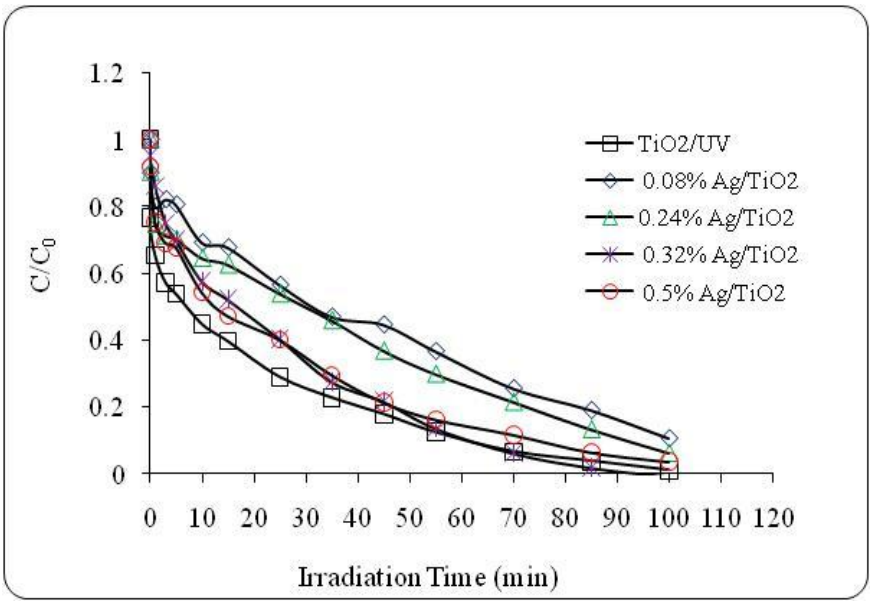

Figure A. 10: Photocatalytic degradation of 20 mg/L RO16 using 1g/L modified catalyst (TiO_2 doped with silver)

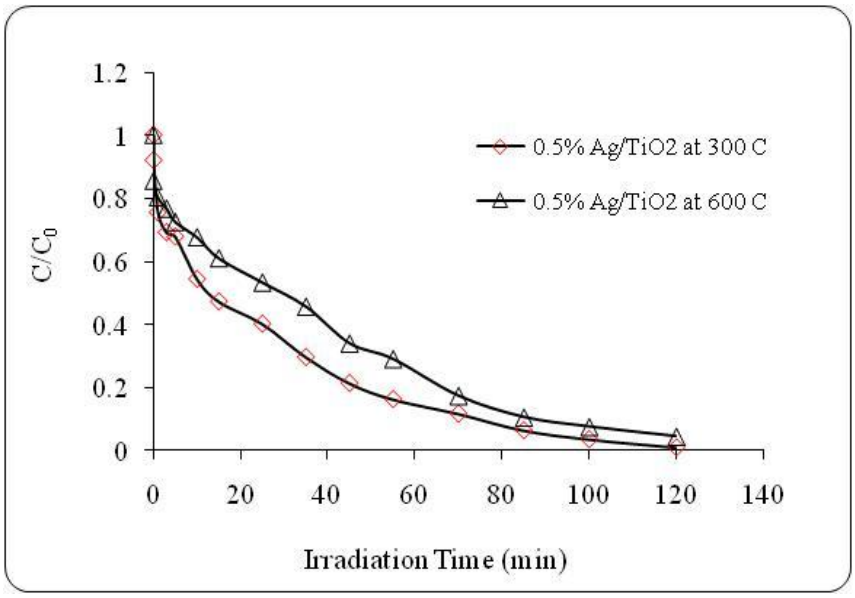

Figure A. 11: Photocatalytic degradation of 20 mg/L RO16 using 1g/L modified catalyst (TiO_2 doped with silver)